ISSN 1881-7815 Online ISSN 1881-7823

BST
BioScience Trends

Volume 15, Number 2
April, 2021

IRCA
BSSA

IACMHR

www.biosciencetrends.com

BST
BioScience Trends

ISSN: 1881-7815
Online ISSN: 1881-7823
CODEN: BTIRCZ
Issues/Year: 6
Language: English
Publisher: IACMHR Co., Ltd.

BioScience Trends is one of a series of peer-reviewed journals of the International Research and Cooperation Association for Bio & Socio-Sciences Advancement (IRCA-BSSA) Group. It is published bimonthly by the International Advancement Center for Medicine & Health Research Co., Ltd. (IACMHR Co., Ltd.) and supported by the IRCA-BSSA.

BioScience Trends devotes to publishing the latest and most exciting advances in scientific research. Articles cover fields of life science such as biochemistry, molecular biology, clinical research, public health, medical care system, and social science in order to encourage cooperation and exchange among scientists and clinical researchers.

BioScience Trends publishes Original Articles, Brief Reports, Reviews, Policy Forum articles, Communications, Editorials, News, and Letters on all aspects of the field of life science. All contributions should seek to promote international collaboration.

Editorial Board

Editorial and Head Office

Pearl City Koishikawa 603,
2-4-5 Kasuga, Bunkyo-ku, Tokyo 112-0003, Japan
E-mail: office@biosciencetrends.com

BioScience Trends

Editorial and Head Office

Pearl City Koishikawa 603, 2-4-5 Kasuga, Bunkyo-ku,
Tokyo 112-0003, Japan

E-mail: office@biosciencetrends.com
URL: www.biosciencetrends.com

Editorial Board Members

CONTENTS

Volume 15, Number 2, 2021

Review

Original Article

Communication

Letter

Review

DOI: 10.5582/bst.2021.01061

COVID-19 vaccine research focusses on safety, efficacy, immunoinformatics, and vaccine production and delivery: a bibliometric analysis based on VOSviewer

Yamin Chen[1,2,§], Luying Cheng[2,§], Rongna Lian[3], Ziwei Song[2], Jinhui Tian[1,4,*]

[1] Key Laboratory of Evidence-based Medicine and Knowledge Translation of Gansu Province, Lanzhou University, Lanzhou, China;
[2] Evidence-Based Nursing Center, School of Nursing, Lanzhou University, Lanzhou, China;
[3] The First Clinical Medical College, Lanzhou University, Lanzhou, China;
[4] Evidence-Based Medicine Center, School of Basic Medical Sciences, Lanzhou University, Lanzhou, China.

SUMMARY Coronavirus Disease 2019 (COVID-19), caused by the severe acute respiratory syndrome coronavirus-2 (SARS-CoV-2), has affected tens of millions of people globally since it was declared a pandemic by the World Health Organization (WHO) on March 11, 2020. There is an urgent need for safe and effective preventive vaccines to curb this pandemic. A growing amount of related research has been published. This study aimed to provide the current status of COVID-19 vaccine using bibliometric analysis. We searched Embase.com and MEDLINE comprehensively and included articles, articles in press, reviews, short surveys, conference abstracts and conference papers about COVID-19 vaccine. VOSviewer1.6.11 (Leiden University, Leiden, Netherlands) was applied to perform the bibliometric analysis of these papers. A total of 1,312 papers were finally included. The BMJ has been the most popular journal in this field. The United States maintained a top position worldwide and has provided a pivotal influence, followed by China, India and United Kingdom. Among all the institutions, Harvard University was regarded as a leader for research collaboration. We analyzed the keywords and identified seven COVID-19 vaccine research hotspot clusters. COVID-19 vaccine research hotspots focus on clinical trials on vaccine safety and efficacy, research on vaccine immunology and immunoinformatics, and vaccine hesitancy. Our analysis results demonstrated that cooperation between countries, institutions, and authors were insufficient. The results suggested that clinical trials on vaccine safety, efficacy, immunology, immunoinformatics, production and delivery are research hotspots. Furthermore, we can predict that there will be a lot of research focusing on vaccine adverse reactions.

Keywords COVID-19, vaccine, bibliometric analysis, VOSviewer

1. Introduction

Coronavirus Disease 2019 (COVID-19), caused by the severe acute respiratory syndrome coronavirus-2 (SARS-CoV-2), has affected tens of millions of people globally since it was declared a pandemic by the World Health Organization (WHO) on March 11, 2020 (*1*). The clinical manifestations of COVID-19 usually include fever, dry cough and fatigue, often accompanied by lung infections (*2*). As of 28 February 2021, the number of confirmed cases has exceeded 110 million, with 2,512,272 reported deaths, indicating this pandemic's significant global impact (*3*). The high transmission rate of the COVID-19 has led to the current heavy burden on public health and the global economy, highlighting the need for a fast and effective method to prevent or treat deadly infections (*4*). An effective treatment strategy is to reduce the symptoms of patients (*4*). Simultaneously, many therapeutic treatments such as antiviral drugs (nucleotide analogue) (*5,6*), antimalarial drugs (those inhibit viral cell entry and its replication) (*7,8*), immunomodulators (*9*), and cell and plasma-based therapy (*10*) have shown therapeutic effects. Despite the various treatment approaches, there are no potential drugs available to treat COVID-19. Some studies reported reinfection in patients who have been declared clinically recovered (*11*). Thus, there is an urgent need for safe and effective preventive vaccines to curb this pandemic. More and more research teams, and pharmaceutical companies are committed to vaccine research and development, which has led to numerous articles about vaccines published in a short time. However, the status of COVID-19 vaccine research

is still unclear.

Bibliometric analysis is a quantitative analysis combining mathematics and statistics, which focuses on the bibliometric characteristics of research in a particular field, and helps investigators grasp the development priorities and trends in the field and guides their follow-up work (*12,13*). Bibliometric methods have expanded the focus on topics, publications, countries, authors, institutions and journals in many research fields (*14,15*). Bibliometrics can assess the research reputation of a large number of units, because individual experts are not capable of handling so much information in a single evaluation procedure (*16*). To a certain degree, bibliometric analysis can systematically estimate the trend of future research hotspots (*17*). A large number of studies have applied bibliometric analyses to identify research trends in various fields (*14*). There are a few published studies about COVID-19 using bibliometric analysis to explore the activity and trends (*18-20*). However, no bibliometric study on recent scientific output and future research trends of COVID-19 vaccine was reported. In order to access the current status and provide a reference for later research of COVID-19 vaccines a bibliometric analysis was performed.

2. Methods

2.1. Data source and collection

We searched *Embase.com* and MEDLINE comprehensively and included articles, articles in press, reviews, short surveys, conference abstracts and conference papers about COVID-19 vaccines. To avoid bias caused by frequent database renewal, all the literature retrieval and data download were completed in a single day, February 18, 2021. There was no restriction on language and data category. The search terms were "coronavirus disease 2019", "severe acute respiratory syndrome coronavirus 2", "COVID-19", "2019-nCov", "SARS-CoV-2", "vaccine", "autovaccine". A detailed search strategy of *Embase.com* is presented in Supplementary Data 1 (*http://www.biosciencetrends.com/action/getSupplementalData.php?ID=71*).

2.2. Study selection

Two reviewers (YMC and LYC) independently extracted data including titles, countries, institutions, journals, authors and so on. Differences of opinion were settled by consensus or referral to a third review author (JHT).

2.3. Data analysis and visualization

We conducted a bibliometric analysis using VOSviewer 1.6.11 (Leiden University, Leiden, Netherlands), and constructed a map based on a co-occurrence matrix and identified clusters from the keywords network (*21,22*). We standardized the data before performing analysis. To be specific, different expressions of the same keywords were standardized into Medical Subject Heading (MeSH) terms in order to avoid bias. The standardizations were carried out manually by the authors (*23,24*). The interpretation of a visualization map produced was based on three characteristics: size, distance, and colors (*25*). A node means a specific element, such as author, country, or keyword, and the size of the node shows the number of publications or frequency (*24*). The larger threshold means the more times it occurs, and the smaller threshold indicates the fewer occurrences. The link between the nodes means that they are connected, and the distance between two terms indicates the affinity and sparseness of the relationship. In other words, the smaller the line, the closer the relationship is, and vice versa. In terms of the cluster analysis of keywords, each color represents a cluster (*25*). In this study, the parameters of VOSviewer were as follows: counting method (fractional counting) and ignore documents with a large number of authors (maximum number of authors per document is 25). We regarded the Emtree Medical Index Terms (Major Focus) as keywords.

3. Results

3.1. Search results, journals, and date of publication

A total of 6,018 records were derived from *Embase.com* and MEDLINE. After two reviewers' independent screening, 1,312 papers were finally included, which were published in 576 journals. The number of journals that published more than five papers and only one study was 7.64% (44/576) and 70.14% (404/576). We have listed the top 20 journals, among them, the top five published journals were BMJ (64/1,312), Vaccines (Basel) (44/1,312), Vaccine (36/1,312), Human Vaccines and Immunotherapeutics (33/1,312), and New England Journal of Medicine (30/1,312) (Table 1). Publication dates of included articles are 2020 and 2021. Since 331 papers have no specific publication information, we only drew a histogram for the remaining 981 papers, as shown in Figure 1. Research on vaccines is increasing month by month, with the most in January 2021 (210/981). Limited by our search until February 18, so it does not mean that there are fewer studies in February and following months.

3.2. Institutions

More than two thousand institutions have paid attention to the research field of COVID-19 vaccine, most of them participated in only one study respectively. We listed the top 20 institutions in the ranking of publications (Table 2). The institutions with more than 20 publications were Harvard University (37 studies), University of Washington (36 studies), University of

Oxford (31 studies), Johns Hopkins University (26 studies), National Institutes of Health (26 studies), Stanford University (18 studies), University of North Carolina (18 studies), University of Toronto (17 studies), Emory University (16 studies), and University of Maryland (16 studies), which demonstrated that most of the contributions came from universities. Network map of institutions with frequency more than seven are shown in Figure 2, which contains 34 nodes and seven clusters. The largest cluster (#1) consisted of Harvard University, Stanford University, University of Florida, University of Kwazulu-Natal, University of Toronto, University of Washington, and University of Yalu, while the second largest cluster (#2) mainly consisted of Baylor College of Medicine, Emory University, New York University, Massachusetts Institute of Technology, University of Maryland, University of North Carolina, and University of Texas. Most of these institutions are in the United States and work closely together. The third cluster (#3) was Chinese Academy of Sciences, Peking University, Fudan University, National Institute for Food and Drug Control, and National Institutes of Health, which are in China and the United States. The fourth cluster (#4) was Duke University, Icahn School of Medicine at Mount Sinai, University of California, University of Michigan and University of Pennsylvania. Among the remaining clusters (#5, #6, #7), each cluster contained three institutions, most of which are universities.

Table 1. Top 20 productive journals of papers on COVID-19 vaccine

Rank	Journal	Frequency
1	BMJ	64
2	Vaccines (Basel)	44
3	Vaccine	36
4	Human Vaccines & Immunotherapeutics	33
5	New England Journal of Medicine	30
6	Frontiers in Immunology	26
7	Nature	22
8	Science	21
9	JAMA	17
10	Annals of Internal Medicine	16
11	Cell	16
12	International Journal of Environmental Research and Public Health	13
13	Clinical Infectious Diseases	12
14	Journal of Biomolecular Structure and Dynamics	12
15	Journal of Medical Virology	12
16	Nature Communications	12
17	Expert Review of Vaccines	10
18	Scientific Reports	10
19	The Lancet	10
20	PLoS One	9

3.3. Countries

In total, 95 countries have engaged in relevant research on COVID-19 vaccine, of them, 28 countries published one study, and 67 countries participated in two studies at least. We presented the top 20 countries in the ranking in Table 3. The United States ranked first, with 424 publications, followed by China (149 publications), India (145 publications), United Kingdom (145 publications), and Canada (57 publications). Figure 3 contains 44 countries with a frequency more than five, which had a connection with others, and seven clusters. It can be said that the United States and China have close ties with other countries. The largest cluster (#1) contained Australia, Germany, Greece, Israel, Italy, Netherlands, Romania, Russian Federation, Spain, and Switzerland. The second largest cluster (#2) contained Bangladesh, China, India, Indonesia, Iran, Japan, Nepal, South Korea, Sudan, and Turkey. The third largest cluster (#3)

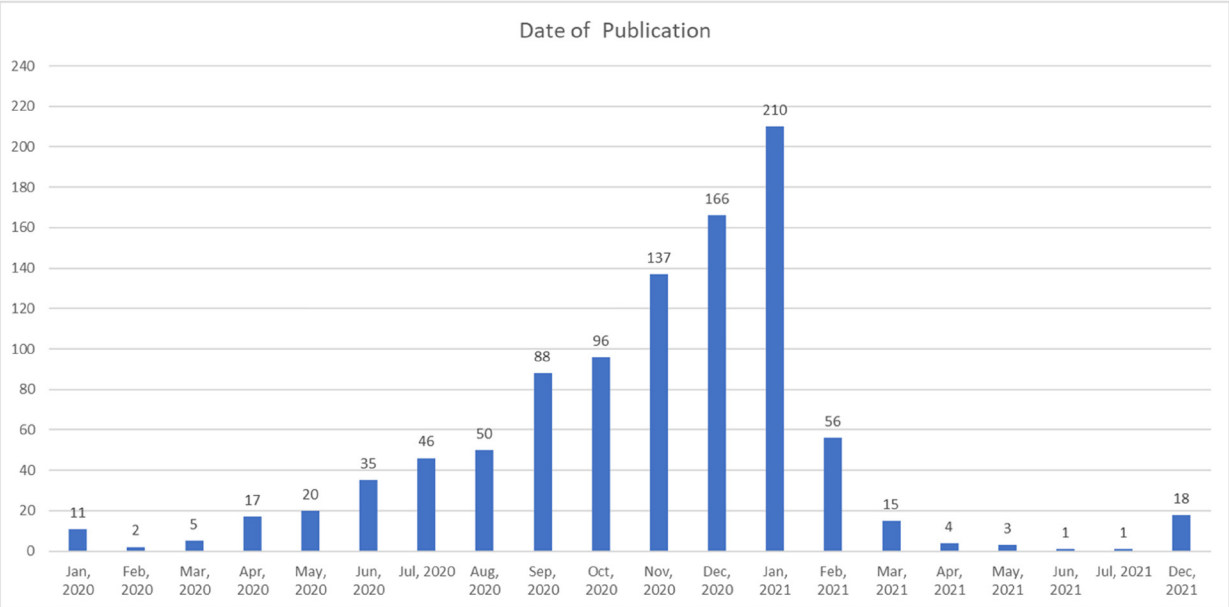

Figure 1. Date of publication of COVID-19 vaccine research.

Table 2. TOP 20 productive institutions of papers on COVID-19 vaccine

Rank	Institution	Frequency
1	Harvard University	37
2	University of Washington	36
3	University of Oxford	31
4	Johns Hopkins University	26
5	National Institutes of Health	26
6	Stanford University	18
7	University of North Carolina	18
8	University of Toronto	17
9	Emory University	16
10	University of Maryland	16
11	Yale University	16
12	Baylor College of Medicine	15
13	Imperial College London	15
14	University of California	15
15	University of Pennsylvania	14
16	Chinese Academy of Sciences	13
17	Icahn School of Medicine at Mount Sinai	13
18	Peking University	12
19	University of Florida	12
20	University of Texas	12

Table 3. Top 20 countries of papers on COVID-19 vaccine

Rank	Country	Frequency
1	United States	424
2	China	149
3	India	145
4	United Kingdom	145
5	Canada	57
6	Germany	56
7	Australia	52
8	Italy	52
9	Spain	38
10	France	36
11	Switzerland	32
12	Iran	31
13	Saudi Arabia	28
14	South Korea	25
15	Netherlands	24
16	Russian Federation	19
17	Brazil	18
18	Israel	18
19	South Africa	18
20	Pakistan	17

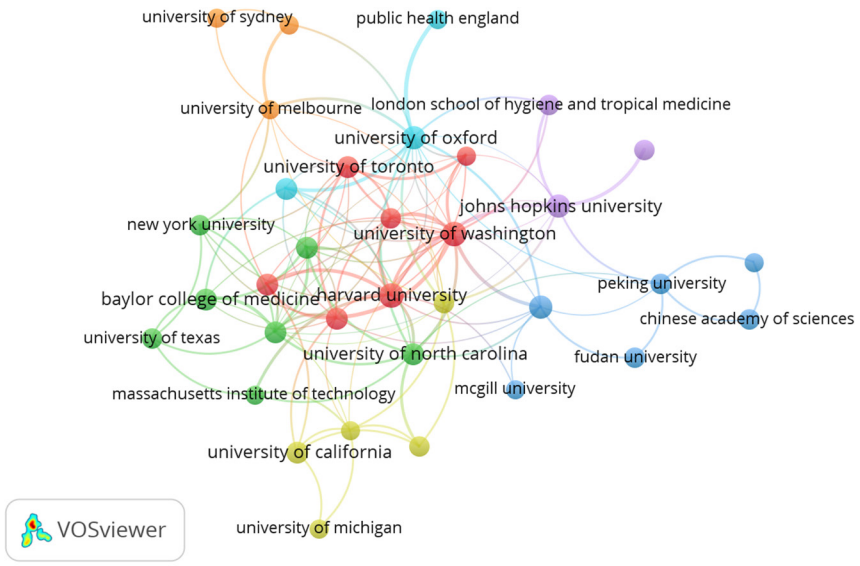

Figure 2. Network map of 19 institutions with frequency more than four.

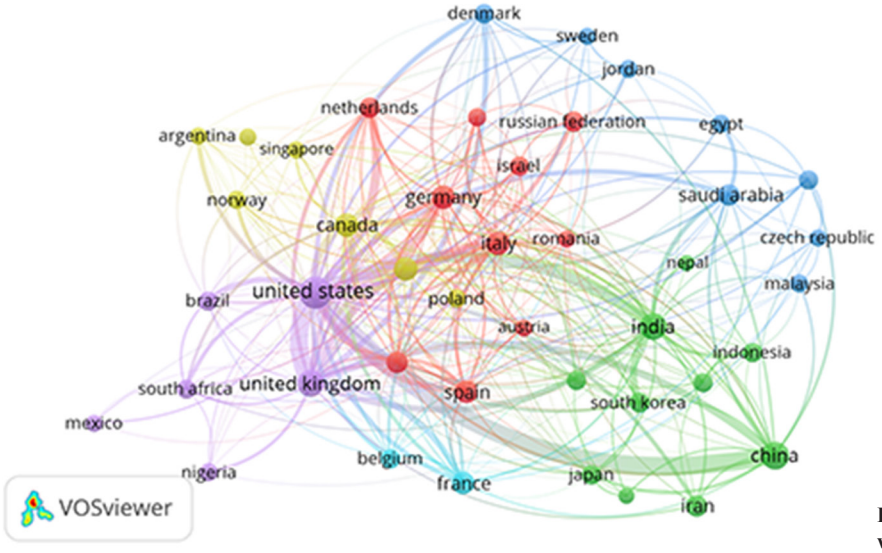

Figure 3. Network map of 40 countries with frequency more than two.

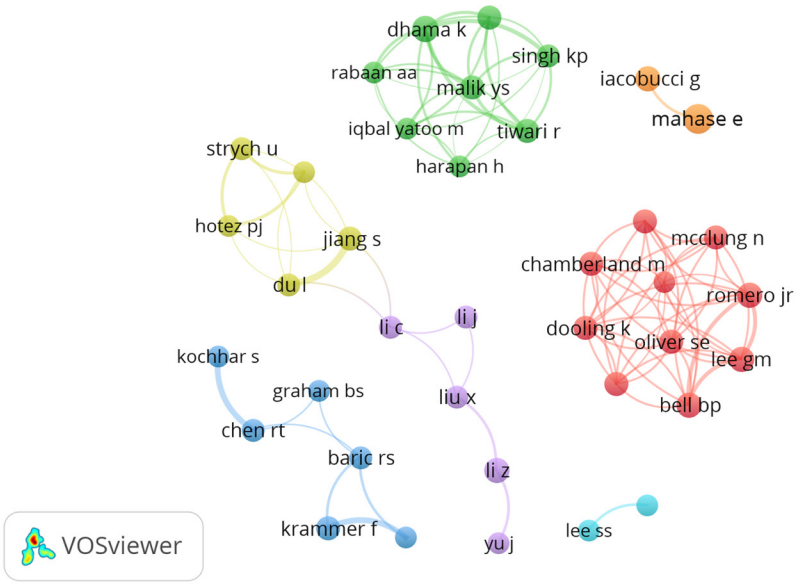

Figure 4. Network map of 29 authors with frequency more than three.

contained Czech Republic, Denmark, Egypt, Jordan, Malaysia, Pakistan, Saudi Arabia, and Sweden.

3.4. Authors

More than five thousand authors contributed to the publications of COVID-19 vaccine. 38 authors who had a connection with others, constituted seven clusters as shown in Figure 4, the threshold is four. The red cluster in the right corner of the picture was the largest cluster containing ten authors from United States, which cooperate closely. The yellow cluster, purple cluster and the blue cluster consisted mainly of American authors, Indian authors, Chinese authors and British authors. The detailed address and nationality of the authors in Figure 4 are shown in Supplementary Data 2 (*http://www.biosciencetrends.com/action/getSupplementalData.php?ID=71*).

3.5. Keywords

869 COVID-19 vaccine research hotspots keywords were extracted from 1,312 publications. Table 4 shows the top 20 keywords, among them, with a frequency of occurrence more than 30 is COVID-19 (1,075 publications), vaccination (212 publications), pandemic (153 publications), immunity (101 publications), vaccine hesitancy (39 publications), prevention and control (32 publications), and drug design (30 publications).

We presented the main keywords density in Figure 5, with frequency greater than eight. 55 nodes are shown in the map, and the brightest three were COVID-19 and vaccination in the center of the map. In Figure 6, 55 keywords that appeared more than eight times are included and classified into seven clusters in the map: cluster 1 (clinical research about vaccination, in red); cluster 2 (immunological research on vaccines, in green); cluster 3 (immunoinformatics on the vaccine, in blue); cluster 4 (infection prevention, in yellow), cluster 5 (herd immunity of public health, in purple), cluster 6 (vaccine delivery in bright blue) and cluster 7 (vaccine production, in orange). Circles with a large size represent the keywords that appeared at a high frequency. Within cluster 1, the following keywords frequently occurred: administration and dosage, age, attitude to health, clinical trial, controlled study, ethics, health care system, influenza vaccination, organization and management, practice guideline, pregnancy, prevention and control, procedures, psychology, trust, and virus pneumonia. In

Table 4. Top 20 keywords of papers on COVID-19 vaccine

Rank	Keywords	Frequency
1	coronavirus disease 2019	1,075
2	vaccination	212
3	pandemic	153
4	immunity	101
5	vaccine hesitancy	39
6	prevention and control	32
7	drug design	30
8	drug efficacy	29
9	public health	28
10	antibody response	27
11	immunogenicity	24
12	middle east respiratory syndrome	22
13	drug safety	21
14	receptor binding	21
15	spike	20
16	t lymphocyte	20
17	drug development	18
18	virus pneumonia	18
19	ethics	17
20	vaccine production	17

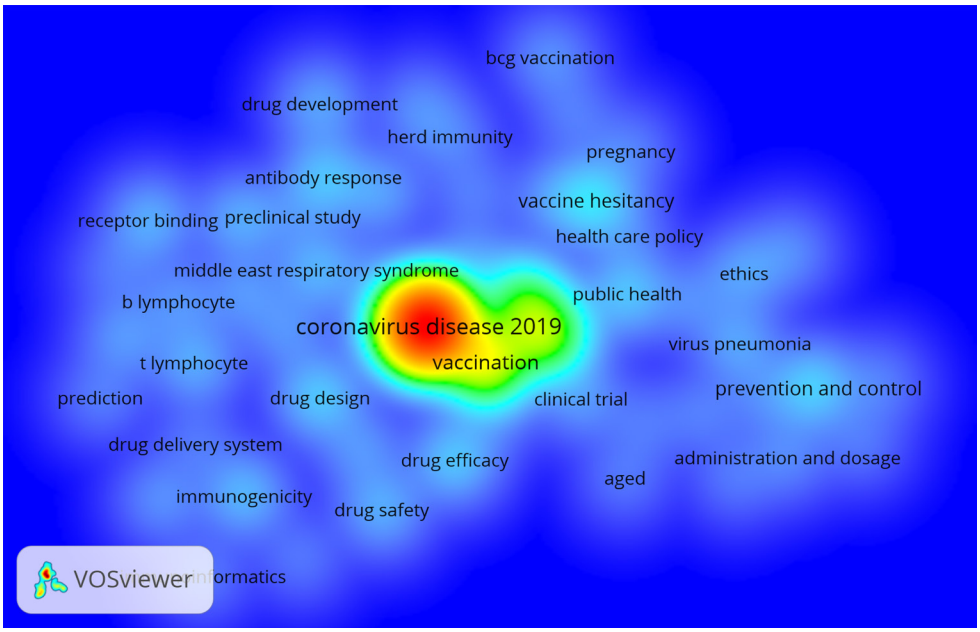

Figure 5. Density map of main keywords.

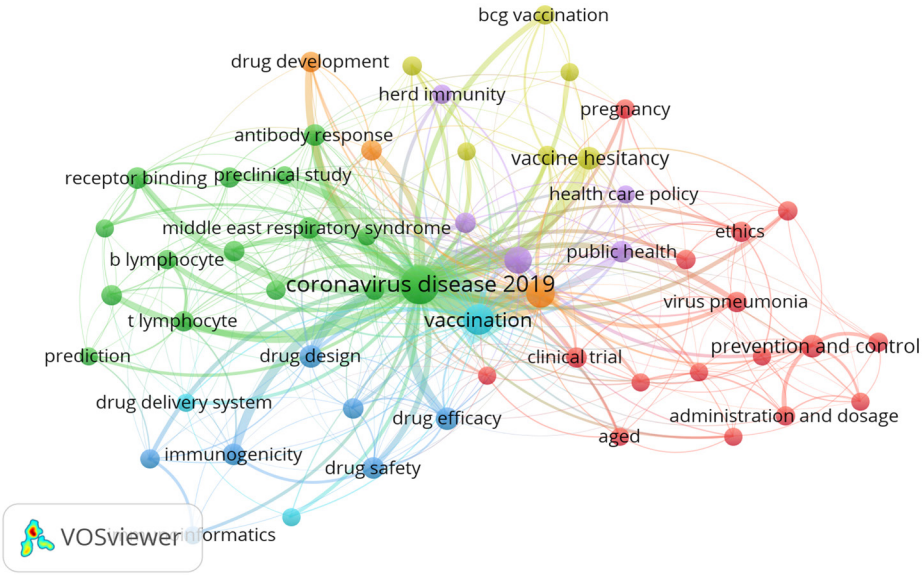

Figure 6. Network map of 44 keywords with frequency more than four.

cluster 2, relevant keywords included antibody response, b lymphocyte, cellular immunity, computer model, coronavirus disease 2019, humoral immunity, innate immunity, middle east respiratory syndrome (MERS), nonhuman, preclinical study, prediction, protein domain, receptor binding, spike, and t lymphocyte. Similarly, in cluster 3, the main keywords are bioinformatics, drug design, drug efficacy, drug safety, immunogenicity, immunoinformatics, and vaccine immunogenicity. In cluster 4, the primary keywords are BCG vaccination, epidemic, health care personnel, infection prevention, mortality, and vaccine hesitancy. In cluster 5, they are communicable disease, health care policy, herd immunity, immunity, and public health. In cluster 6, the keywords are drug delivery system, nanomedicine, and vaccination. The keywords of the last cluster are drug development, pandemic, and vaccine production. To sum up, COVID-19 vaccine research hotspots can be classified as clinical trials on vaccine safety and efficacy, research on vaccine immunology and immunoinformatics, herd immunity of public health and vaccine production and delivery.

4. Discussion

As we all know, the pandemic of COVID-19 has caused high alarm worldwide because of its morbidity and mortality. The battle against COVID-19 is still going on,

and there are still new cases of COVID-19 in China (*18*). The most urgent task for medical doctors or scientists is to control COVID-19, including the development of a safe and effective vaccine. Many diverse studies addressing COVID-19 vaccine have sprung up owing to the urgent necessity of prevention and control. Global efforts should continue on vaccines for COVID-19.

In this study, we analyzed the journals, date of publication, institutions, countries, authors, and keywords of published studies on COVID-19 vaccine based on bibliometric and visualization methods, in order to reveal the current status of COVID-19 vaccine worldwide.

Based on the results of the analysis about journals, the BMJ was the top journal with publications on the COVID-19 vaccine up to February 18, 2021. Medical journals with high impact such as the BMJ, JAMA, Science, Cell, Nature, Lancet and the New England Journal of Medicine have also published papers for COVID-19 vaccine, which means that the vaccine received extensive attention from researchers around the world and had a crucial role in the prevention of COVID-19. Studies with high impact factors have involved COVID-19 vaccine development, safety and immunogenicity of the vaccine, vaccine hesitancy, and COVID-19 vaccine trials (*26-29*). Variations in the number of academic papers on a certain research field are important indicators for the developing trend. Plotting the number of publications over time and conducting multivariate statistical analysis help to comprehend the research level and future trends (*19*). As for 981 publications with specific dates, the quantity increased month by month from January 2020 to January 2021. Since our search was completed on February 18, 2021, the publications of February and the following months are incomplete. We predict that the publications will be more than that shown in Figure 1, according to the fact that some vaccines have been widely introduced. Thus, vaccines will be a research hotspot in the future until COVID-19 is controlled.

Our observations indicate that multiple institutions published studies about COVID-19 vaccines, attributed to the fact that COVID-19 has affected more than 200 countries or regions around the world. After analyzing the top 20 institutions, we realized that most of the institutions are universities and located in the United States. The network map illustrated that research teams are formed between different institutions, which were connected but not close to each other. Regarding the contributions of countries, both the United States and China have played important roles in COVID-19 vaccine research, and their total numbers of studies ranked first and second, respectively. The United States seems to have superior conditions for basic medical research or clinical trials, which include adequate funding, advanced equipment, and professional researchers. All the characteristics also showed that the United States is leading the field (*30*). The four institutions from China (Fudan University, Peking University, National Institute for Food and Drug Control and Chinese Academy of Sciences) also made some contributions. Part of the reason for this phenomenon was that China is one of the countries severely affected by the epidemic, which also demonstrated China's scientific research strength has increased in recent years. Notably, approximately two thousand authors contributed to the publication of COVID-19 vaccine, however, most were involved in one publication. The network map of more than four authors illustrated that independent research teams formed between different authors. The same result was attributed to the author's institution. More connections between different nodes indicate more cooperation between different countries. The biggest problem at present is insufficient cooperation between various countries, institutions, and authors, which greatly reduces research efficiency. If the exchanges and cooperation about research methods and results between institutions in various countries are improved, vaccine research on COVID-19 will make a huge breakthrough.

As for the keywords involved, 869 hotspots keywords were encountered, which covered common words used in COVID-19 vaccine research. The most frequent words were COVID-19, vaccination, pandemic, vaccine hesitancy, prevention and control, and drug design. Only 6.3% (55/869) of keywords had a frequency of ≥ 8, indicating the importance of a few keywords. In bibliometrics, a network map of keyword co-occurrences reflects hot topics (*31*). Cluster analysis of co-occurrence keywords demonstrated that there were seven clusters in this field. Cluster 1 consisted of 16 keywords, mainly related to clinical research about vaccination, because clinical research on vaccination was carried out in many countries. WHO reported that at least seven different vaccines across three platforms have been rolled out. Vulnerable populations in all countries are the highest priority for vaccination. At the same time, there are currently more than 200 additional vaccine candidates in development, of which more than 60 are in clinical development, as of February 18, 2021 (*32*). Issues such as ethics and informed consent involved in vaccines are also hot topics in current research (*33-37*). Cluster 2 consisted of 15 keywords mainly about immunological research on vaccines, which was the key to vaccine development. The viral surface spike (S) protein of SARS-CoV-2 is a key target for prophylactic measures as it is critical for the viral replication cycle and the primary target of neutralizing antibodies, thus, researchers all over the world are targeting the S protein for the development of potential vaccines (*38*). A previous study showed that 4A8 binds to the N-terminal domain (NTD) of S protein with potent neutralizing activity, which means that the development of vaccines has made some progress (*39*). For cluster 3, seven keywords were mainly related to vaccine immunoinformatics. Some research

focused on designing a multi-epitope vaccine, using an immunoinformatics approach (*40*). Six keywords, BCG vaccination, epidemic, health care personnel, infection prevention, mortality, and vaccine hesitancy, formed cluster 4. Some studies have elaborated the vital role of vaccines in preventing infections and controlling epidemics (*41,42*). Study data supports the hypothesis that BCG vaccination is beneficial in reducing the morbidity and mortality of COVID-19. The data supporting this result may be inaccurate due to many confounders such as Polymerase Chain Reaction (PCR) testing rate, population characteristics, and protection strategies. The reliability of this result still needs to be verified by clinical trials (*43*). Vaccine hesitancy remains a challenge to full population inoculation against highly infectious diseases. Concern about the safety of COVID-19 vaccine could contribute to vaccine hesitancy (*44*). The effort of the scientific community in searching for a COVID-19 vaccine may be hampered by a diffused vaccine hesitancy. Some researchers have paid attention to factors that affect vaccine hesitancy, such as race, educational attainment, and whether to receive influenza vaccine (*45*). Cluster 5 that consisted of 5 keywords paid attention to research on vaccine research on herd immunity for public health. COVID-19 vaccines will be essential in the future for reducing morbidity and mortality and inducing herd immunity (*46,47*). In cluster 6, keywords were drug delivery system, nanomedicine, and vaccination. The recent success of mRNA vaccines in SARS-CoV-2 clinical trials is in part due to the development of lipid nanoparticle delivery systems, which not only efficiently express the mRNA-encoded immunogen after intramuscular injection, but also play roles as adjuvants and in vaccine reactogenicity (*48*). The last cluster that consisted of 3 keywords paid attention to research on vaccine production, which is one of the current challenges of COVID-19 vaccine. To sum up, COVID-19 vaccine research hotspots can be classified as clinical trials on vaccine safety and efficacy, research on vaccine immunology and immunoinformatics, the importance of vaccine to public health and vaccine production and delivery.

It is worth noting that two versions of the AstraZeneca/Oxford vaccine, produced by AstraZeneca-SK Bioscience (AZ-SKBio) and the Serum Institute of India (AZ-SII), were approved for emergency use, which were cheaper and easier to distribute than some rivals, including that of Pfizer-BioNTech (*49*). As of 24 February 2021, eight vaccines have been approved for emergency use. Among them, the vaccine named BNT162b2/COMIRNATY Tozinameran, which platform is nucleoside modified mNRA. The platforms of two vaccines that named AZD1222 and Covishield (ChAdOx1_nCoV-19) were Recombinant ChAdOx1 adenoviral vector encoding the spike protein antigen of SARS-CoV-2. The platform of SARS-CoV-2 Vaccine (Vero Cell), Inactivated (lnCoV) and SARS-CoV-2 Vaccine (Vero Cell), inactivated, were produced in Vero cells. The platform of mRNA-1273 is mNRA-based vaccine encapsulated in a lipid nanoparticle. Meanwhile, the Ad26.COV2.S is Recombinant as well as replication-incompetent adenovirus type 26 vectored vaccine encoding the S protein. The last vaccine named Ad5-nCoV platform is Recombinant Novel Coronavirus Vaccine (Adenovirus Type 5 Vector)) (*50*). One widespread concern is adverse events after vaccination. It was reported that severe allergy-like reactions in at least 12 people who received BNT162b2 mRNA Covid-19 Vaccine may be due to a compound in the packaging of the mRNA that forms the vaccine's main ingredient (*51*). A similar mRNA vaccine developed by Moderna, which was authorized for emergency use in the United States, also contains the compound, polyethylene glycol (PEG). Therefore, attention should be paid to adverse reactions when performing large-scale clinical vaccinations. In summary, adverse reactions of vaccines will be other research hotspots.

To be the best of our knowledge, this is the first study to perform bibliometric analysis on COVID-19 vaccine research. To comprehensively capture the current status of research on COVID-19 vaccine, VOSviewer was used to identify the hotspots, cooperation among authors, countries, and institutions in this field. However, this study has some limitations. At first, the data was retrieved from *Embase.com* and MEDLINE. Nevertheless, the amount of data in our analysis is large enough to reflect the current status of COVID-19 vaccine. Second, since some authors have the same short name, some keywords have different expression, bias may still exist, although we have standardized them. At last, our study has been undertaken at the vortex of the epidemic, which may miss the most updated information. Therefore, all the results and conclusions of this study should be interpreted considering these limitations.

5. Conclusion

With the spread of the pandemic, more and more academic papers have been published. It is particularly important to evaluate the quality of such a great number of COVID-19 vaccine research papers and obtain valuable information. The results of bibliometrics show that the top one published journal was the BMJ. The United States and China have played important roles in COVID-19 vaccine research. Simultaneously, there is no doubt that universities have contributed the most publications. COVID-19 vaccine research hotspots are as follows: clinical research on vaccine safety and efficacy, research on vaccine immunology and immunoinformatics, infection prevention and herd immunity, and vaccine delivery and production. Furthermore, we can predict that there will be a lot of research focusing on vaccine adverse reactions. We also revealed that cooperation between countries, institutions,

and authors were insufficient. If the exchanges and cooperation between institutions in various countries are improved from now on, vaccine research of COVID-19 will make a huge breakthrough.

Acknowledgements

The authors thank all investigators and supporters involved in this study.

Funding: This work is supported by Gansu Province Science and Technology Plan Funded Project (Grant No. 20CX4ZA027). The funders had no role in the design and conduct of the study; collection, management, analysis, and interpretation of the data; preparation, review, or approval of the manuscript; and decision to submit the manuscript for publication.

Conflict of Interest: The authors have no conflicts of interest to disclose.

References

1. Polack FP, Thomas SJ, Kitchin N, *et al.* Safety and efficacy of the BNT162b2 mRNA Covid-19 vaccine. N Engl J Med. 2020; 383:2603-2615.
2. Shi Y, Wang G, Cai XP, Deng JW, Zheng L, Zhu HH, Zheng M, Yang B, Chen Z. An overview of COVID-19. J Zhejiang Univ Sci B. 2020; 21:343-360.
3. World Health Organization. Coronavirus disease (COVID-19) pandemic. *https://www.who.int/emergencies/diseases/novel-coronavirus-2019* (accessd December 22, 2020).
4. Clarke L. An introduction to economic studies, health emergencies, and COVID-19. J Evid Based Med. 2020;13:161-167.
5. Cao B, Wang Y, Wen D, *et al.* A trial of lopinavir-ritonavir in adults hospitalized with severe Covid-19. N Engl J Med. 2020; 382:1787-1799.
6. Wang M, Cao R, Zhang L, Yang X, Liu J, Xu M, Shi Z, Hu Z, Zhong W, Xiao G. Remdesivir and chloroquine effectively inhibit the recently emerged novel coronavirus (2019-nCoV) *in vitro*. Cell Res. 2020; 30:269-271.
7. Gao J, Tian Z, Yang X. Breakthrough: Chloroquine phosphate has shown apparent efficacy in treatment of COVID-19 associated pneumonia in clinical studies. Biosci Trends. 2020; 14:72-73.
8. Campos DMO, Fulco UL, de Oliveira CBS, Oliveira JIN. SARS-CoV-2 virus infection: Targets and antiviral pharmacological strategies. J Evid Based Med. 2020; 13:255-260.
9. Twomey JD, Luo S, Dean AQ, Bozza WP, Nalli A, Zhang B. COVID-19 update: The race to therapeutic development. Drug Resist Updat. 2020; 53:100733.
10. Leng Z, Zhu R, Hou W, *et al.* Transplantation of ACE2(-) mesenchymal stem cells improves the outcome of patients with COVID-19 pneumonia. Aging Dis. 2020; 11:216-228.
11. Xing Y, Mo P, Xiao Y, Zhao O, Zhang Y, Wang F. Post-discharge surveillance and positive virus detection in two medical staff recovered from coronavirus disease 2019 (COVID-19), China, January to February 2020. Euro Surveill. 2020; 25:2000191.
12. Ellegaard O, Wallin JA. The bibliometric analysis of scholarly production: How great is the impact? Scientometrics. 2015; 105:1809-1831.
13. Glanville J, Kendrick T, McNally R, Campbell J, Hobbs FD. Research output on primary care in Australia, Canada, Germany, the Netherlands, the United Kingdom, and the United States: bibliometric analysis. BMJ. 2011; 342:d1028.
14. Li G, Lin J, Jiang C, Feng Q, Wen L. Trends in chronic hepatitis B treatment-related research from 1973 to 2018: a bibliometric and visual analysis. J Int Med Res. 2020; 48:300060519893234.
15. Zyoud SH, Smale S, Waring WS, Sweileh WM, Al-Jabi SW. Global research trends in microbiome-gut-brain axis during 2009-2018: a bibliometric and visualized study. BMC Gastroenterol. 2019; 19:158.
16. Bornmann L, Leydesdorff L. Scientometrics in a changing research landscape: bibliometrics has become an integral part of research quality evaluation and has been changing the practice of research. EMBO Rep. 2014; 15:1228-1232.
17. Qiu Y, Yang W, Wang Q, Yan S, Li B, Zhai X. Osteoporosis in postmenopausal women in this decade: a bibliometric assessment of current research and future hotspots. Arch Osteoporos. 2018; 13:121.
18. Fan J, Gao Y, Zhao N, Dai R, Zhang H, Feng X, Shi G, Tian J, Chen C, Hambly BD, Bao S. Bibliometric analysis on COVID-19: a comparison of research between English and Chinese studies. Front Public Health. 2020; 8:477.
19. Mao X, Guo L, Fu P, Xiang C. The status and trends of coronavirus research: A global bibliometric and visualized analysis. Medicine (Baltimore). 2020; 99:e20137.
20. Yu Y, Li Y, Zhang Z, Gu Z, Zhong H, Zha Q, Yang L, Zhu C, Chen E. A bibliometric analysis using VOSviewer of publications on COVID-19. Ann Transl Med. 2020; 8:816.
21. van Eck NJ, Waltman L. Software survey: VOSviewer, a computer program for bibliometric mapping. Scientometrics. 2010; 84:523-538.
22. Farzanegan R, Feizabadi M, Ghorbani F, Movassaghi M, Vaziri E, Zangi M, Lajevardi S, Shadmehr MB. An overview of tracheal stenosis research trends and hot topics. Arch Iran Med. 2017; 20:598-607.
23. Romero L, Portillo-Salido E. Trends in sigma-1 receptor research: a 25-year bibliometric analysis. Front Pharmacol. 2019; 10:564.
24. Gao Y, Ge L, Shi S, Sun Y, Liu M, Wang B, Shang Y, Wu J, Tian J. Global trends and future prospects of e-waste research: a bibliometric analysis. Environ Sci Pollut Res Int. 2019; 26:17809-17820.
25. Shi S, Gao Y, Liu M, Bu Y, Wu J, Tian J, Zhang J. Top 100 most-cited articles on exosomes in the field of cancer: a bibliometric analysis and evidence mapping. Clin Exp Med. 2020. doi: 10.1007/s10238-020-00624-5.
26. Whitehead CL, Walker SP. Consider pregnancy in COVID-19 therapeutic drug and vaccine trials. Lancet. 2020; 395:e92.
27. Hotez PJ, Corry DB, Bottazzi ME. COVID-19 vaccine design: the Janus face of immune enhancement. Nat Rev Immunol. 2020; 20:347-348.
28. Thanh Le T, Andreadakis Z, Kumar A, Gómez Román R, Tollefsen S, Saville M, Mayhew S. The COVID-19 vaccine development landscape. Nat Rev Drug Discov. 2020; 19:305-306.
29. Heaton PM. The Covid-19 vaccine-development multiverse. N Engl J Med. 2020; 383:1986-1988.

30. Tao Z, Zhou S, Yao R, Wen K, Da W, Meng Y, Yang K, Liu H, Tao L. COVID-19 will stimulate a new coronavirus research breakthrough: a 20-year bibliometric analysis. Ann Transl Med. 2020; 8:528.
31. Liang YD, Li Y, Zhao J, Wang XY, Zhu HZ, Chen XH. Study of acupuncture for low back pain in recent 20 years: a bibliometric analysis *via* CiteSpace. J Pain Res. 2017; 10:951-964.
32. World Health Organization. COVID-19 vaccines. *https://www.who.int/emergencies/diseases/novel-coronavirus-2019/covid-19-vaccines* (accessd December 26, 2020).
33. Jamrozik E, Selgelid MJ. COVID-19 human challenge studies: ethical issues. Lancet Infect Dis. 2020; 20:e198-e203.
34. Wibawa T. COVID-19 vaccine research and development: ethical issues. Trop Med Int Health. 2021; 26:14-19.
35. Wendler D, Ochoa J, Millum J, Grady C, Taylor HA. COVID-19 vaccine trial ethics once we have efficacious vaccines. Science. 2020; 370:1277-1279.
36. Calina D, Hartung T, Docea AO, Spandidos DA, Egorov AM, Shtilman MI, Carvalho F, Tsatsakis A. COVID-19 vaccines: ethical framework concerning human challenge studies. Daru. 2020; 28:807-812.
37. Ma X, Wang Y, Gao T, He Q, He Y, Yue R, You F, Tang J. Challenges and strategies to research ethics in conducting COVID-19 research. J Evid Based Med. 2020; 13:173-177.
38. Bos R, Rutten L, van der Lubbe JEM, *et al.* Ad26 vector-based COVID-19 vaccine encoding a prefusion-stabilized SARS-CoV-2 Spike immunogen induces potent humoral and cellular immune responses. NPJ Vaccines. 2020; 5:91.
39. Chi X, Yan R, Zhang J, *et al.* A neutralizing human antibody binds to the N-terminal domain of the Spike protein of SARS-CoV-2. Science. 2020; 369:650-655.
40. Dong R, Chu Z, Yu F, Zha Y. Contriving multi-epitope subunit of vaccine for COVID-19: immunoinformatics approaches. Front Immunol. 2020; 11:1784.
41. Lotfi M, Hamblin MR, Rezaei N. COVID-19: Transmission, prevention, and potential therapeutic opportunities. Clin Chim Acta. 2020; 508:254-266.
42. Yang L, Tian D, Liu W. Strategies for vaccine development of COVID-19. Sheng Wu Gong Cheng Xue Bao. 2020; 36:593-604.
43. Gong W, Wu X. Is the tuberculosis vaccine BCG an alternative weapon for developing countries to defeat COVID-19? Indian J Tuberc. 2020; doi: 10.1016/j.ijtb.2020.10.012.
44. Dror AA, Eisenbach N, Taiber S, Morozov NG, Mizrachi M, Zigron A, Srouji S, Sela E. Vaccine hesitancy: the next challenge in the fight against COVID-19. Eur J Epidemiol. 2020; 35:775-779.
45. Fisher KA, Bloomstone SJ, Walder J, Crawford S, Fouayzi H, Mazor KM. Attitudes toward a potential SARS-CoV-2 vaccine : a survey of U.S. adults. Ann Intern Med. 2020; 173:964-973.
46. Lee L, Peterson GM, Naunton M, Jackson S, Bushell M. Protecting the herd: why pharmacists matter in mass vaccination. Pharmacy (Basel). 2020; 8:199.
47. Frederiksen LSF, Zhang Y, Foged C, Thakur A. The long road toward COVID-19 herd immunity: vaccine platform technologies and mass immunization strategies. Front Immunol. 2020; 11:1817.
48. Buschmann MD, Carrasco MJ, Alishetty S, Paige M, Alameh MG, Weissman D. Nanomaterial delivery systems for mRNA vaccines. Vaccines (Basel). 2021; 9:65.
49. World Health Organization. COVAX statement on WHO emergency use listing for AstraZeneca/Oxford COVID-19 vaccine. *https://www.who.int/news/item/16-02-2021-covax-statement-on-who-emergency-use-listing-for-astrazeneca-oxford-covid-19-vaccine* (Access February 16, 2021).
50. World Health Organization. Status of COVID-19 vaccines within WHO EUL/PQ evaluation process. *https://extranet.who.int/pqweb/sites/default/files/documents/Status_COVID_VAX_24Feb2021.pdf* (Access February 24, 2021).
51. de Vrieze J. Pfizer's vaccine raises allergy concerns. Science. 2021; 371:10-11.

Received February 6, 2021; Revised March 8, 2021; Accepted March 12, 2021.

[§]These authors contributed equally to this work.
**Address correspondence to:*
Jinhui Tian, Evidence-Based Medicine Centre, School of Basic Medical Sciences, Lanzhou University, No.199, Donggang West Road, Lanzhou 730000, Gansu, China.
E-mail: tianjh@lzu.edu.cn

Released online in J-STAGE as advance publication March 19, 2021.

Review

DOI: 10.5582/bst.2021.01041

The role of Toll-like receptors in neurobiology of alcoholism

Marat Airapetov[1,2,*], Sergei Eresko[1,3], Andrei Lebedev[1], Evgenii Bychkov[1], Petr Shabanov[1,4]

[1] Department of Neuropharmacology, Institute of Experimental Medicine, St. Petersburg, Russia;
[2] Department of Pharmacology, St. Petersburg State Pediatric Medical University, St. Petersburg, Russia;
[3] Research and Education Center for Molecular and Cellular Technologies, St. Petersburg State Chemical Pharmaceutical University, St Petersburg, Russia;
[4] Department of Pharmacology, Kirov Military Medical Academy, St. Petersburg, Russia.

SUMMARY Alcoholism is a global socially significant problem and still remains one of the leading causes of disability and premature death. One of the main signs of the disease is the loss of cognitive control over the amount of alcohol consumed. Among the mechanisms of the development of this pathology, changes in neuroimmune mechanisms occurring in the brain during prolonged alcohol consumption and its withdrawal have recently become the focus of numerous studies. Ethanol consumption leads to the activation of neuroimmune signaling in the central nervous system through many subtypes of Toll-like receptors (TLRs), as well as release of their endogenous agonists (high-mobility group protein B1 (HMGB1), S100 protein, heat shock proteins (HSPs), and extracellular matrix degradation proteins). TLR activation triggers intracellular molecular cascades of reactions leading to increased expression of genes of the innate immune system, particularly, proinflammatory cytokines, causing further development of a persistent neuroinflammatory process in the central nervous system. This leads to death of neurons and neuroglial cells in various brain structures, primarily in those associated with the development of a pathological craving for alcohol. In addition, there is evidence that some subtypes of TLRs (TLR3, TLR4) are able to form heterodimers with neuropeptide receptors, thereby possibly playing other roles in the central nervous system, in addition to participating in the activation of the innate immune system.

Keywords alcoholism, brain, neuroinflammation, Toll-like receptors, neuroimmune signaling

1. Introduction

The pathological effect on neuroimmune mechanisms in the brain caused by long-term ethanol consumption has attracted increased interest among researchers over the past two decades. One of the earliest studies in this area was performed by Lewohl *et al.* in 2000 (*1*). Using DNA microarray technology, the authors discovered an unexpected abundance of changes in the genes of the innate immune system in postmortem samples of the cerebral cortex of people with alcoholism (*1*). The very first experimental data showing that long-term ethanol consumption can activate the innate immune system in the central nervous system, promoting the production of pro-inflammatory cytokines and the death of nerve cells, were published by Valles *et al.* in 2004 (*2*). These results have been repeatedly confirmed and expanded in subsequent studies (*3*-*8*).

Impairments in the coordinated work of mechanisms at the cellular and molecular levels in various structures of the brain induced by prolonged use of ethanol lead to serious consequences such as emotional disorders (increased levels of anxiety and anxiety, deterioration in attention, aggression) and, worst of all, loss of cognitive control over the amount of alcohol consumed. These signs serve as criteria for the transition from the abuse of alcoholic beverages (drunkenness) to the formation of a complex and incurable mental illness, alcohol dependence (*9*-*14*).

For our review, we use the term "alcoholism" to mean a human disease, whereas "long-term ethanol consumption" is modeling of alcoholism in animals.

Long-term ethanol consumption leads to activation of microglial cells in the brain (*15*). Microglial activation is characterized by small morphological changes and increased expression of signaling molecules involved in the immune response (components of the major histocompatibility complex, Toll-like receptors (TLRs), and pro/anti-inflammatory cytokines) (*16*). In the brain, microglial cells, being resident macrophages in the central nervous system, express diverse receptors of the innate immune system, particularly members of

the TLR superfamily. The latter plays an important role in triggering the inflammatory response to various pathogens (*17,18*).

TLRs are activated by exogenous or PAMP (pathogen-associated molecular pattern; molecular fragments associated with pathogens) ligands, as well as by endogenous or DAMP (damage-associated molecular-pattern) ligands; their level increased in the brain during prolonged use of ethanol (*4*). Animal experiments have shown that the use of ethanol leads to increased expression and extracellular release of an endogenous ligand, HMGB1 protein (High-mobility group protein B1) (*4*). The interaction of the ligand with TLRs is a signal that triggers complex intracellular cascades of reactions, activating transcription factors NF-κB (nuclear factor kappa-light-chain-enhancer of activated B cells), AP-1 (activator protein 1), and IRFs (interferon regulatory factors). This leads to a subsequent increase in expression of genes encoding various pro-inflammatory signaling molecules (pro-inflammatory cytokines, oxidases, nitric oxide synthase, proteases, and components of the major histocompatibility complex) (*3-7,18-21*). It should be noted that an increase in the level of pro-inflammatory cytokines correlates with an increase in the level of expression of certain subtypes of TLRs in the central nervous system (TLR2, TLR3, TLR4, TLR7) (*3-7*). These changes cause the development of a long-term neurotoxic effect, which further leads to proteasomal degradation of proteins, demyelination of axons, destruction of synaptic terminals due to damage of synaptic proteins and, ultimately, to the death of many cells in the central nervous system. Neurodegenerative changes in all parts of the brain of patients with alcoholism are a consequence of the neurotoxic effect of ethanol on the brain (*3,22-25*).

Besides microglia, neurons and neuroglial cells are able to respond to the pro-inflammatory factors of the immune system by expressing many different cytokine receptors such as TNFαR, IL-1βR, IL-6R (CD126), IFNγR, and IFNαR. Fractalin (also known as CX3CL), a protein secreted by nerve cells in the brain, is involved in the regulation of the migration of microglial cells in the central nervous system (*18,26*).

Microglial cells are considered a major component of the immune system in the central nervous system (CNS). However, accumulating evidence suggests that astrocytes serve as important effector cells and regulators of the local immunity in pathophysiological conditions due to expression of a wide spectrum of molecules involved in the innate or adaptive immune response, secretion of cytokines and complement components, and differential response to various stimuli inducing either the innate or adaptive immune response. Moreover, ethanol can alter the function of CNS glial cells including microglia and astrocytes which normally maintain homeostasis in the CNS (*27,28*).

Astrocytes are the major glial cell type in the CNS and can also express TLR2-3 and TLR9 (*17*). Based on this, it is assumed that the effect of ethanol/ethanol metabolites on astrocytes can also be mediated through the TLR; but this assumption requires further research.

Thus, the release of pro-inflammatory cytokines can lead to the activation of an increasing number of microglial cells, as well as astrocytes, oligodendrocytes and neurons, enhancing the mechanisms of neuroimmune signaling (*2,29-31*).

This review work summarizes the results of studies that bear compelling evidence about TLR-signaling that changes in the brain when using ethanol, and that many types of brain cells are involved in this process due to the fact that different subtypes of TLR-receptors are localized on different types of nervous system cells. There is still no complete understanding of the ultimate cause that starts these changes when ethanol is consumed. It is anticipated that endogenous TLR agonists are essential to this process, because they are secreted during ethanol consumption. Such agonists, for example, include HMGB1, heat shock proteins, uric acid, microRNA (*6,32*).

The research results of recent studies bring out clearly that TLR overexpression mediates the development of a neurotoxic effect in the CNS when ethanol is used. Possibly, TLR signaling contributes to the regulation of functional activity of neurotransmitter systems, which can contribute to the formation of pathological alcohol craving. Disturbances in the coordinated operation of neuroimmune signaling mechanisms in various brain structures as a result of ethanol use may result in consequences such as emotional disrepairs (increased anxiety level, impaired concentration, aggression) and reduced cognitive control over the amount of alcohol consumed. These signs serve as criteria for change from abusive drinking behavior to the formation of a complex and incurable mental illness – alcoholism (*5,6*).

2. Toll-like receptors (TLRs)

During the last decade a large number of pattern recognition receptors (PRRs) have been discovered and intensively studied. They have been found in all multicellular organisms, ranging from invertebrates (*e.g.*, sponges) to mammals, including humans (*18*). To date, 5 families of signaling PRRs are known: Toll-like receptors (TLRs), C-type lectin receptors, scavenger receptors, Nucleotide-binding and oligomerization domain-like receptors (NLRs), and CARD (Caspase recruitment domain) helicases (*18*). All PRRs bind specifically to various molecular structures of microorganisms, including bacteria, fungi, viruses, and unicellular protozoa. PRRs specifically react to a number of plant substances and complex synthetic molecules. All these compounds serve as exogenous ligands of PRRs. PRRs can also respond to a number of substances from their own body, endogenous ligands (*18*).

TLRs represent the best studied family. In humans, 10 representatives have been found, while mice have of 13 representatives of this family (TLR1-TLR13) (*18,33*). All TLRs share a similar structure: they are integral transmembrane proteins, consisting of 3 parts that differ in their functions. The extracellular N-terminal region, responsible for ligand binding, has 19-25 leucine-rich repeats. This is followed by a cysteine-rich transition region, which is responsible for the attachment of the receptor to membrane proteins. Finally, the cytoplasmic region, represents the TIR domain (Toll / IL-1 receptor), which interacts with TLRs and adapter proteins, triggering intracellular signaling cascades (*18*) (Table 1).

Table 1. TLR adaptor proteins (modified from (*53*))

Receptor	Adaptor protein
TLR2/TLR1 (heterodimer)	Myd88/TIRAP
TLR3	TRIF
TLR4	Myd88/TIRAP; TRIF/TRAM
TLR2/TLR6 (heterodimer)	Myd88/TIRAP
TLR7	Myd88
TLR8	Myd88
TLR9	Myd88
TLR11/TLR12 (heterodimer)	Myd88
TLR13	Myd88

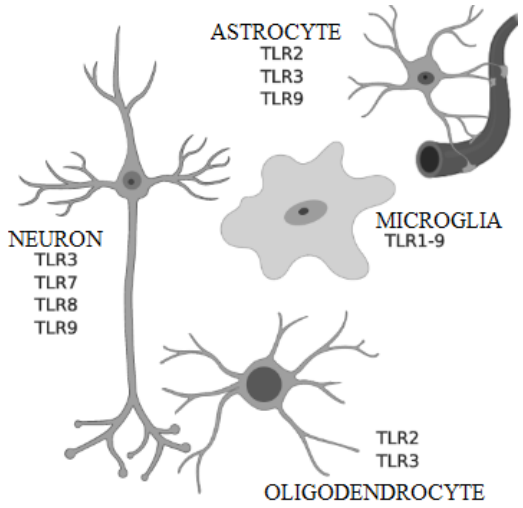

Figure 1. Expression of TLRs in cells of the central nervous system.

All subtypes of TLRs are expressed in the central nervous system: TLR1-TLR9 are expressed by microglial cells, TLR3 and TLR7-9 are expressed by neurons, TLR2-3 and TLR9 are expressed by astrocytes, and TLR2-3 are expressed by oligodendrocytes (*17,34*) (Figure 1).

It is important to note that TLR1-2 and TLR4-6 are expressed on the surface of the cytoplasmic membrane, while TLR3 and TLR7-13 are expressed on endosomes inside the cell (*35,36*).

3. TLR signaling cascades

All TLRs function as homo- or heterodimers: TLR2 forms heterodimers with TLR1 or TLR6, TLR11 forms heterodimers with TLR12, while TLR3-5, TLR7-9, and TLR13 form homodimers (*36*). After ligand recognition (Table 2) TLR undergoes dimerization with formation of a heterodimer or homodimer, followed by conformational changes in the receptor necessary for the interaction of the cytoplasmic TIR domain with intracellular adapter proteins and subsequent activation of the intracellular signaling cascade (*32*).

The most common case includes binding of the TIR receptor domain of TLR to the adapter protein MyD88 (Myeloid differentiation primary response 88) (Figure 2). After that, MyD88 interacts with kinases

Table 2. TLR ligands (summarized using data from (*47-53*))

Receptor	Exogenous ligands	Endogenous ligands
TLR1	Triacetylated peptides	Unknown
TLR2	Zymosan, diacetylated peptides, triacetylated peptides, lipoteichoic acid	rHSP70, gp96, HMGB1, uric acid, hyaluronic acid, -synuclein
TLR3	Double- stranded RNA (dsRNA), poly (I:C)	mRNA, statmin,
TLR4	Lipopolysaccharide (LPS)	HMGB1, HSP60, HSP70, HSP72, hyaluronic acid, fibrinogen, protein S100, uric acid, heparan sulfate fragments, tenascin-C
TLR5	Flagellin	Unknown
TLR6	Zymosan, diacetylated peptides, triacetylated peptides, lipoteichoic acid, lipoarabinoman	Unknown
TLR7	Imiquimod, gardiquimod, single-stranded RNA (ssRNA), miRNAs let-7, microRNA-21, imidazoquinoline, loxoribine, bropyrimin	Unknown
TLR8	Single-stranded RNA (ssRNA), ssRNA40/Lyovec, gardiquimod	Unknown
TLR9	DNA with unmethylated CpG oligodeoxynucleotides	Chromatin-IgG complexes
TLR10*	Double- stranded RNA (dsRNA)	Unknown
TLR11**	Profilin and profilin-like proteins	Unknown
TLR12**	Profilin	Unknown
TLR13**	Single-stranded RNA (ssRNA)	Unknown

*- Found only in humans, **- found only in mice.

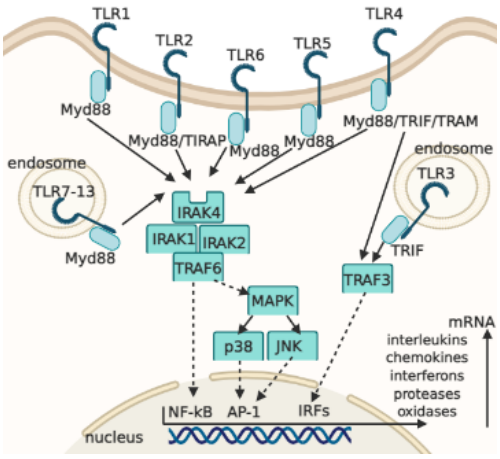

Figure 2. Signaling cascades realizing TLRs effects.

of the IRAK family (IL-1 receptor associated kinase); the family consists of several enzymes: IRAK1-4 and IRAK-M. Initially, IRAK4 is activated, and then IRAK1. Activated IRAK1 interacts with TRAF6 (TNF receptor-associated factor 6). This factor can trigger two signaling pathways including: (*i*) activation of the transcription factor AP-1 by MAP-kinases (mitogen-activated protein kinases), JNK-kinases (c-Jun N-terminal kinases), and p38; (*ii*) activation of the TAK1/TAB (Transforming growth factor-β (TGF-β)-activated kinase 1/ TAK1-binding protein) and IKK (IκB kinase) complex. After IKK activation, the inhibitory protein IκB is phosphorylated and degraded; this leads to release of the NF-κB dimer and its subsequent translocation into the nucleus, where NF-κB binds to the promoter regions of genes that activate and regulate the development of the inflammatory response. This intracellular signaling mechanism functions when almost all known TLRs (with the exception of TLR3) are activated. This indicates that different pathogens that activate different TLRs initiate a common universal pathway for the activation of the inflammatory response (*18*). The Toll/interleukin-1 (IL-1) receptor (TIR) domain of TLR3 and TLR4 can interact with the adapter protein TIR domain containing adapter inducing IFNβ (TRIF) (*37*). The TRIF protein activates TRAF6 (TNF receptor-associated factor 6) and TRAF3 (TNF receptor-associated factor 3). This results in activation of the intracellular factor TBK1 (TANK-binding kinase 1) followed by activation of IRF3 (Interferon regulatory factor 3). Activated IRF3 triggers expression of the IFNα and IFNβ genes required for the development of an antiviral response (*18*).

Other adapter proteins, besides those considered above, required for signal transduction from certain TLRs have been identified. These include TIRAP protein (TIR-domain-containing adapter protein), which together with MyD88 participates in signal transduction from TLR2 and TLR4, but not from other TLRs (*38*). The adapter protein TRAM (TRIF-related adapter molecule), which interacts with TRIF, is used for signal transduction from TLR4 (*39*).

The activation of TLRs triggers several intracellular signaling pathways. This results in activation of complex intracellular cascades, which can cause both the enhancement and inhibition of the final effect of cytokine expression. For example, activation of TLR3 and TLR4 can enhance expression of TLR2 on the surface of macrophages in a Myd88-independent manner, while activation of TLR7 and TLR9 induces its expression in a Myd88-dependent manner (*40*). TLR4 activation can positively regulate TLR2, TLR4, and TLR9 (*39*). Such regulation (TLR-TLR) often leads to an enhancement of the immune response, attracting more TLRs; however, the initial stimulating dose and the activation time of the second TLR involved in the process can have a significant impact on the immune response (*18,40-43*). In addition, different subtypes of TLRs can jointly form a synergistic effect or create feedback with respect to another TLR. Stimulation of a dendritic cell with a TLR2 agonist counteracts the expression of IL10 and IL12, which is initiated by TLR3 and TLR4 agonists. TLR8 inhibits TLR7 and TLR9, while TLR9 inhibits TLR7 as a result of direct or indirect interactions between them (*44*).

4. The role of TLRs in neuroimmune mechanisms of alcoholism development

Ethanol consumption promotes TLR-mediated activation of the innate immune system manifested by increased levels of pro-inflammatory signaling molecules (*7*). Among TLRs involved in the pathogenesis of alcoholism, researchers pay particular attention to TLR3, TLR4, TL7 (*3-7,17, 22,45-48*).

Increased levels of pro-inflammatory cytokines play an important role in the development of neurotoxicity, with the subsequent death of many cells in the central nervous system. Although microglia are considered the main source of pro-inflammatory cytokines in the central nervous system, the role of neurons in the ethanol-induced neuroimmune signaling networks is not fully understood (*26*). The activity of TLRs depends on the level of exogenous and endogenous ligands by which these receptors are activated. Ethanol consumption is accompanied by an increase in the level of endogenous ligands, such as HMGB1 (*7*), heat shock proteins (*49*), proteins involved in extracellular matrix degradation (*50*), and various variants of microRNA (*51-55*). Endogenous ligands are released in response to the activation of the inflammatory process in the brain and during apoptotic cell damage in the central nervous system (*3-7*). Exogenous ligands and various cytokines can be transported by blood to the central nervous system from the periphery (*6*).

5. The role of TLRs in the pathogenesis of alcoholism

5.1. The Role of TLR3 in the pathogenesis of alcoholism

An increased level of TLR3 mRNA was found in postmortem samples of the brain's orbifrontal cortex from patients with alcoholism (*4*). Rodent experiments have shown that TLR3-dependent signaling affects the level of voluntary ethanol consumption (*56,57*). Alcoholization of mice for 10 days increased the brain level of TLR3 mRNA and the expression level of the TLR3 protein in the orbifrontal and entorhinal cortex (*4*).

A single intraperitoneal injection of a TLR3 agonist poly (I:C) (poly-inosine-polycytidylic acid, a synthetic analogue of the viral double-stranded RNA) to mice increased the level of voluntary ethanol consumption in the two-bottle choice test (ethanol solution or water); at the same time, the increase in the level of ethanol consumption developed during several days (*57*).

The study of the poly (I:C) effects on gene expression in the rat brain nucleus accumbens has shown that activation by the TLR3 agonist leads to an increase in the mRNA levels of TLR3, COX2 (cyclooxygenase 2) and genes of the glutamatergic system (mGluR2 - metabotropic glutamate receptor 2; mGluR3; GLT1 - glutamate transporter 1), as well as the BDNF gene (brain-derived neurotrophic factor). Moreover, an increase in the mRNA of each of these genes correlated with an increase in TLR3 mRNA (*58*).

The use of poly (I:C) led to an increase in the expression of a number of pro-inflammatory genes (CCL5, CCL2, IL-1b, IL-6, *etc.*) in the prefrontal cortex of the mouse brain. Under conditions of free access to ethanol (two-bottle choice drinking) during the peak activation of the pro-inflammatory response in the brain, the level of voluntary ethanol consumption by mice decreased and remained unchanged when access to ethanol was provided to mice with descending limb of activation of the innate immune system. These results suggest that a gradual increase in the inflammatory response may indirectly contribute to an increase in alcohol craving in mice. According to the authors (*57*), specific pathways and the balance between cytokines can regulate the level of craving for alcohol.

Using a model of 10-day alcoholization of mice with ethanol, it was shown that a single administration of the TLR3 agonist poly (I:C) resulted in an increase in the TRAIL (TNF-related apoptosis-inducing ligand) mRNA level in the orbitofrontal and entorhinal cortex of the mouse brain (*59*). Treatment of cell cultures with ethanol activated TLR3, which promoted release of IFNβ and IFNγ by neurons and astrocytes. Afterward, addition of poly (I:C) into the cell culture resulted in increased activity of the TRAIL gene. TRAIL blockage *via* neutralizing antibody led to a decrease in the levels of IFNβ and IFNγ in both astrocytes and neurons. The combined effect of ethanol and a TLR3 agonist (poly (I:C)) showed an increase in the levels of TNF-α, IL-1β, and IL-6 mRNA, as well as an increase in the levels of p38 and IRF3 proteins in microglial and neuronal cell cultures (*59*).

TLR3 mRNA and components of the TRIF-dependent pathway were increased in the prefrontal cortex of mice 24 hours after ethanol withdrawal (*56*). Expression of TLR3-related components of the TRIF-dependent pathway increased in the nucleus accumbens, but decreased in the amygdala. In addition, Amlexanox, an inhibitor of the IKKε/TBK1 complex, reduced immune activation of the TRIF-dependent pathway in the brain and decreased ethanol consumption. This suggests that the TRIF-dependent pathway regulates the level of ethanol consumption (*56*).

Decreased activity of the MyD88-dependent pathway correlates with decreased ethanol consumption and increased levels of the TRIF-dependent pathway. To test the mediated action of poly (I:C) *via* MyD88, female Myd88 knockout mice were used and showed that administration of poly (I:C) did not alter alcohol consumption in Myd88 knockouts, indicating that poly (I:C)-induced changes in alcohol consumption depended on the MyD88-dependent pathway (*57*).

Based on the experimental data obtained using various models, it can be concluded that TLR3 plays an important role in the pathogenesis of alcoholism; however, the exact mechanisms of TLR3-dependent signaling remain completely unclear.

5.2. The Role of TLR4 in the Pathogenesis of Alcoholism

In the context of alcoholism, most studies were focused on the involvement of TLR4 in the mechanisms of pro-inflammatory signaling activation as a result of ethanol consumption (*37,60-65*).

A large amount of data was obtained on rats and mice using genetic and pharmacological manipulations (TLR4 knockout and antagonist use); these studies showed that although TLR4 activity did not regulate the level of ethanol consumption, subsequently consumed alcohol influenced TLR4-mediated signaling (*61,62*).

Ethanol consumption by mice for 2 weeks led to the activation of TLR4-dependent pro-inflammatory processes, which were characterized by the activation of MAP kinases and NF-κB, followed by release of COX-2 (Cyclooxygenase 2), iNOS (Inducible nitric oxide synthase), and HMGB1. The development of the inflammatory process under conditions of increased activity of these pro-inflammatory signaling molecules led to demyelination of axons and structural synaptic changes due to the damage to myelin proteins and synaptic proteins. Subsequently, such mice were characterized by impaired parameters in tests of object recognition, passive avoidance, and olfactory behavior (*66*). Knockdown of the TLR4 gene was accompanied by inhibition of the production of pro-inflammatory mediators, blockade of the activation of MAP kinases and NF-κB pathways in astrocytes (*67*). *Tlr4* gene knockout mice were protected from an increase in the concentration of cytokines and chemokines in the brain

caused by prolonged consumption of ethanol (for 5 months), while the presence of a functionally competent *Tlr4* gene led to an increase in the concentration of cytokines (IL-1β, IL-17, TNF-α) and chemokines (MCP-1, MIP-1α, CX3CL1) in the blood and striatum (*39*).

It was shown that ethanol caused accumulation of polyubiquitinated forms of proteins in the cerebral cortex and promoted activation of immunoproteasomes and autophagolysosomes (*48*). Mice lacking TLR4 receptors were protected from such changes induced by ethanol (*64*).

There is evidence that TLR4/MCP-1-mediated signaling in the amygdala and ventral tegmental area (VTA) predisposes rats to increased ethanol consumption. This signaling is supported by increased expression of corticotropin-releasing factor (CRF), which is capable of downregulating TLR4 (*61*). In addition, there is evidence that the level of MCP-1, with a simultaneous increase in the level of microglia activity, was increased in the VTA, amygdala, substantia nigra, and hippocampus of postmortem brain samples from patients with alcoholism (*68*).

It is suggested that TLR4-MyD88-dependent signaling mediates acute depressive disorders, which develop after ethanol consumption, and may also be involved in the regulation of GABAergic transmission in the central nervous system (*61*). TLR4 gene knockdown rats had a decreased level of voluntary alcohol consumption (*60*). It is suggested that this was associated with a decrease in the expression of the GABAA a2 subunit in the amygdala (*60*). Intraperitoneal administration of the TLR4 ligand, LPS (lipopolysaccharide), accelerated the development of anxious behavior in animals subsequently exposed to ethanol (*69*). Mice lacking TLR4 or MyD88 became less sensitive to the sedative and intoxicating effects of ethanol, while mice lacking TLR2 did not differ from control mice in these tests (*69*).

These data suggest that TLR4 may indirectly interact with neurotransmitter receptors (or other targets), thereby indirectly regulating the level of ethanol consumption.

5.3. The Role of TLR7 in the Pathogenesis of Alcoholism

In addition to the above described studies on TLR3 and TLR4, there are a small number of studies aimed at studying TLR7 in the pathogenesis of alcoholism. For example, TLR7 expression was higher in the hippocampus of postmortem human brain samples (*47*). There is evidence that ethanol induces secretion of the TLR7 agonist (miRNA let-7b), which leads to TLR7-mediated activation of neurodegenerative processes in the central nervous system (*47*). The effect of ethanol on TLR7 and let-7b was studied in a cultured section of the hippocampal-entorhinal cortex of rats: the tissue of the alcoholized hippocampus was characterized by increased expression of TLR7 (*47*). In addition, it was found that ethanol induced formation of HMGB1-miR-let-7 complexes in microvesicles, which induced the development of a neurotoxic effect through TLR7 activation (*47*). Ethanol causes an increase in TLR7 expression and release of let-7b and HMGB1 from microglia. Inhibition of HMGB1 by glycyrrhizin prevented the development of neurotoxicity (*47*).

Findings obtained in one of the recent research papers attest to the fact that TLR7 may serve as one of their potential targets during development of treatment therapy options for alcoholism. The chemical mixture imidazoquinoline R848 and protagonist TLR7 used in the work, lead to a decrease in ethanol absorption with single dosing to Kunming mice, but prolonged activation of TLR7 lead to an increase in ethanol absorption. It is anticipated that these effects are associated with molecular non-responsiveness of intracellular signaling cascades and with the fact that the access time connected with signaling of constitutive immunity plays an important role in regulating ethanol absorption behavior. In addition, there is available evidence in favor of the fact that the peak of neuroimmune response is crucial for ethanol consumption-related behavior. The peak immune activation response results in reduced ethanol consumption, but ethanol consumption increases several hours or days after immune system activation. There are some suggestions that IRF7 and the genes regulated by it in this case may become potential targets for correcting ethanol consumption behavior, since Irf7 is the only gene that was activated after 24 hours following both a single dose of R848 (the TLR7 protagonist) and repeated injection of R848 (*70*).

Our laboratory also obtained information regarding the proportion of mRNA TLR7 in various cerebral structures of rats after alcoholization with a 20% ethanol solution during 1 month. In the group of prolonged alcoholization, there were no changes in mRNA levels in any of the brain structures that we studied. However, during the period of alcohol cessation, on the 1st day, there was an increased level of TLR7 mRNA in the hippocampus and amygdala and a decrease in the striatum. This data once more emphasizes the fact that the TLR7 mRNA level can have multidirectional changes not only in different cerebral structures, but also during different conditions of the organism. Alcohol ingestion and cessation of alcohol at different times serves as the reason for multidirectional changes in the proportion of TLR7 mRNA. It is important to consider this when searching for targets and choosing the date for beginning pharmaceutical correction of alcoholism (*10*).

6. Conclusions

Over the past 20 years, research on the role of TLRs in the pathogenesis of alcoholism has been focused mainly on two subtypes of TLRs; TLR3 and TLR4. Several

studies have investigated the role of TLR7. Attention was mainly paid to the analysis of the expression of these receptors, as well as the components involved in intracellular signaling (mainly at the mRNA level), mediated by the interaction of TLRs with their specific ligands. Most of the work was carried out on cell cultures and mice exposed to various models of alcohol intoxication. The results presented in these works convincingly show that TLRs mediate the development of a neurotoxic effect in the central nervous system when ethanol is consumed. Moreover, TLR signaling not only contributes to the development of the neuroinflammatory process in the brain, but is probably also involved in the mechanisms of regulation of the functional activity of neurotransmitter systems, which may contribute to the formation of a pathological craving for alcohol. However, it would be interesting to study how the TLR signaling components change during alcohol withdrawal at different withdrawal periods and how long in this case the neuroinflammatory process in the central nervous system, mediated by TLRs, persists. The level of cytokine expression at the protein level in the brain in pathological conditions caused by exposure to ethanol needs detailed investigation. It would also be interesting to investigate how the expression level of TLRs and components of intracellular signaling change in various brain structures that are primarily involved in changes in the course of alcohol intoxication. Understanding the intracellular mechanisms mediated by TLR activation may open up new targets for the development of effective drugs for the treatment of alcoholism.

Funding: The study was financed from the budget of Institute of Experimental Medicine (state assignment Pharmacological analysis of the action of neurotropic agents, the study of intracellular targets and the creation of targeted delivery systems», no. 0557-2019-0004) and Saint-Petersburg State Pediatric Medical University.

Conflict of Interest: The authors have no conflicts of interest to disclose.

References

1. Lewohl JM, Wang L, Miles MF, Zhang L, Dodd PR, Harris RA. Gene expression in human alcoholism: Microarray analysis of frontal cortex. Alcohol Clin Exp Res. 2000; 24:1873-1882.
2. Valles SL, Blanco AM, Pascual M, Guerri C. Chronic ethanol treatment enhances inflammatory mediators and cell death in the brain and in astrocytes. Brain Pathol. 2004; 14:365-371.
3. Crews FT, Zou J, Qin L. Induction of innate immune genes in brain create the neurobiology of addiction. Brain Behav Immun. 2011; 25:S4-S12.
4. Crews FT, Qin L, Sheedy D, Vetreno RP, Zou J. HMGB1/TLR receptor danger signaling increases brain neuroimmune activation in alcohol dependence. Biol Psychiatry. 2013; 73: 602-612.
5. Crews FT, Vetreno RP. Neuroimmune basis of alcoholic brain damage. Int Rev Neurobiol. 2014; 118:315-357.
6. Crews FT, Lawrimore CJ, Walter TJ, Coleman LG. The role of neuroimmune signaling in alcoholism. Neuropharmacology. 2017; 122:56-73.
7. Crews FT, Walter TJ, Coleman LG, Vetreno RP. Toll-like receptor signaling and stages of addiction. Psychopharmacology (Berl). 2017; 234:1483-1498.
8. Vetreno RP, Crews FT. Alcohol and the Nervous System. Handbook of Clinical Neurology. (Aminoff MJ, Boller F, Swaab DF). Elsevier Amsterdam, Netherlands 2014; pp. 477-497.
9. Airapetov MI, Sexte EA, Eresko SO, Bychkov ER, Lebedev AA, Shabanov PD. Chronic alcoholism influences the mRNA level of the orexin receptor type 1 (OX1R) in emotiogenic structures of the rat brain. Biomed Khim. 2018; 64:451-454.
10. Airapetov MI, Eresko SO, Bychkov ER, Lebedev AA, Shabanov PD. Expression of Toll-like receptors in emotiogenic structures of rat brain is changed under longterm alcohol consumption and ethanol withdrawal. Medical Immunology. 2020; 22:77-86.
11. Eryshev OF, Rybakova TG, Shabanov PD. Alcohol Dependence: Formation, Course, Anti-Relapse Therapy. Elby-SPb, St. Petersburg, Russia, 2002. pp. 20-45. (in Russian)
12. Shabanov PD, Kalishevich SY. Biology of Alcoholism. Lan', St. Petersburg, Russia, 1998. pp. 35-58. (in Russian)
13. Shabanov PD, Lebedev AA, Streltsov VF. Hormonal mechanisms of reinforcement. Elby-SPb, St. Petersburg, Russia, 2008. pp. 10-58. (in Russian)
14. Becker, H.C., Alcohol and the Nervous System. Handbook of Clinical Neurology. (Aminoff MJ, Boller F, Swaab DF). Elsevier Amsterdam, Netherlands 2014, pp. 133-156.
15. Walter TJ, Vetreno RP, Crews FT. Alcohol and Stress Activation of Microglia and Neurons: Brain Regional Effects. Alcohol Clin Exp Res., 2017; 41:2066-2081.
16. Graeber MB, Li W, Rodriguez ML. Role of microglia in CNS inflammation. FEBS Lett. 2011; 585:3798-3805.
17. Hanke ML, Kielian T. Toll-like receptors in health and disease in the brain: mechanisms and therapeutic potential. Clin Sci (Lond). 2011; 121:367-387.
18. Lebedev KA, Ponyakina ID. Immunology of Image Recognizing Receptors. Lenand Moscow Russia, 2017. pp. 10-55. (in Russian)
19. Crews FT, Braun CJ, Hoplight B, Switzer RC, Knapp DJ. Binge ethanol consumption causes differential brain damage in young adolescent rats compared with adult rats. Alcohol Clin Exp Res. 2000; 24:1712-1723.
20. Zou J, Crews F. Induction of innate immune gene expression cascades in brain slice cultures by ethanol: key role of NF-κB and proinflammatory cytokines. Alcohol Clin Exp Res. 2010; 34:777-789.
21. Zou J, Crews FT. Inflammasome-IL-1β signaling mediates ethanol inhibition of hippocampal neurogenesis. Front Neurosci. 2012; 6:77.
22. Qin L, Crews FT. Chronic ethanol increases systemic TLR3 agonist-induced neuroinflammation and neurodegeneration. J Neuroinflammation. 2012; 9:130.
23. Blednov YA, Benavidez JM, Geil C, Perra S, Morikawa H, Harris RA. Activation of inflammatory signaling by lipopolysaccharide produces a prolonged increase of voluntary alcohol intake in mice. Brain Behav Immun. 2011; 25:S92-S105.
24. Qin L, He J, Hanes R, Pluzarev O, Hong J, Crews FT.

Increased systemic and brain cytokine production and neuroinflammation by endotoxin following ethanol treatment. J Neuroinflammation. 2008; 5:10.
25. Qin L, Liu Y, Hong JS, Crews FT. NADPH oxidase and aging drive microglial activation, oxidative stress, and dopaminergic neurodegeneration following systemic LPS administration. Glia. 2013; 61:855-868.
26. Lawrimore CJ, Crews FT. Ethanol, TLR3, and TLR4 agonists have unique innate immune responses in neuron-like SH-SY5Y and microglia-like BV2. Alcohol Clin Exp Res. 2017; 41:939-954.
27. Kane CJM, Drew PD. Neuroinflammatory contribution of microglia and astrocytes in fetal alcohol spectrum disorders. *https://publons.com/publon/10.1002/jnr.24735* (accessed February 22, 2021).
28. Linnerbauer M, Wheeler MA, Quintana FJ. Astrocyte crosstalk in CNS inflammation. Neuron. 2020; 108:608-622.
29. Alfonso-Loeches S, Guerri C. Molecular and behavioral aspects of the actions of alcohol on the adult and developing brain. Crit Rev Clin Lab Sci. 2011; 48:19-47.
30. Fernandez-Lizarbe S, Pascual M, Guerri C. Critical role of TLR4 response in the activation of microglia induced by ethanol. J Immunol. 2009; 183:4733-4744.
31. Pascual M, Balino P, Alfonso-Loeches S, Aragon CM, Guerri C. Impact of TLR4 on behavioral and cognitive dysfunctions associated with alcohol-induced neuroinflammatory damage. Brain Behav Immun. 2011; 25:S80-S91.
32. Akira S, Takeda K. Toll-like receptor signalling. Nat Rev Immunol. 2004; 4:499-511.
33. Yamamoto M, Sato S, Mori K, Hoshino K, Takeuchi O, Takeda K, Akira S. Cutting edge: a novel Toll/IL-1 receptor domain-containing adapter that preferentially activates the IFN-beta promoter in the Toll-like receptor signaling. J Immunol. 2002; 169:6668-6672.
34. Esen N., Kielian T. Toll-like receptors in brain abscess. Curr Top Microbiol Immunol. 2009; 336:41-61.
35. Leifer CA, Medvedev AE. Molecular mechanisms of regulation of Toll-like receptor signaling. J Leukoc Biol. 2016; 100:927-941.
36. Nie L, Cai SY, Shao JZ, Chen J. Toll-like receptors, associated biological roles, and signaling networks in non-mammals. Front Immunol. 2018; 9:1523.
37. Smith KM, Eaton AD, Finlayson LM, Garside P. Oral tolerance. Am J Respir Crit Care Med. 2000; 162:S175-S178.
38. Sinch-Jasuja H, Hilf N, Arnold-Schild D, Schild H. Biol Chem. The role of heat shock proteins and their receptors in the activation of the immune system. 2001; 382:629-639.
39. Fitzgerald K, Rowe D, Barnes B, Caffrey DR, Visintin A, Latz E, Monk B, Pitha PM, Golenbock DT. LPS-TLR4 signaling to IRF-3/7 and NF-kappaB involves the toll adapters TRAM and TRIF. J Exp Med. 2003; 198:1043-1055.
40. Nilsen N, Nonstad U, Klan N, Knetter CF, Akira S, Sundan A, Espevik T, Lienl E. Lipopolysaccharide and double-stranded RNA up-regulate toll-like receptor 2 independently of myeloid differentiation factor 88. J Biol Chem. 2004; 279:39727-39735.
41. An H, Zhao W, Hou J, Zhang Y, Xie Y, Zheng Y, Xu H, Qian C, Zhou J, Yu Y, Liu S, Feng G, Cao X. SHP-2 phosphatase negatively regulates the TRIF adaptor protein-dependent type I interferon and proinflammatory cytokine production. Immunity. 2006; 25:919-928.
42. Lee MC, Kim YJ. Signaling pathways downstream of pattern-recognition receptors and their cross talk. Annu Rev Biochem. 2007; 76:447-480.
43. Napolitani G, Rnaldi A, Bertoni F. Selected Toll-like receptor agonist combinations synergistically trigger a T helper type 1-polarizing program in dendritic cells. Nat Immunol. 2005; 6:769-776.
44. Wang J, Shao Y, Benett TA, Shankar RA, Wightman PD, Reddy LG. The functional effects of physical interactions among Toll-like receptors 7, 8, and 9. J Biol Chem. 2006; 281:37427-37434.
45. Vabulas RM, Wagner H, Schild H. Heat shock proteins as ligands of toll-like receptors. Curr Top Microbiol Immunol. 2002; 270:169-184.
46. Okun E, Griffioen KJ, Lathia JD, Tang SC, Mattson MP, Arumugam TV. Toll-like receptors in neurodegeneration. Brain Res Rev. 2009; 59:278-292.
47. Coleman LG, Zou J, Crews FT. Microglial-derived miRNA let-7 and HMGB1 contribute to ethanol-induced neurotoxicity *via* TLR7. J Neuroinflammation. 2017; 14:22.
48. Pascual M, Baliño P, Aragón CMG, Guerri C. Cytokines and chemokines as biomarkers of ethanol-induced neuroinflammation and anxiety-related behavior: role of TLR4 and TLR2. Neuropharmacology. 2015; 89:352-359.
49. Qin L, Wu X, Block ML, Liu Y, Breese GR, Hong JS, Knapp DJ, Crews FT. Systemic LPS causes chronic neuroinflammation and progressive neurodegeneration. Glia. 2007; 55:453-462.
50. Koval'chuk LV, Khoreva MV, Varivoda AS. Congenital components of immunity: Toll-like receptors in the normal state and in immunopathology. Zh Mikrobiol Epidemiol Immunobiol. 2005; 4:96-104. (in Russian)
51. Volkov MY. Role of Toll-like receptors and their endogenous ligands in the pathogenesis of rheumatoid arthritis: a review of literature. Rheumatology Science and Practice. 2016; 54:78-85.
52. Takagi M, Takakubo Y, Pajarinen J, Naganuma Y, Oki H, Maruyama M, Goodman SB. Danger of frustrated sensors: Role of Toll-like receptors and NOD-like receptors in aseptic and septic inflammations around total hip replacements. J Orthop Translat. 2017; 10:68-85.
53. Jang TH, Badri Narayanan K, Ho Park H. *In vitro* reconstitution of the Toll/Interleukin-1 receptor (TIR) domain complex between TLR5/6 and Myd88. Protein Pept Lett. 2015; 23:55-62.
54. Murphy K, Weaver C. Janeway's Immunobiology. 9th Edition. Garland Science. New York. USA. 2017. pp. 60-80.
55. Scheibner KA, Lutz MA, Boodoo S, Fenton MJ, Powell JD, Horton MR. Hyaluronan fragments act as an endogenous danger signal by engaging TLR2. J Immunol. 2006; 177:1272-1281.
56. McCarthy GM, Warden AS, Bridges CR, Blednov YA, Harris RA. Chronic ethanol consumption: role of TLR3/TRIF-dependent signaling. Addict Biol. 2018; 23:889-903.
57. Warden AS, Azzam M, DaCosta A, Mason S, Blednov YA, Messing RO, Harris RA. Toll-like receptor 3 dynamics in female C57BL/6J mice: Regulation of alcohol intake. Brain Behav Immun. 2019; 77:66-76.
58. Randall PA, Vetreno RP, Makhijani VH, Crews FT, Besheer J. The Toll-like receptor 3 agonist poly(I:C)

induces rapid and lasting changes in gene expression related to glutamatergic function and increases ethanol self-administration in rats. Alcohol Clin Exp Res. 2019; 43:48-60.
59. Lawrimore CJ, Coleman LG, Crews FT. Ethanol induces interferon expression in neurons *via* TRAIL: role of astrocyte-to-neuron signaling. Psychopharmacology (Berl). 2019; 236:2881-2897.
60. Liu J, Yang AR, Kelly T, Puche A, Esoga C, June HL, Aurelian L. Binge alcohol drinking is associated with GABAA alpha2-regulated Toll-like receptor 4 (TLR4) expression in the central amygdala. Proc Natl Acad Sci U S A. 2011; 108:4465-4470.
61. Blednov YA, Black M, Benavidez JM, Da Costa A, Mayfield J, Harris RA. Sedative and Motor Incoordination Effects of Ethanol in Mice Lacking CD14, TLR2, TLR4, or MyD88. Alcohol Clin Exp Res. 2017; 41:531-540.
62. Harris RA, Bajo M, Bell RL, *et al.* Genetic and pharmacologic manipulation of TLR4 has minimal impact on ethanol consumption in rodents. J Neurosci. 2017; 37:1139-1155.
63. June HL, Liu J, Warnock KT, Bell KA, Balan I, Bollino D, Aurelian L. CRF-amplified neuronal TLR4/MCP-1 signaling regulates alcohol self-administration. Neuropsychopharmacology. 2015; 40:1549-1559.
64. Pla A, Pascual M, Renau-Piqueras J, Guerri C. TLR4 mediates the impairment of ubiquitin-proteasome and autophagy-lysosome pathways induced by ethanol treatment in brain. Cell Death Dis. 2014; 5:e1066.
65. Montesinos J, Alfonso-Loeches S, Guerri C. Impact of the innate immune response in the actions of ethanol on the central nervous system. Alcohol Clin Exp Res. 2016; 40:2260-2270.
66. Montesinos J, Pascual M, Pla A, Maldonado C, Rodríguez-Arias M, Miñarro J, Guerri C. TLR4 elimination prevents synaptic and myelin alterations and long-term cognitive dysfunctions in adolescent mice with intermittent ethanol treatment. Brain Behav Immun. 2015; 45:233-244.
67. Alfonso-Loeches S, Pascual-Lucas M, Blanco AM, Sanchez-Vera I, Guerri C. Pivotal role of TLR4 receptors in alcohol-induced neuroinflammation and brain damage. J Neurosci. 2010; 30:8285-8295.
68. He J, Crews FT. Increased MCP-1 and microglia in various regions of the human alcoholic brain. Exp Neurol. 2008; 210:349-358.
69. Breese GR, Knapp DJ, Overstreet DH, Navarro M, Wills TA, Angel RA. Repeated lipopolysaccharide (LPS) or cytokine treatments sensitize ethanol withdrawal-induced anxiety-like behavior. Neuropsychopharmacology. 2008; 33:867-876.
70. Grantham EK, Warden AS, McCarthy GS, DaCosta A, Masona S, Blednov Y, Mayfiel RD, Harris RA. Role of toll-like receptor 7 (TLR7) in voluntary alcohol consumption. Brain Behav Immun. 2020; 89:423-432.

Received January 24, 2021; Revised February 22, 2021; Accepted February 26, 2021.

**Address correspondence to:*
Marat Airapetov, Department of Neuropharmacology, Institute of Experimental Medicine, 12 Academician Pavlova Street, St. Petersburg, 197376, Russia.
E-mail: interleukin1b@gmail.com

Released online in J-STAGE as advance publication March 12, 2021.

Review

DOI: 10.5582/bst.2021.01072

The E2F transcription factor 2: What do we know?

Luwen Li[1,2,3], Shiguan Wang[4], Yihang Zhang[1,2,3], Jihong Pan[1,2,3,*]

[1] Biomedical Sciences College & Shandong Medicinal Biotechnology Centre, Shandong First Medical University, Ji'nan, China;
[2] Key Lab for Biotech-Drugs of National Health Commission, Ji'nan, China;
[3] Key Lab for Rare & Uncommon Diseases of Shandong Province, Shandong First Medical University, Ji'nan, China;
[4] Medical College, Shandong University, Ji'nan, China.

SUMMARY E2F transcription factor 2 (E2F2) is a member of the E2F family of transcription factors. The classical view is that some E2Fs act as "activators" and others "inhibitors" of cell cycle gene expression. However, the so-called "activator" E2F2 is particularly enigmatic, with seemingly contradictory roles in the cell cycle, proliferation, apoptosis, inflammation, and cell migration and invasion. How can we rationalize the apparently opposing functions of E2F2 in different situations? This is difficult because different methods of studying E2F2 have yielded conflicting results, so extrapolating mechanisms from an observed endpoint is challenging. This review will attempt to summarize and clarify these issues. This review focuses on genetic studies that have helped elucidate the biological functions of E2F2 and that have enhanced our understanding of how E2F2 is integrated into pathways controlling the cell cycle, proliferation, apoptosis, inflammation, and cell migration and invasion. This review will also discuss the function of E2F2 in cancer and other diseases. This review provides a strong basis for further research on the biological function and clinical potential of E2F2.

Keywords E2F2, biological effect, diseases

1. Introduction

The E2F transcription factor family, a cellular factor required for activation of the E2 adenoviral promoter (*1*), came to the forefront of cancer research when it was found to be associated with and regulated by the retinoblastoma protein RB. There are now eight known subclasses of E2F proteins (*2*); some are considered "activators" and others "inhibitors" of expression (*3,4*). This makes E2F2 enigmatic and unique, and despite being known for 35 years, its functions remain an active topic of research in diverse arenas such as biochemistry, cell and developmental biology, and oncology.

2. Structure and regulation

E2F2 contains a winged-helix DNA binding domain (DBD) (*5*) (Figure 1), a highly conserved domain that contributes to dimerization, expressed from eight chromosomal loci to regulate the transcriptional activity of other genes. The E2F2 protein also contains multiple protein-protein interaction domains, including a helix-loop-helix binding domain that mediates heterodimerization with Sp1, resulting in synergistic activation of transcription (*6,7*). Other domains include a cyclinA/cdk2 binding domain, hydrophobic heptad repeat dimerization domain, and Rb protein binding domain.

The activity of E2F2 is controlled by acetylation by P/CAF, p300/CBP, or a related acetyltransferase, which increases the protein stability and DNA binding and transactivation activity of E2F2. However, this acetylation can be reversed by "pocket proteins" (*i.e.*, the retinoblastoma protein (pRb) and Rb-related proteins p107 and p130) (*8,9*), which are regulated by cyclin dependent kinases (CDKs), form the CDK-E2F-pRb complex, and take part in transcriptional activities (*10*). pRb acts as a transcriptional repressor complex by recruiting histone deacetylase (HDAC) and remodeling chromatin. During transcriptional activation of cell cycle progression, pRb is phosphorylated by G1 cyclin-dependent kinase complexes (cyclinD/cdk4 and cyclinE/cdk2) that inhibit its ability to bind E2F2, which is released and becomes transcriptionally active (*11*).

The dimerization domain of E2F2 mediates heterodimerization with a DP protein such as DP-1, DP-2, or DP-3. This interaction is required for formation of functional transcription factors that can bind to DNA with high affinity. DP proteins were originally identified as binding to differentiation to regulate transcription

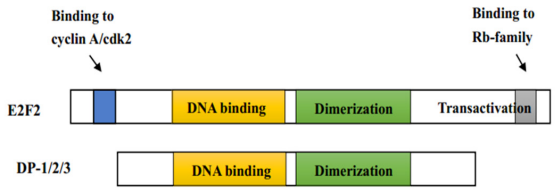

Figure 1. The structure of E2F2 as well as the similar structure of DP proteins. The highly conserved winged-helix DNA binding domain (DBD) is indicated in yellow, and the hydrophobic heptad repeat domain required for dimerization is shown in green. Other domains required for interaction with cyclin A/cdk2 and Rb family members are also indicated.

factor 1 (DRTF1). The consensus DNA-binding site of DRTF1 was later found to be the same as that of E2F2, and DRTF1 was also found to interact with Rb (*12*). Evidence is now clear that DRTF1 and E2F2 are the same factor (*13*) and that E2F proteins regulate complex cellular functions by forming heterodimeric protein complexes with a member of the DP family of proteins (DP-1 or DP-2).

3. Role and function

3.1. Interaction between E2F2 and cell cycle proteins

E2F2 plays a significant role in promoting the cell cycle (*14*), which is regulated by CDKs and CDK inhibitors (CKIs). E2F2 is often referred to as an activator because it transcriptionally activates certain target genes, such as cyclin E. Analysis of the cell cycle regulatory machinery has indicated that expression of E2F2 can greatly induce cyclin A and E while not affecting the expression of CKIs such as p21. For example, E2F2-mediated expression of cyclin A and E can induce limited proliferation of cardiomyocytes (*15,16*). In addition, E2F2 has nuclear localization signals adjacent to its cyclin A-binding domain. This ensures its movement into the nucleus, thereby modulating E2F2 activity in a cell cycle-dependent manner.

The "pRb pathway" is one of the most significant pathways in normal cell cycle control. Unphosphorylated pRb binds to E2F2 in G0/G1, forming a complex that actively represses E2F2-responsive genes (*17*). Once activated by mitogenic signals, CDKs phosphorylate pRb, p107, and p130, causing the release and accumulation of sequestered E2F2 (*18*). In many cell types, pRb family members play an important role in regulating terminal differentiation by directly controlling cell division through regulation of E2F-dependent promoters. For example, TNF-α stimulates proliferation of vascular smooth muscle cells by activating the Raf-1/MEK/ERK pathway and stimulating Rb-Raf-1, resulting in high expression of E2F2 that regulates cell proliferation (*19*). Rb-mediated control of E2F2 creates complex signaling and regulatory loops. For example, Rb-E2F2 controls angiogenesis by regulating VEGF (vascular endothelial growth factor A) receptors. In a hypoxic environment, E2F2 is released and activated, ultimately regulating angiogenesis *via* interaction with hypoxia-inducible factor 1 to activate *VEGF*, allowing the secretion of VEGF and eventual interaction with its receptor on endothelial cells (*20*). Rb-E2F2 also regulates angiogenesis with other mediators – for example, p53 binds to E2F2 to form a transcriptional complex that inhibits VEGF expression (*21*).

Mice with targeted deletion of *E2f2* exhibit impaired liver regeneration, and their hepatocytes display delayed cell-cycle entry from quiescence. In addition, E2F2-mediated transcription promotes adult hepatocyte proliferation and liver regeneration (*22*). Overexpression of E2F2 in cultured cells stimulates their entry into the S phase (*23*), indicating that E2F2 promotes cell cycle progression. In light of this, E2F2-responsive genes are potent transcriptional activators (*24,25*), and overexpression of E2F2 is sufficient to induce quiescent cells to re-enter the cell cycle (*26-28*) by promoting activation of target genes that are important to the G1/S transition (*29*). Knockdown of E2F2 expression reduces the proliferation of glioma and GSCs (cancer stem-like cells), while overexpression of E2F2 partially reverses the inhibitory effect of Let-7b (a member of the Let-7 microRNA family) on the proliferation of glioma and GSCs (*30*). These findings are consistent with the positive role E2F2 presumably plays in progression from the G1 to the S phase (*31*).

3.2. E2F2 can promote or inhibit proliferation

Current evidence suggests that E2F2 may act both as a suppressor and promoter of proliferation, depending on the cellular context (Table 1).

3.2.1. Promoting proliferation

Studies of multiple E2Fs have revealed both redundant and specific roles for E2F2 in proliferation. $E2F1^{-/-}$ $E2F2^{-/-}$ T cells exhibit profound defects in homeostatic proliferation (*31*). Intriguingly, *E2F2* and *E2F1* double knockout (DKO) mice are severely impaired in all hematopoietic cell lineages because of defective S phase progression in progenitor populations (*32*). E2F2 is expressed in a cell cycle-regulated manner and is highest in the late G1 and S phases (*33*). In cultured neonatal rat cardiomyocytes, directed expression of E2F2, but not E2F1, E2F3, or E2F4, stimulates cell division without affecting apoptosis, indicating that E2F2 offers promise as a specific candidate for regenerating cardiomyocytes (*34*). Moreover, a combination of *E2f1*, *E2f2*, and *E2f3* mutations is sufficient to completely block proliferation of mouse embryonic fibroblasts (MEFs) (*35*).

3.2.2. Inhibiting proliferation

Table 1. Effect of E2F2 on cell proliferation

Genotype	Cell type or tissue	Effect on proliferation	Phenotypic consequences
E2F2$^{-/-}$	T cells	Increases antigen-dependent proliferation	
	Cardiomyocytes	Inhibits proliferation	
	Glioma cells	Inhibits proliferation	
	GSCs	Inhibits proliferation	
	hESCs	Inhibits proliferation	
	ECs	Promotes proliferation	
Elevated E2F2	Adult hepatocytes	Promotes proliferation	liver regeneration
	Cardiomyocytes	Promotes proliferation	
E2F1$^{-/-}$	T cells	Promotes antigen-dependent proliferation	
E2F2$^{-/-}$	Exocrine pancreas	Promotes endoreduplication	polyploidy, exocrine de-generation, and diabetes
	T cells	Inhibits homeostatic prolifera-tion	T-cell lymphopenia
	Hematopoietic progenitors	Impairs S-phase progression	defective hematopoiesis, anemia, and leukopenia
E2F1$^{-/-}$ *E2F2*$^{-/-}$ *E2F3*$^{-/-}$	MEFs	Arrests the cell cycle throughout	

Table 2. The effect of E2F2 on apoptosis

Genotype	Cell type or tissue	Effect on apoptosis	The reason
E2F2$^{-/-}$	Myc-induced T cell lymphomagenesis	Inhibits apoptosis	p53-dependent apoptosis
	cone cells	Inhibits apoptosis	p53-dependent apoptosis
	MEF	Inhibits apoptosis	p53-dependent apoptosis
	melanocytes	Inhibits apoptosis	p53-independent apoptosis
dE2F2$^{-/-}$	wing proliferative tissue of Drosophila	Inhibits apoptosis	p53-independent apoptosis
	peripheral nervous system of Drosophila	Inhibits apoptosis	p53-independent apoptosis
E2F2$^{-/-}$	cardiomyocytes	Promotes apoptosis	p53-dependent apoptosis
	melanoma cells	Promotes apoptosis	p53-dependent apoptosis
E2F1$^{-/-}$ *E2F2*$^{-/-}$	differentiating cells	Promotes apoptosis	p53-dependent apoptosis

Conversely, a study has indicated that E2F1/E2F2 transcription factors play a key role in slowing the rate of proliferation during terminal cell differentiation (*36*). T lymphocytes deficient in E2F2 proliferate with TCR stimulation. An E2F2 deficiency, or more significantly loss of both E2F1 and E2F2, results in increased proliferation of T cells in peripheral blood, which is consistent with a reduced threshold of antigen activation (*37,38*). In addition, hind-limb ischemia was surgically induced in E2F2$^{-/-}$ mice and their wild-type littermates; two weeks later, laser Doppler perfusion measurements, capillary density, and endothelial cell proliferation were significantly enhanced in E2F2$^{-/-}$ mice (*16*). Zhou *et al.* found that loss of E2F2 expression improved endothelial cell growth, proliferation, gene expression in the G1/S phase, and neovascularization after myocardial infarction (*16,39*).

Since E2Fs can both suppress and stimulate proliferation, the balance between various signal intensities is what determines whether cells proliferate or differentiate (*40*). In the microenvironment of the body, E2F-mediated control of cell proliferation results from the balance between repressor and activator E2F proteins. Therefore, E2F2 may upset this balance and induce different regulation of proliferation in different *in vivo* microenvironments.

3.3. E2F2 can promote or inhibit apoptosis

Apoptosis, the process of programmed cell death, occurs throughout the lifespan of multicellular organisms. Apoptosis acts to maintain homeostasis of tissues and organs by removing unwanted or damaged cells. Depending on the cells or tissues, E2F2 can have pro- or anti-apoptotic effects. Indeed, E2F2 expression induces apoptosis in different proliferative tissues, but this effect is not observed in differentiated post-mitotic cells. This phenomenon suggests that the regulation of apoptosis by E2F2 may be related to cell type and developmental status (Table 2).

3.3.1. Promoting apoptosis

The alternative expression or combination of any of the eight *E2F* family genes can induce strong apoptotic activity. This apoptosis is widely is believed to be a result of high levels of E2F activity because ectopic expression of E2F2 can induce both p53-dependent and p53-independent apoptosis (*41*).

p53-dependent apoptosis: Removing one allele of *E2f2* reduces apoptosis and promotes the formation of Myc-driven murine T-cell lymphomas (*42*). Mechanistically, this may be due to the E2f2-dependent

Ser15 phosphorylation of P53 (*43*), which in cone cells leads to concomitant induction of the p53 targets Noxa and Siva. Deleting p53 in a context of elevated E2f2 ($Rb^{-/-}$) inhibits the induction of apoptosis in cone cells, indicating the process is p53-dependent. E2f2 also maintains levels of Tradd, which inhibits Trip12/Ulf-mediated Arf ubiquitylation and degradation (*44,45*). Removing E2f2 reduces Arf levels, increases the Arf target Mdm2, and ultimately activates the p53 pathway (*46*).

p53-independent apoptosis: Rbf1, the *Drosophila* homolog of Rb, is pro-apoptotic in proliferative tissue. In flies, E2F2 is the main partner of Rbf1 (*47*). In that study, Clavier *et al.* found that dE2F2 and dDP are required for Rbf1-induced apoptosis. Moreover, Rbf1 and dE2F2 reduce the expression of two major anti-apoptotic genes in *Drosophila*: buffy, an anti-apoptotic member of the Bcl-2 family; and diap1, possibly encoding a caspase inhibitor. Rbf1/dE2F2 represses buffy at the transcriptional level, contributing to cell death. In addition, Rbf1 and dE2F2 upregulate HOW expression. HOW is an RNA binding protein involved in diap1 regulation. HOW is essential for cell survival and key to mRNA degradation (*48*). In summary, Rbf1 appears to coordinate with dE2F2 and some complexes to downregulate the anti-apoptotic genes buffy and diap1, thereby promoting cell death in proliferating tissues (*47*). In *Drosophila*, Rovani *et al.* found that the dREAM complex, which includes dE2F2, cooperates with the proapoptotic factor Grim to induce cell death in the peripheral nervous system (*49*). In melanocytes, Raj *et al.* found that E2F2 binds to the *Survivin* (an anti-apoptotic factor) promoter and that mutation of either the p53 or E2F2-binding sites within the promoter is sufficient to increase transcription (*50*).

3.3.2. Inhibiting apoptosis

Expression of E2F2 in cardiomyocytes reduces expression of various apoptosis-related genes, including *p53*, *p21CIP/WAF*, and *mdm2*, and it represses the activity of proapoptotic pathways (*34*). Iglesias *et al.* found that $E2f1^{-/-}$/$E2f2^{-/-}$DKO mice exhibited apoptosis of pancreatic cells and mitochondria (*51,52*). Providing insight into the mechanisms underlying apoptosis, typical p53 direct transcriptional target genes involved in intrinsic (*Bax*, *Puma*, *Apaf-1*, and *Pidd*) and extrinsic (*Dr5*) pathways are significantly overexpressed in DKO pancreatic samples, and disruption of p53 in *E2f1/E2f2*-deficient mice prevents apoptosis and restores a normal pancreatic phenotype (*52*). Interestingly, p21 was found to be optional for the aberrant pancreatic phenotype developed by cells lacking E2F1/E2F2. In melanoma, however, E2F2 regulates SIRT1 to inhibit p53-dependent apoptosis (*53*).

3.4. E2F2 can promote or inhibit inflammation

The function of inflammation is to eliminate the initial cause of cell injury, clear out necrotic cells and tissue damage arising from the original insult or the inflammation process itself, and initiate tissue repair. According to a recent study, E2F2 has both pro-inflammatory and anti-inflammatory action in mammals (Table 3).

3.4.1. Promoting inflammation

Silencing E2F2 significantly decreases expression of the inflammatory cytokine IL-6 in J774A.1 macrophages and MES 13 mesangial cells (*54*). A previous gene chip analysis by the current authors revealed that expression of E2F2 is higher in synovial tissue from patients with rheumatoid arthritis (RA) than from patients with osteoarthritis (OA) (*55*). The current authors previously found that its increased expression contributes to the abnormal proliferation, invasion, and cytokine production of RA synovial fibroblasts (RASFs). Further research revealed that TNF-α can facilitate the nuclear translocation of E2F2, NF-κB can bind to the E2F2 promoter, and E2F2 can directly bind to the IL-6 promoter (*56*). Moreover, E2F2 affects the formation of the STAT1/MYD88 complex by directly binding to STAT1 and MYD88 promoters. This, in turn, influences entry of STAT1 into the nucleus and activation of the PI3K/AKT/NF-κB pathway, which ultimately regulates expression of inflammatory cytokines including IL-1α, IL-1β, and TNF-α (*55*). Moreover, Wu *et al.* demonstrated that *E2F1/E2F2* DKO significantly reduces neuronal death, neuroinflammation, and associated neurological deficits (*57*), which is consistent with results from the current authors.

Table 3. The effect of E2F2 on inflammation

Genotype	Cell type or tissue	Effect on inflammation	Mechanism	Consequence
$E2F2^{-/-}$	J774A.1 macrophages, MES 13 mesangial cells	Inhibits inflammation	decreased let-7a expression	decreased IL-6 production
	RASFs	Inhibits inflammation	PI3K/AKT/NF-κB	decreased IL-1α, IL-1β, and TNF-α production
	T lymphocytes	Promotes inflammation		inflammatory infiltrates
$E2F1^{-/-}$ $E2F2^{-/-}$	neuronal cells	Inhibits inflammation		reduced neuronal death, neuroinflammation, and tissue damage

3.4.2. Inhibiting inflammation

E2F2 functions as a negative regulator of the immune response in mice by suppressing cellular proliferation of activated lymphocytes. As they age, *E2f2*$^{-/-}$ animals develop an autoimmune disorder with features of splenomegaly, multiorgan inflammatory infiltrates, glomerulonephritis, and serum anti-DNA antibodies, and the animals die prematurely. In these mice, E2F2-deficient T cells are hyperresponsive to TCR stimulation, responding with increased proliferation to lower concentrations of ligand. Thus, low levels of self-ligands may be sufficient to trigger autoimmune disease in these mice, resulting in a dramatic, abnormal expansion of the CD44^{hi}/CD69-effector/memory population of T cells (*58*).

3.5. Migration and invasion

Cell migration and invasion are central processes in the development and maintenance of multicellular organisms. Wound healing, immune response, and tissue formation and shaping during embryonic development all require orchestrated movement of cells. Cell migration is usually in response to specific external signals, both chemical and mechanical. Errors during this process have serious consequences, including intellectual disability, vascular disease, and tumor metastasis. Zhang *et al.* silenced E2F2 to suppress the migration and invasion of RASFs *in vitro* (*56*). Yoon *et al.* found that expression of an E2F2 mutant deficient in DNA-binding interfered with H-RAS dependent invasion of SUM-159 cells, suggesting transcriptionally active E2F2 is required for this process (*59*). Active E2F2 may promote H-RAS-dependent invasion in part by increasing expression of the B4 integrin subunit, a component of the A6B4 integrin that is known to enhance carcinoma invasion. Specifically, expression of E2F2 increases B4 mRNA, protein, and cell surface expression. These aspects link active H-RAS, transcriptionally active E2F2, and A6B4 integrins in a common pathway that enhances A6B4-dependent invasion. H-RAS also can activate E2F2 and A6H4 integrins through a common pathway, ultimately enhancing A6H4-dependent invasion.

4. E2F2 in malignancies

The effect of E2F2 on tumors cannot be ignored; it seems to be more inclined to promote tumor progression. There is scant evidence that E2F2 inhibits tumor progression (Table 4).

4.1. Promoting malignant tumors

4.1.1. Breast cancer

Aberrant E2F2 expression is associated with cancer progression and metastasis (*60*). Fujiwara *et al.* found that activation of the E2F2 pathway is associated with a lower relapse-free survival (RFS) rate in patients with breast cancer (*61*). In particular, E2F2 expression impacts cell-matrix adhesion, with potential consequences for metastatic colonization during breast cancer (*62*). Moreover, levels of gene expression have revealed that tumors from *E2f2* knockout mice have reduced expression of genes associated with the epithelial-mesenchymal transition (EMT), corresponding with a reduced probability of Ras activation. A study has found that the low likelihood of E2F2 pathway activation in human breast cancer is related to longer recurrence-free survival (*61*). That finding also illustrates the unique genetic requirements of individual E2Fs in mediating tumorigenesis in human breast cancer. Li *et al.* analyzed Oncomine data and found that *E2F2* mRNA levels are higher in breast cancer ($p < 0.001$) than in normal tissues (*63*).

4.1.2. Lung cancer

Immunohistochemical analysis of lung cancer biopsies from 119 patients detected E2F2 expression in 18% of patient samples and predominantly in patients with adenocarcinoma rather than squamous cell carcinoma (*64*). Sun *et al.* examined *E2F2* transcription and data on the survival of patients with lung cancer using the Oncomine, GEPIA, Kaplan-Meier Plotter, and cBioPortal databases. Analyses indicated that levels of *E2F2* expression were higher in lung adenocarcinoma and squamous cell lung carcinoma tissues than in

Table 4. The effect of E2F2 on cancer

Genotype	Type of cancer	Effect on cancer	Consequence
E2F2$^{-/-}$	breast cancer	Inhibits cancer	increased latency fewer tumors with EMT inhibited cell-matrix adhesion
	lung cancer	Inhibits cancer	decreases the CSC population reduces cell viability and colony formation
	liver cancer	Inhibits cancer	
E2F2 polymor-phisms	squamous cell carcinoma of oropharynx	Alters the risk of SCCOP recurring	
High E2F2 expression	ovarian cancer	Promotes cancer	worsens overall survival
	gastric cancer	Promotes cancer	
E2F2$^{-/-}$	lymphoma	Promotes cancer	

normal lung tissues, and levels of *E2F2* expression correlated with a tumor in an advanced stage. Moreover, survival analysis using the Kaplan-Meier Plotter database revealed that high levels of *E2F2* mRNA are associated with a low RFS rate in the patients with lung cancer that were studied (*65*). In addition, Chen *et al.* immunohistochemically analyzed 86 non-small cell lung cancer (NSCLC) samples and found that E2F2 expression was markedly increased in 62.8% (54/86) of samples compared to that in non-tumor lung tissue. Further studies have found that E2F2 expression is closely related to clinical stage ($p = 0.039$) and tumor size ($p = 0.045$). E2F2 acts as an activator in the progression of NSCLC and may serve as a promising indicator of prognosis for patients with NSCLC (*66*).

4.1.3. Liver cancer

Bioinformatic analysis of TCGA data revealed that the expression of E2F2 in HCC samples was significantly correlated with histological grade, clinical stage, and tumor status. Therefore, elevated E2F2 can be used as an independent prognostic marker and therapeutic target for liver cancer (*67*). Moreover, HCC tumor tissues exhibited overexpression of the BRD4-E2F2-cell cycle regulation axis, and E2F2 overexpression was significantly associated with a poor prognosis in those patients with HCC (*68*). Thus, E2F2 overexpression appears to play a central role in dysregulation of the cell cycle in HCC.

4.1.4. Squamous cell carcinoma of the oropharynx

Li *et al.* investigated associations between genetic variants in five *E2F2* promoter polymorphisms and the risk of recurrence of squamous cell carcinoma of the oropharynx (SCCOP) in 1,008 patients (*69,70*). Compared to patients with the variant *E2F2* genotypes rs2742976 and rs3218123, patients with the common homozygous genotypes had better disease-free survival (both log-rank, $p < 0.001$) and lower risk of SCCOP recurrence (HR: 0.4; 95% CI: 0.3-0.6; and HR: 0.3: 95% CI: 0.2-0.5, respectively) after multivariable adjustment. This finding suggests that *E2F2* polymorphisms may individually or jointly modify the risk of SCCOP recurrence.

4.1.5. Ovarian cancer

Xie *et al.* examined 308 ovarian cancer samples and found that E2F2 is significantly upregulated in ovarian cancer epithelial cells (CEPIs) (*71*). That study also indicated that increased E2F2 expression significantly enhances MCM4, CCNE2, and WHSC1 transcription in the SKOV3 and A2780 ovarian cancer cell lines. In addition, high levels of E2F2 and CCNE2 expression were associated with poorer overall survival. The high level of E2F2 expression offsets the effect of an LBX2-AS1 knockdown in ovarian cancer cells (*72*). LBX2-AS1 is a new type of lncRNA that promotes the progression of ovarian cancer. Therefore, E2F2 promotes ovarian cancer.

4.1.6. Gastric cancer

miRNA chip analysis indicated that miR-31 decreased in gastric cancer. E2F2 is the direct target of miR-31. E2F2 expression is up-regulated in gastric cancer tissues and is inversely proportional to the level of miR-31. miR-31 plays a vital role as a tumor suppressor by inhibiting the expression of E2F2s (*73*). Bioinformatic analysis using multiple databases revealed that the level of E2F2 expression in GC tissue was significantly higher than that in normal tissues and that the expression of E2F2 was related to survival (*74*). E2F2 is a potential biomarker and therapeutic target for the treatment of differentially expressed genes in GC (*75*).

4.2. Inhibiting malignant tumors

Opavsky *et al.* used a bitransgenic mouse model of Myc-induced T cell lymphomagenesis and analyzed tumor progression in E2F-deficient mice (*42*). Interestingly, the targeted inactivation of E2F1 or E2F3 has no significant effect on tumor progression while the loss of E2F2 accelerates the development of lymphoma. The loss of a single copy of E2F2 also accelerates the development of tumors, albeit to a lesser extent. In terms of its mechanism, E2F2 acts as a tumor suppressor through its ability to regulate apoptosis.

5. E2F2 in other diseases

Huntington's disease (OMIM 143100) is a neurodegenerative disorder characterized by movement abnormalities (chorea and hypokinesia), cognitive decline, and psychiatric symptoms, which are usually noticeable at ages 35-50 (*76*). Valcárcel-Ocete *et al.* found that presence of the *E2F2* rs2742976 T allele is associated with onset age of Huntington's disease and the level of *E2F2* expression. This highly significant E2F2 signal warrants further investigation. Moreover, Valcárcel-Ocete *et al.* speculated that a lower level of *E2F2* expression in symptomatic patients with Huntington's disease could be associated with a delay in the age of onset (*77*).

In degenerative diseases such as Stargardt disease and age-related macular degeneration, the leading cause of blindness in the developed world, retinal pigmented epithelial (RPE) cell loss is followed by photoreceptor cell death. RPE cells can proliferate upon *E2F2* gene transfer, suggesting an intrinsic regenerative potential. These findings provide proof-of-concept for an *E2F2*-mediated strategy to induce in situ regeneration of RPE

to treat degeneration (*78*).

6. Conclusion and perspectives for the future

Like other members of the E2F family, E2F2 typically binds to the promoter region of genes to control gene expression, playing a vital role in controlling the cell cycle. Mounting data suggest that *E2F2* plays different roles in the body and is an indispensable gene. E2F2 is not only involved in cell cycle progression but also in apoptosis, inflammation, and cell migration and invasion. As discussed in this review, E2F2 is a complex molecule that can promote the proliferation of hepatocytes and cardiomyocytes but that can also inhibit the proliferation of peripheral blood T cells; E2F2 induces the apoptosis of cone photoreceptor cells but also can inhibit the apoptosis of pancreatic cells. These and other findings have revealed the complex role of E2F2 in the human body and have challenged the traditional view that E2F2 is consistently and solely an "activator" of cell cycle gene expression. This view does not reflect the complexity of E2F2's function in the human microenvironment—its function seems to depend on the tissue and state of development.

E2F2 may have the opposite effect in even the same phenotype or disease. Whether E2F2 promotes or inhibits apoptosis depends on the tissue and state of development. In cone cells, E2F2 promotes apoptosis, and this promotion is dependent on P53. The promotion of apoptosis by E2F2 sometimes does not depend on P53. In melanocytes, E2F2 can directly bind to anti-apoptotic factors to promote apoptosis. However, an interesting aspect is that E2F2's anti-apoptotic action seems to depend on P53. Therefore, E2F2 is both an "activator" and an "inhibitor" of apoptosis. Inflammation seems to be a symptom of all diseases, so the effect of E2F2 on inflammation is also an issue that cannot be ignored. A number of studies have found that E2F2 can both promote and inhibit inflammation. In RA and neuroinflammation, E2F2 acts as an "activator" of inflammation to promote inflammation. However, E2F2 acts as a negative regulator of the immune response in mice by inhibiting the proliferation of activated lymphocytes. There is, nonetheless, an interesting phenomenon in terms of the effect that E2F2 has on tumors. E2F2 is more inclined to be an "activator" of the development and progression of tumors. A large amount of the literature indicates that E2F2 can promote the progression of tumors such as breast, lung cancer, and liver cancer, but the loss of E2F2 in transgenic mouse models of lymphoma accelerates the development of lymphoma. This seems to be the only evidence that E2F2 acts as an "inhibitor" of tumors. Therefore, E2F2 acts as an "activator" of the cell cycle as well as an "activator" of cell proliferation, apoptosis, and inflammation. Because of the tissue and state of development, it can inhibit the cell cycle, apoptosis, inflammation, and other processes. In short, the role of E2F2 in the human microenvironment is very complicated. Thus, it should not be simply labeled as an "activator" or "inhibitor." Its effect on the biological activity of cells depends on the tissue and state of development.

Although modern molecular technology and experimental models have revealed many functions of the intriguing transcription factor E2F2, there is still much to learn about its roles in the body. Further research on E2F2 needs to be conducted to clarify its role in diseases so that its potential as a diagnostic and therapeutic target can be fully realized. In fact, numerous studies have focused on its potential prognostic value in different types of diseases because of the importance of E2F2 in both normal homeostasis and tissue pathologies. E2F2 is also an attractive drug target, particularly with regard to cancer, and we may yet discover that E2F2 has other valuable functions, warranting many more years of study.

Funding: This work was supported by the National Natural Science Foundation of China (Grant No. 81671624), The Innovation Project of the Shandong Academy of Medical Sciences, and the program to promote academics of the Shandong First Medical University (LJ001).

Conflict of Interest: The authors have no conflicts of interest to disclose.

References

1. Kumin D, Hofmann C, Uckert W, Both GW, Loser P. Identification of an ovine atadenovirus gene whose product activates the viral E2 promoter: Possible involvement of E2F-1. Virology. 2004; 318:79-89.
2. Chen HZ, Tsai SY, Leone G. Emerging roles of E2Fs in cancer: An exit from cell cycle control. Nat Rev Cancer. 2009; 9:785-797.
3. Fischer M, Müller GA. Cell cycle transcription control: DREAM/MuvB and RB-E2F complexes. Crit Rev Biochem Mol Biol. 2017; 52:638-662.
4. Ebelt H, Liu Z, Müller-Werdan U, Werdan K, Braun T. Making omelets without breaking eggs: E2F-mediated induction of cardiomyoycte cell proliferation without stimulation of apoptosis. Cell Cycle. 2006; 5:2436-2439.
5. Lammens T, Li J, Leone G, De Veylder L. Atypical E2Fs: New players in the E2F transcription factor family. Trends Cell Biol. 2009; 19:111-118.
6. Lin SY, Black AR, Kostic D, Pajovic S, Hoover CN, Azizkhan JC. Cell cycle-regulated association of E2F1 and Sp1 is related to their functional interaction. Mol Cell Biol. 1996; 16:1668-1675.
7. Karlseder J, Rotheneder H, Wintersberger E. Interaction of Sp1 with the growth- and cell cycle-regulated transcription factor E2F. Mol Cell Biol. 1996; 16:1659-1667.
8. Martínez-Balbás MA, Bauer UM, Nielsen SJ, Brehm A, Kouzarides T. Regulation of E2F1 activity by

acetylation. EMBO J. 2000; 19:662-671.
9. Marzio G, Wagener C, Gutierrez MI, Cartwright P, Helin K, Giacca M. E2F family members are differentially regulated by reversible acetylation. J Biol Chem. 2000; 275:10887-10892.
10. Harbour JW, Luo RX, Dei Santi A, Postigo AA, Dean DC. Cdk phosphorylation triggers sequential intramolecular interactions that progressively block Rb functions as cells move through G1. Cell. 1999; 98:859-869.
11. Halaban R, Cheng E, Smicun Y, Germino J. Deregulated E2F transcriptional activity in autonomously growing melanoma cells. J Exp Med. 2000; 191:1005-1016.
12. Bandara LR, La Thangue NB. Adenovirus E1a prevents the retinoblastoma gene product from complexing with a cellular transcription factor. Nature. 1991; 351:494-497.
13. Girling R, Partridge JF, Bandara LR, Burden N, Totty NF, Hsuan JJ, La Thangue NB. A new component of the transcription factor DRTF1/E2F. Nature. 1993; 365:468.
14. Attwooll C, Lazzerini Denchi E, Helin K. The E2F family: Specific functions and overlapping interests. Embo j. 2004; 23:4709-4716.
15. Suzuki DE, Nakahata AM, Okamoto OK. Knockdown of E2F2 inhibits tumorigenicity, but preserves stemness of human embryonic stem cells. Stem Cells Dev. 2014; 23:1266-1274.
16. Zhou J, Cheng M, Wu M, Boriboun C, Jujo K, Xu S, Zhao TC, Tang YL, Kishore R, Qin G. Contrasting roles of E2F2 and E2F3 in endothelial cell growth and ischemic angiogenesis. J Mol Cell Cardiol. 2013; 60:68-71.
17. Cobrinik D. Pocket proteins and cell cycle control. Oncogene. 2005; 24:2796-2809.
18. Roskoski R Jr. Cyclin-dependent protein serine/threonine kinase inhibitors as anticancer drugs. Pharmacol Res. 2019; 139:471-488.
19. Davis R, Pillai S, Lawrence N, Sebti S, Chellappan SP. TNF-α-mediated proliferation of vascular smooth muscle cells involves Raf-1-mediated inactivation of Rb and transcription of E2F1-regulated genes. Cell Cycle. 2012; 11:109-118.
20. Yang D, Wang J, Xiao M, Zhou T, Shi X. Role of Mir-155 in controlling HIF-1α level and promoting endothelial cell maturation. Sci Rep. 2016; 6:35316.
21. Deshpande R, Mansara P, Kaul-Ghanekar R. Alpha-linolenic acid regulates Cox2/VEGF/MAP kinase pathway and decreases the expression of HPV oncoproteins E6/E7 through restoration of p53 and Rb expression in human cervical cancer cell lines. Tumour Biol. 2016; 37:3295-3305.
22. Delgado I, Fresnedo O, Iglesias A, Rueda Y, Syn WK, Zubiaga AM, Ochoa B. A role for transcription factor E2F2 in hepatocyte proliferation and timely liver regeneration. Am J Physiol Gastrointest Liver Physiol. 2011; 301:G20-G31.
23. Maldonado EN, Delgado I, Furland NE, Buqué X, Iglesias A, Aveldaño MI, Zubiaga A, Fresnedo O, Ochoa B. The E2F2 transcription factor sustains hepatic glycerophospholipid homeostasis in mice. PLoS One. 2014; 9:e112620.
24. Helin K, Lees JA, Vidal M, Dyson N, Harlow E, Fattaey A. A cDNA encoding a pRB-binding protein with properties of the transcription factor E2F. Cell. 1992; 70:337-350.
25. Lees JA, Saito M, Vidal M, Valentine M, Look T, Harlow E, Dyson N, Helin K. The retinoblastoma protein binds to a family of E2F transcription factors. Mol Cell Biol. 1993; 13:7813-7825.
26. Johnson DG, Schwarz JK, Cress WD, Nevins JR. Expression of transcription factor E2F1 induces quiescent cells to enter S phase. Nature. 1993; 365:349-352.
27. Qin XQ, Livingston DM, Kaelin WG, Jr., Adams PD. Deregulated transcription factor E2F-1 expression leads to S-phase entry and p53-mediated apoptosis. Proc Natl Acad Sci U S A. 1994; 91:10918-10922.
28. Lukas J, Petersen BO, Holm K, Bartek J, Helin K. Deregulated expression of E2F family members induces S-phase entry and overcomes p16INK4A-mediated growth suppression. Mol Cell Biol. 1996; 16:1047-1057.
29. DeGregori J, Leone G, Miron A, Jakoi L, Nevins JR. Distinct roles for E2F proteins in cell growth control and apoptosis. Proc Natl Acad Sci U S A. 1997; 94:7245-7250.
30. Song H, Zhang Y, Liu N, Zhang D, Wan C, Zhao S, Kong Y, Yuan L. Let-7b inhibits the malignant behavior of glioma cells and glioma stem-like cells *via* downregulation of E2F2. J Physiol Biochem. 2016; 72:733-744.
31. DeGregori J. The genetics of the E2F family of transcription factors: Shared functions and unique roles. Biochim Biophys Acta. 2002; 1602:131-150.
32. Li FX, Zhu JW, Hogan CJ, DeGregori J. Defective gene expression, S phase progression, and maturation during hematopoiesis in E2F1/E2F2 mutant mice. Mol Cell Biol. 2003; 23:3607-3622.
33. Cam H, Dynlacht BD. Emerging roles for E2F: Beyond the G1/S transition and DNA replication. Cancer Cell. 2003; 3:311-316.
34. Ebelt H, Hufnagel N, Neuhaus P, Neuhaus H, Gajawada P, Simm A, Müller-Werdan U, Werdan K, Braun T. Divergent siblings: E2F2 and E2F4 but not E2F1 and E2F3 induce DNA synthesis in cardiomyocytes without activation of apoptosis. Circ Res. 2005; 96:509-517.
35. Wu L, Timmers C, Maiti B, Saavedra HI, Sang L, Chong GT, Nuckolls F, Giangrande P, Wright FA, Field SJ, Greenberg ME, Orkin S, Nevins JR, Robinson ML, Leone G. The E2F1-3 transcription factors are essential for cellular proliferation. Nature. 2001; 414:457-462.
36. Iglesias-Ara A, Zenarruzabeitia O, Fernandez-Rueda J, Sánchez-Tilló E, Field SJ, Celada A, Zubiaga AM. Accelerated DNA replication in E2F1- and E2F2-deficient macrophages leads to induction of the DNA damage response and p21(CIP1)-dependent senescence. Oncogene. 2010; 29:5579-5590.
37. DeGregori J, Johnson DG. Distinct and overlapping roles for E2F family members in transcription, proliferation and apoptosis. Curr Mol Med. 2006; 6:739-748.
38. Azkargorta M, Fullaondo A, Laresgoiti U, Aloria K, Infante A, Arizmendi JM, Zubiaga AM. Differential proteomics analysis reveals a role for E2F2 in the regulation of the Ahr pathway in T lymphocytes. Mol Cell Proteomics. 2010; 9:2184-2194.
39. Zhou J, Wu M, Xu S, Cheng M, Ding C, Liu Y, Yan H, Biyashev D, Kishore R, Qin G. Contrasting roles of E2F2 and E2F3 in cardiac neovascularization. PLoS One. 2013; 8:e65755.
40. Müller H, Bracken AP, Vernell R, Moroni MC, Christians F, Grassilli E, Prosperini E, Vigo E, Oliner JD, Helin K. E2Fs regulate the expression of genes involved in differentiation, development, proliferation, and apoptosis. Genes Dev. 2001; 15:267-285.
41. Stravopodis DJ, Karkoulis PK, Konstantakou EG,

Melachroinou S, Thanasopoulou A, Aravantinos G, Margaritis LH, Anastasiadou E, Voutsinas GE. Thymidylate synthase inhibition induces p53-dependent and p53-independent apoptotic responses in human urinary bladder cancer cells. J Cancer Res Clin Oncol. 2011; 137:359-374.
42. Opavsky R, Tsai SY, Guimond M, Arora A, Opavska J, Becknell B, Kaufmann M, Walton NA, Stephens JA, Fernandez SA, Muthusamy N, Felsher DW, Porcu P, Caligiuri MA, Leone G. Specific tumor suppressor function for E2F2 in Myc-induced T cell lymphomagenesis. Proc Natl Acad Sci U S A. 2007; 104:15400-15405.
43. Chen D, Chen Y, Forrest D, Bremner R. E2f2 induces cone photoreceptor apoptosis independent of E2f1 and E2f3. Cell Death Differ. 2013; 20:931-940.
44. Chen D, Shan J, Zhu WG, Qin J, Gu W. Transcription-independent ARF regulation in oncogenic stress-mediated p53 responses. Nature. 2010; 464:624-627.
45. Morris EJ, Michaud WA, Ji JY, Moon NS, Rocco JW, Dyson NJ. Functional identification of Api5 as a suppressor of E2F-dependent apoptosis *in vivo*. PLoS Genet. 2006; 2:e196.
46. Iaquinta PJ, Aslanian A, Lees JA. Regulation of the Arf/p53 tumor surveillance network by E2F. Cold Spring Harb Symp Quant Biol. 2005; 70:309-316.
47. Clavier A, Baillet A, Rincheval-Arnold A, Coléno-Costes A, Lasbleiz C, Mignotte B, Guénal I. The pro-apoptotic activity of Drosophila Rbf1 involves dE2F2-dependent downregulation of diap1 and buffy mRNA. Cell Death Dis. 2014; 5:e1405.
48. Reuveny A, Elhanany H, Volk T. Enhanced sensitivity of midline glial cells to apoptosis is achieved by HOW(L)-dependent repression of Diap1. Mech Dev. 2009; 126:30-41.
49. Rovani MK, Brachmann CB, Ramsay G, Katzen AL. The dREAM/Myb-MuvB complex and Grim are key regulators of the programmed death of neural precursor cells at the Drosophila posterior wing margin. Dev Biol. 2012; 372:88-102.
50. Raj D, Liu T, Samadashwily G, Li F, Grossman D. Survivin repression by p53, Rb and E2F2 in normal human melanocytes. Carcinogenesis. 2008; 29:194-201.
51. Iglesias A, Murga M, Laresgoiti U, Skoudy A, Bernales I, Fullaondo A, Moreno B, Lloreta J, Field SJ, Real FX, Zubiaga AM. Diabetes and exocrine pancreatic insufficiency in E2F1/E2F2 double-mutant mice. J Clin Invest. 2004; 113:1398-1407.
52. Iglesias-Ara A, Zenarruzabeitia O, Buelta L, Merino J, Zubiaga AM. E2F1 and E2F2 prevent replicative stress and subsequent p53-dependent organ involution. Cell Death Differ. 2015; 22:1577-1589.
53. Zhao H, Tang W, Chen X, Wang S, Wang X, Xu H, Li L. The NAMPT/E2F2/SIRT1 axis promotes proliferation and inhibits p53-dependent apoptosis in human melanoma cells. Biochem Biophys Res Commun. 2017; 493:77-84.
54. Chafin CB, Regna NL, Caudell DL, Reilly CM. MicroRNA-let-7a promotes E2F-mediated cell proliferation and NFκB activation *in vitro*. Cell Mol Immunol. 2014; 11:79-83.
55. Wang S, Wang L, Wu C, Sun S, Pan JH. E2F2 directly regulates the STAT1 and PI3K/AKT/NF-κB pathways to exacerbate the inflammatory phenotype in rheumatoid arthritis synovial fibroblasts and mouse embryonic fibroblasts. Arthritis Res Ther. 2018; 20:225.
56. Zhang R, Wang L, Pan JH, Han J. A critical role of E2F transcription factor 2 in proinflammatory cytokines-dependent proliferation and invasiveness of fibroblast-like synoviocytes in rheumatoid arthritis. Sci Rep. 2018; 8:2623.
57. Wu J, Sabirzhanov B, Stoica BA, Lipinski MM, Zhao Z, Zhao S, Ward N, Yang D, Faden AI. Ablation of the transcription factors E2F1-2 limits neuroinflammation and associated neurological deficits after contusive spinal cord injury. Cell Cycle. 2015; 14:3698-3712.
58. Murga M, Fernández-Capetillo O, Field SJ, Moreno B, Borlado LR, Fujiwara Y, Balomenos D, Vicario A, Carrera AC, Orkin SH, Greenberg ME, Zubiaga AM. Mutation of E2F2 in mice causes enhanced T lymphocyte proliferation, leading to the development of autoimmunity. Immunity. 2001; 15:959-970.
59. Yoon SO, Shin S, Mercurio AM. Ras stimulation of E2F activity and a consequent E2F regulation of integrin alpha6beta4 promote the invasion of breast carcinoma cells. Cancer Res. 2006; 66:6288-6295.
60. Gao Y, Ma X, Yao Y, Li H, Fan Y, Zhang Y, Zhao C, Wang L, Ma M, Lei Z, Zhang X. miR-155 regulates the proliferation and invasion of clear cell renal cell carcinoma cells by targeting E2F2. Oncotarget. 2016; 7:20324-20337.
61. Fujiwara K, Yuwanita I, Hollern DP, Andrechek ER. Prediction and genetic demonstration of a role for activator E2Fs in Myc-induced tumors. Cancer Res. 2011; 71:1924-1932.
62. Bollig-Fischer A, Marchetti L, Mitrea C, Wu J, Kruger A, Manca V, Drăghici S. Modeling time-dependent transcription effects of HER2 oncogene and discovery of a role for E2F2 in breast cancer cell-matrix adhesion. Bioinformatics. 2014; 30:3036-3043.
63. Li Y, Huang J, Yang D, Xiang S, Sun J, Li H, Ren G. Expression patterns of E2F transcription factors and their potential prognostic roles in breast cancer. Oncol Lett. 2018; 15:9216-9230.
64. Feliciano A, Garcia-Mayea Y, Jubierre L, *et al.* miR-99a reveals two novel oncogenic proteins E2F2 and EMR2 and represses stemness in lung cancer. Cell Death Dis. 2017; 8:e3141.
65. Sun CC, Zhou Q, Hu W, *et al.* Transcriptional E2F1/2/5/8 as potential targets and transcriptional E2F3/6/7 as new biomarkers for the prognosis of human lung carcinoma. Aging (Albany NY). 2018; 10:973-987.
66. Chen L, Yu JH, Lu ZH, Zhang W. E2F2 induction in related to cell proliferation and poor prognosis in non-small cell lung carcinoma. Int J Clin Exp Pathol. 2015; 8:10545-10554.
67. Zhan L, Huang C, Meng XM, Song Y, Wu XQ, Miu CG, Zhan XS, Li J. Promising roles of mammalian E2Fs in hepatocellular carcinoma. Cell Signal. 2014; 26:1075-1081.
68. Hong SH, Eun JW, Choi SK, Shen Q, Choi WS, Han JW, Nam SW, You JS. Epigenetic reader BRD4 inhibition as a therapeutic strategy to suppress E2F2-cell cycle regulation circuit in liver cancer. Oncotarget. 2016; 7:32628-32640.
69. Li Y, Sturgis EM, Zhu L, Cao X, Wei Q, Zhang H, Li G. E2F transcription factor 2 variants as predictive biomarkers for recurrence risk in patients with squamous cell carcinoma of the oropharynx. Mol Carcinog. 2017; 56:1335-1343.
70. Li Y, Sturgis EM, Yuan Y, Lu M, Cao X, Wei Q, Li G.

Effect of human papillomavirus seropositivity and E2F2 promoter variants on risk of squamous cell carcinomas of oropharynx and oral cavity. Carcinogenesis. 2016; 37:1070-1078.
71. Xie L, Li T, Yang LH. E2F2 induces MCM4, CCNE2 and WHSC1 upregulation in ovarian cancer and predicts poor overall survival. Eur Rev Med Pharmacol Sci. 2017; 21:2150-2156.
72. Cao J, Wang H, Liu G, Tang R, Ding Y, Xu P, Wang H, Miao J, Gu X, Han S. LBX2-AS1 promotes ovarian cancer progression by facilitating E2F2 gene expression *via* miR-455-5p and miR-491-5p sponging. J Cell Mol Med. 2020; 25:1178-1189.
73. Wang H, Zhang X, Liu Y, Ni Z, Lin Y, Duan Z, Shi Y, Wang G, Li F. Downregulated miR-31 level associates with poor prognosis of gastric cancer and its restoration suppresses tumor cell malignant phenotypes by inhibiting E2F2. Oncotarget. 2016; 7:36577-36589.
74. Yu J, Fang C, Zhang Z, Zhang G, Shi L, Qian J, Xiong J. H19 rises in gastric cancer and exerts a tumor-promoting function *via* miR-138/E2F2 axis. Cancer Manag Res. 2020; 12:13033-13042.
75. Liu X, Hu C. Novel potential therapeutic target for E2F1 and prognostic factors of E2F1/2/3/5/7/8 in human gastric cancer. Mol Ther Methods Clin Dev. 2020; 18:824-838.
76. McColgan P, Tabrizi SJ. Huntington's disease: A clinical review. Eur J Neurol. 2018; 25:24-34.
77. Valcárcel-Ocete L, Alkorta-Aranburu G, Iriondo M, *et al.* Exploring genetic factors involved in huntington disease age of onset: E2F2 as a new potential modifier gene. PLoS One. 2015; 10:e0131573.
78. Kampik D, Basche M, Luhmann UFO, Nishiguchi KM, Williams JAE, Greenwood J, Moss SE, Han H, Azam S, Duran Y, Robbie SJ, Bainbridge JWB, Larkin DF, Smith AJ, Ali RR. In situ regeneration of retinal pigment epithelium by gene transfer of E2F2: A potential strategy for treatment of macular degenerations. Gene Ther. 2017; 24:810-818.

Received February 17, 2021; Revised April 8, 2021; Accepted April 25, 2021.

**Address correspondence to:*
Jihong Pan, Biomedical Sciences College & Shandong Medicinal Biotechnology Centre, Shandong First Medical University, No. 6699 Qingdao Road, Ji'nan 250117, China.
E-mail: panjihong@sdfmu.edu.cn

Released online in J-STAGE as advance publication April 29, 2021.

Original Article

DOI: 10.5582/bst.2021.01090

Rapid SARS-CoV-2 antigen detection potentiates early diagnosis of COVID-19 disease

Ying Lv[1,§], Yuanyuan Ma[2,§], Yanhui Si[3], Xiaoyi Zhu[4], Lin Zhang[5], Haiyan Feng[6], Di Tian[7], Yixin Liao[7], Tiefu Liu[7,*], Hongzhou Lu[8,*], Yun Ling[8,*]

[1] Department of Integrative Medicine, Shanghai Public Health Clinical Center, Fudan University, Shanghai, China;
[2] Department of Drug Clinical Trial, Shanghai Public Health Clinical Center, Fudan University, Shanghai, China;
[3] Department of Surgery, Shanghai Public Health Clinical Center, Fudan University, Shanghai, China;
[4] Department of Pediatrics, Shanghai Public Health Clinical Center, Fudan University, Shanghai, China;
[5] Department of Nursing, Shanghai Public Health Clinical Center, Fudan University, Shanghai, China;
[6] Department of Pain Rehabilitation, Shanghai Public Health Clinical Center, Fudan University, Shanghai, China;
[7] Scientific Department, Shanghai Public Health Clinical Center, Fudan University, Shanghai, China;
[8] Department of Infectious Disease, Shanghai Public Health Clinical Center, Shanghai, China.

SUMMARY As the COVID-19 epidemic is still ongoing, a more rapid detection of SARS-CoV-2 infection such as viral antigen-detection needs to be evaluated for early diagnosis of COVID-19 disease. Here, we report the dynamic changes of SARS-CoV-2 viral antigens in nasopharyngeal swabs of COVID-19 patients and its association with the viral nucleic acid clearance and clinical outcomes. Eighty-five COVID-19 patients were enrolled for detection of SARS-CoV-2 viral antigens, including 57 anti-SARS-CoV-2 antibody negative cases and 28 antibody positive cases. The viral antigen could be detected in 52.63% (30/57) patients with SARS-CoV-2 antibody negative at the early stage of SARS-CoV-2 infection, especially in the first 5 days after disease onset ($p = 0.0018$) and disappeared in about 8 days after disease onset. Viral antigens were highly detectable in patients with low Ct value (less than 30) of SARS-CoV-2 nucleic acid RT-PCT assay, suggesting the expression of viral antigen was associated with high viral load. Furthermore, positive antigen detection indicated disease progression, nine cases with positive antigen (9/30, 30.0%), in contrast to two cases (2/27, 7.40%) ($p = 0.0444$) with negative antigen, which progressed into severe disease. Thus, the viral antigens were persistent in early stages of infection when virus was in highly replicating status, and viral antigen detection promises to rapidly screen positive patients in the early stage of SARS-CoV-2 infection.

Keywords COVID-19, nasopharyngeal swab virus nucleic acid, antigen-detection, RT-qPCR Ct value, radiographic progression

1. Introduction

The pandemic of SARS-CoV-2 virus infections has caused 113,315,218 confirmed cases of coronavirus disease COVID-19, including 2,517,964 deaths up to 28 February 2021 in the world by World Health Organization (WHO) (*1*). Despite tremendous efforts to prevent the spread of SARS-CoV-2 worldwide, the high rate of person-to-person transmission with a large number of deaths poses a significant threat to global public health (*2*). The mortality in several countries exceeded 10% in the early stage of COVID-19 pandemic, which brought substantial economic losses and life threats. According to Chinese Center for Disease Control and Prevention, the overall mortality of COVID-19 patients is approximately 2.3% (*3*), which is obviously lower than Severe Acute Respiratory Syndrome (SARS) and Middle East Respiratory Syndrome (MERS) (*4*), however, the number of COVID-19 deaths is still high because of the lager quantity of COVID-19 patients (*5*).

At present, the diagnosis of COVID-19 mainly depends on RT-qPCR-based nucleic acid testing of SARS-CoV-2 virus (*6*). Specific testing for SARS-CoV-2 has significantly contributed to controlling this public health emergency and clinical practice. Further studies have demonstrated that the combined RT-qPCR detection with serological testing enhances diagnostic sensitivity and specificity (*7*). Recently new methods have developed to detect SARS-CoV-2 antigen(s) for diagnosis of acute or early infections, because SARS-CoV-2 antigen(s) are highly expressed in the respiratory

tract when the virus is actively replicating. For instance, monoclonal antibodies (mAbs) against the nucleocapsid protein of SARS-CoV-2 have promised a rapid antigen detection test (*2*).

To validate the diagnostic significance of SARS-CoV-2 antigen detection, here, we focused on the dynamic changes of virus antigen in COVID-19 patients during the course of SARS-CoV-2 nucleic acid clearance and the correlation of SARS-CoV-2 antigen existence with clinical outcome.

2. Materials and Methods

2.1. Subjects

This study included 85 patients (≥ 18 years old) with COVID-19 from December 9, 2020 to January 26, 2021, in the Shanghai Public Health Clinical Center. All patients were imported cases and diagnosed with COVID-19 according to the Eighth Edition of the Guidance for COVID-19 of China (5) and confirmed by nasopharyngeal swab nucleic acid test at the airport or quarantine hotels. This study was approved by the Ethics Committee of Shanghai Public Health Clinical Center (No. 2020-E142-01) and all participants consented.

All patients were classified into anti-SARS-CoV-2 antibody positive and negative groups based on the serological test of anti-SARS-CoV-2 IgG and IgM antibodies on admission day. Clinical and lab data were collected at admission, including sex, age, blood cell counts of $CD4^+$ and $CD8^+$ T lymphocytes, $CD19^+$ B lymphocyte and $CD14^+$ monocytes, erythrocyte sedimentation rate (ESR), and chest Computed Tomography (chest CT). The participant's histories of clinical and lab exams, together with the SARS-CoV-2 viral RNA detection data, were prospectively collected.

2. 2. Detection of SARS-CoV-2 viral RNA

Total RNA was extracted from a 200-mL sample of nasopharyngeal swabs using a magnetic bead-based nucleic acid extraction kit in a fully automated nucleic acid extraction instrument (Master Biotechnology, China). Dual fluorescence RT-PCR (Applied Biosystems 7500 Real-Time PCR Systems, Foster City, CA, USA) was performed according to the manufacturer's instructions. Gene ORF-1ab and gene N of SARS-CoV-2 virus were used as target sequences of PCR primers, respectively. A Ct value of greater than 40 was considered as negative detection.

2.3. Detection of SARS-CoV-2 viral antigen in nasopharyngeal swab specimens

As the low antigen expression in antibody positive cases, a rapid chromatographic immunoassay for the qualitative detection of specific antigens of SARS-CoV-2 virus in human nasopharynx was performed in antibody negative patients on different days of hospitalization using Diagnostic Kit for COVID-19 Antigen Test (Colloidal Gold) (Kehua Bio-engineering, China). This test device contains two antibody pre-coated lines, the "C" (control) and "T" (test) lines on the surface of the nitrocellulose membrane. The C line was pre-coated with anti-Chicken IgY antibody and the T line with anti-SARS-CoV-2 antibody. Color particle-conjugated anti-SARS-CoV-2 antibody was used as detector for SARS-CoV-2 antigen. During the test, SARS-CoV-2 antigens in the specimen interact with color particle-conjugated monoclonal anti-SARS-CoV-2 antibody, forming a color antigen-antibody complex. This complex migrates on the membrane *via* capillary action until the test line, where it will be captured by pre-coated anti-SARS-CoV-2 antibody. A colored test line would be visible in the result window if SARS-CoV-2 antigens are present in the specimen. The intensity of colored test line varies with the amount of SARS-CoV-2 antigen in the specimen. Color particle-conjugated Chicken IgY was used as detector for the control line.

2.4. Definitions

Based on the fact that some patients have no clinical symptoms at the time of COVID-19 disease confirmation, disease onset time was defined as first appearance of symptoms or first positive viral nucleic acid screening. The severity of COVID-19 was categorized into 4 groups according to the Chinese management guidelines for COVID-19 (version 8.0) (*8*): mild cases presented with mild symptoms without manifestation of pneumonia on imaging; moderate cases have fever, cough, sputum production, and other respiratory tract or non-specific symptoms along with manifestation of pneumonia on imaging; severe cases suffer from respiratory distress with respiratory frequency ≥ 30/min, SaO_2/SpO_2 below 94% on room air or a PaO_2 to FiO_2 ratio of 300 or lower; and critical cases show respiratory failure and need for mechanical ventilation, or shock or combination with other organ failure and need ICU care. Disease progression indicates that (*9*) mild or moderate disease on admission progressed to moderate or severe/critical disease; or (*10*) severe disease on admission progressed to critical disease.

2.5. Statistical analysis

Statistical analyses were performed using SPSS 25.0 (International Business Machines Corporation, IBM, Armonk, New York, USA). Non-normally distributed data were presented as median and interquartile range (IQR) as appropriate. Categorical variables were

expressed as counts and percentages for each category. The Wilcoxon rank-sum tests and Kruskal-Wallis tests were applied to test differences between two groups, Fisher exact tests or Chi-square tests were used for categorical variables. Multiple linear regression was applied to determine the relationship between outcomes and the exploratory factor. $p < 0.05$ was considered significant. Figures were constructed using GraphPad Prism 8.0.

3. Results

3.1. Comparison of antibody positive and negative groups

This study enrolled 85 COVID-19 confirmed patients who are Chinese citizens returning from Italy, Russia, US, UK, Nigeria and France and their age ranged from 18 to 67 years old. Twenty-eight patients (32.94%) were positive for serum anti-SARS-Cov-2 IgG/IgM and 57 patients (67.06%) were negative. The age in antibody positive group was older than antibody negative group (Z = -2.256, p = 0.0241). There was no difference in sex (p = 0.3434) and body mass index (BMI) (Z = -0.683, p = 0.4949) between the two groups. Twenty-seven (31.76%) patients had radiographic progression during the first week of hospitalization, 24 of them (88.9%) were from antibody negative group, and 3 of them (11.1%) from antibody positive group. As a consequence, 8 cases (8/24, 33.3%) progressed from mild to moderate type, and 3 cases (3/24, 12.5%) from mild to severe type in the antibody negative group, in contrast to 3 of 3 cases (100%) from mild to moderate type with no severe progression in antibody positive group. The cell counts of $CD4^+$ T cells, $CD8^+$ T cells and $CD19^+$ B cells in antibody negative group were significantly lower than those in antibody positive group (Z = -3.469, p = 0.0005; Z = -4.119, $p < 0.0001$; Z = -3.932, $p < 0.0001$, respectively), whereas, the thyroid stimulating hormone (TSH) level in antibody negative group was higher than antibody positive group (Z = -2.525, p = 0.0116). There was no significant difference between the two groups in ESR (Z = -0.595, p = 0.5519) and $CD14^+$ monocyte (Z = -0.463, p = 0.6434) level (Table 1).

3.2. Comparison of SARS-CoV-2 antigen positive and negative groups

Among the 57 antibody negative patients, 30 patients (52.63%) were SARS-CoV-2 antigen positive and 27 patients (47.36%) were negative. There was no difference in sex (χ^2 = 0.4838, p = 0.6285), age (Z = -0.392, p = 0.6951), BMI (Z = -0.655, p = 0.5123) and disease severity on admission (χ^2 = 1.233, p = 0.2174) between SARS-CoV-2 antigen positive and negative groups. Positive SARS-CoV-2 antigen detection likely indicates disease progression, as nine cases with positive antigen (9/30, 30.0%) progressed, in contrast to disease progression in 2 cases (2/27, 7.40%) with negative antigen detection (p = 0.0444). In the antigen positive group, there were 18 cases (18/30, 60.00%) with radiographic progression during the first week of hospitalization, in contrast to 6 of 27 cases (22.22%, p = 0.0068) in antigen negative group. There was no significant difference in levels of $CD4^+$ T cells, $CD8^+$ T

Table 1. The comparison of the groups with positive antibody and negative antibody

Items	Antibody (-) n = 57	Antibody (+) n = 28	Statistics	P
Gender (n,%)			-	0.3434
Female	23 (43.33%)	8 (28.57%)		
Male	34 (56.67%)	20 (71.43%)		
Age (Median)	38.0 (24.0-52.0)	29.5 (23.0-34.8)	Z = -2.256	0.0241
BMI (kg/m^2)	22.60 (20.35-25.14)	23.12 (21.37-26.02)	Z = -0.683	0.4949
Nasopharyngeal swab virus nucleic acid negative time*				
days of hospitalization	16.0 (8.0-24.0)	12.0 (3.0-22.0)	Z = -3.173	0.0015
days after onset	20.0 (10.0-25.0)	ND	ND	ND
Severity on admission (n, %)			-	0.0163
Mild	31 (46.67%)	23 (82.14%)		
Moderate	26 (53.33%)	5 (17.86%)		
Severe	0 (0)	0 (0)		
Disease progression (n, %)	11 (19.29%)	3 (10.71%)	-	0.3707
Mild to moderate	8 (14.03%)	3 (10.71%)	-	1.0000
Mild to severe	3 (5.26%)	0 (0)	-	-
Radiographic progression (n, %)	24 (42.11%)	3 (10.7%)	-	< 0.0001
$CD4^+$ cells (/μL)	480.0 (350.5-664.5)	647.5 (539.5-808.8)	Z = -3.469	0.0005
$CD8^+$ cells (/μL)	344.0 (216.5-426.5)	527 (362.3-639.0)	Z = -4.119	< 0.0001
$CD19^+$ cells (/μL)	171.0 (115.0-210.0)	277.0 (190.3-385.0)	Z = -3.932	< 0.0001
ESR (mm/H)	27.0 (8.5-41.5)	18.5 (9.3-33.0)	Z = -0.595	0.5519
Peripheral blood monocyte (10^9/L)	0.570 (0.365-0.720)	0.50 (0.423-0.593)	Z = -0.463	0.6434
TSH (μIU/mL)	2.38 (1.29-3.09)	1.64 (1.15-2.15)	Z = -2.525	0.0116

*55 cases with negative antibody were followed up until nasopharyngeal swab virus clearance.

Table 2. Comparison of groups with positive and negative antigen

Items	Antigen (+) n = 30	Antigen (-) n = 27	Statistics	P
Gender (n,%)			χ^2 = 0.4838	0.6285
Female	13 (43.33%)	10 (37.04%)		
Male	17 (56.67%)	17 (62.96%)		
Age (Median)	39.0 (24.75-56.25)	33.0 (24.00-50.00)	Z = -0.392	0.6951
BMI (kg/m^2)	23.09 (21.03-25.98)	22.04 (19.69-24.22)	Z = -0.655	0.5123
Nasopharyngeal swab virus nucleic acid negative time				
days of hospitalization	19.5 (13.3-25.0)	12.0 (3.0-22.0)	Z = -2.521	0.0117
days after onset	30.5 (15.3-27.0)	14.0 (5.0-23.0)	Z = -1.432	0.1520
Antigen negative time				
days of hospitalization	6.5 (5-9)	-	-	-
days after onset	8 (6-11)	-	-	-
Antibody appearance time				
days of hospitalization	12.0 (9.0-16.0)	10.0 (7.8-16.3)	Z = -0.813	0.4160
days after onset	13.0 (10.0-17.0)	12.5 (9.0-17.5)	Z = 0.000	1.0000
Severity on admission (n,%)			χ^2 = 1.233	0.2174
Mild	14 (46.67%)	17 (62.96%)		
Moderate	16 (53.33%)	10 (37.04%)		
Severe	0 (0)	0 (0)		
Disease progression (n,%)	9 (30.00%)	2 (7.41%)	-	0.0444
Mild to moderate	7 (23.34%)	1 (3.70%)	-	0.0543
Mild to severe	2 (6.67%)	1 (3.70%)	-	1.0000
Radiographic progression (n,%)	18 (60.0%)	6 (22.2%)	-	0.0068
CD4$^+$ cells (/μL)	465.5 (342.5-552.0)	513.0 (401.5-677.3)	Z = -1.135	0.2565
CD8$^+$ cells (/μL)	286 (162.8-446)	369 (228-420)	Z = -0.967	0.3336
CD19$^+$ cells (/μL)	143 (113.8-207)	183 (116-219)	Z = -1.031	0.3026
ESR (mm/H)	27.0 (10.0-38.8)	27.0 (8.0-47.0)	Z = -0.160	0.8728
Peripheral blood monocyte (10^9/L)	0.67 (0.40-0.76)	0.45 (0.35-0.66)	Z = -1.823	0.0684
TSH (μIU/mL)	2.33 (1.13-2.95)	2.47 (1.33-3.26)	Z = -0.751	0.4526

cells, CD19$^+$ B cells, CD14$^+$ monocyte, ESR, and TSH between the two groups (p > 0.05) (Table 2).

3.3. Dynamic changes of serum antibody and antigen and virus nucleic acid in nasopharyngeal swabs

All of the 30 cases positive for SARS-CoV-2 antigen detection were followed up until negative for antigen detection. The mean time of virus antigen disappearance was about 6.5(5-9) days of hospitalization or 8 (6-11) days after disease onset (Table 2). The median nasopharyngeal swab SARS-CoV-2 virus RNA clearance time in the antibody negative group was 20 (10.0-25.0) days after onset and 16.0 (8.0-24.0) days of hospitalization, which was significantly longer than that in antibody positive group {12.0 (3.0-22.0), Z = -3.173, p = 0.0015} (Table 1). The median hospitalization time for virus nucleic acid disappearance in nasopharyngeal swabs was significantly different between antigen positive group {19.5 days (13.3-25.0)} and antigen negative group {12.0 days (3.0-22.0)}(Z = -2.521, p = 0.0117), however, there was no difference on virus clearance time after disease onset (Z = -1.432, p = 1.1520). There was also no difference in antibody positive time between the two groups (p > 0.05) (Table 2). The positive rate of antigen was 57.78% (26/45) in 3 days, 60% (3/5) in 5 days and 0% (0/1) in 8 days of hospitalization (χ^2 = 4.0474, p = 0.0436). After 14 days of hospitalization, the antigen positive rate dropped to 20% (1/5). Taking the disease course into consideration, the antigen positive rate was 72% (18/25) in 3 days, 52.94% (9/17) in 5 days, 40% (2/5) in 7 days and 12.5%(1/8) after onset (p < 0.05) (Figure 1A, B). The viral antigen can be detected from nasopharyngeal swabs in 52.63% (30/57) patients with COVID-19 antibody negative at the early stage of SARS-CoV-2 infection, especially in the first 5 days after admission (p = 0.0007) (Table 4). According to follow-up data in 30 patients with positive antigen, the positive rate of antigen began to decrease gradually on the 3rd day, while the antibody began to appear gradually. The time for virus nucleic acid disappearance in nasopharyngeal swabs was longer than that for viral antibody and antigen disappearance (Figure 1C, D).

3.4. Factors related to antigen detection

A total of 35 samples, including 10 antigen negative samples and 25 antigen positive samples, were classified into three grades based on CT values of SARS-CoV-2 nucleic acid RT-PCR assay: less than 30, 30-35, 35-40, and two grades by the days after disease onset: less than 5 days, more than 5 days. The antigen was highly detected in cases with less than 30 CT value of the gene ORF-1ab (86.96%, 20/23, p = 0.0048) or gene N (84.62%, 22/26, p = 0.0074) (Table 3). In multi-analysis, the CT value of gene N (less than 30) and days after disease onset (less than 5 days) were positively correlated with the positive rate of antigen detection (p = 0.0018, p = 0.0018) (Table 4).

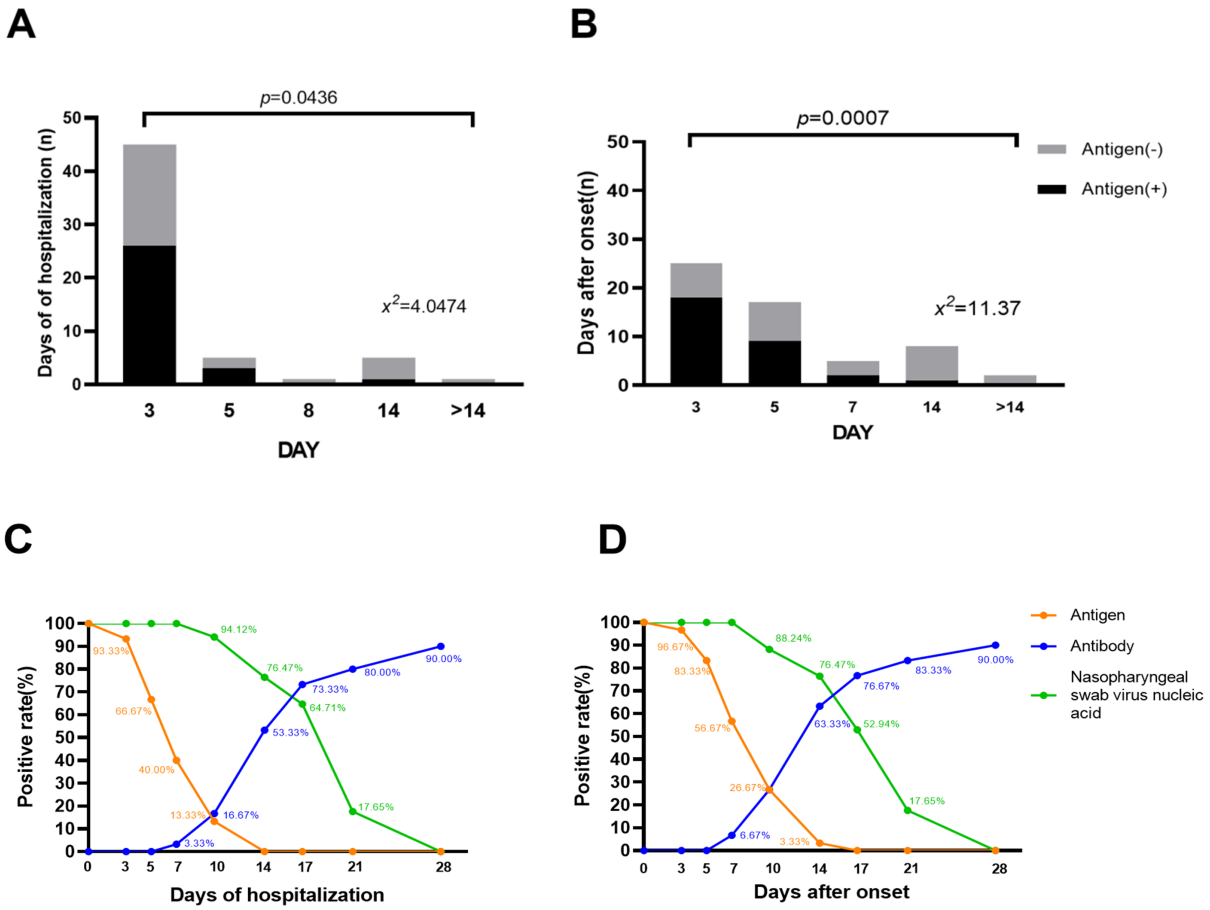

Figure 1. Positive rate of antigen in different days of hospitalization or after onset. The rate in different hospitalizations is shown in **(A)**. The positive rate of antigen was 57.78% (26/45) in 3 days, 60% (3/5) in 5 days, 0% (0/1) in 8 days and 20% (1/5) of hospitalization ($\chi^2 = 4.0474$, $p = 0.0436$). The rate in different days after onset is shown in **(B)**. Taking the disease course into consideration, the antigen positive rate was 72% (18/25) in 3 days, 52.94% (9/17) in 5 days, 40% (2/5) in 7 days and 12.5% (1/8) after onset ($p < 0.05$). Dynamic changes of antigen, antibody and viral RNA in nasopharyngeal swab of 17 antigen positive patients on the days after hospitalization **(C)** and disease onset **(D)**.

Table 3. The correlation of RT-qPCR Ct value of viral RNA and antigen detection

RT-qPCR (Ct value)	Gene ORF-1ab			Gene N		
	Antigen (+)	Antigen (-)	$P^{\ddagger}$	Antigen (+)	Antigen (-)	$P^{\ddagger}$
- 30.0	20	3	0.0048	20	3	0.0074
30.0 - 35.0	2	2		2	2	
35.0 - 40.0	1	3		1	3	
40.0 -	1	2		1	2	

‡The p value was calculated by comparison between the patients with Ct value less than 30 and those with more than 30.

Table 4. Multiple linear regression analysis of parameters with respect to virus antigen detection

Independent variables	Coefficient	St. Error	Beta	*t*	*P*
CT value < 30 (Gene N)	0.496	0.137	0.450	3.403	0.0018
Disease course (≤ 5 days)	0.496	0.137	0.450	3.403	0.0018

4. Discussion

The dynamic changes of SARS-CoV-2 antigens, serum anti-SARS-CoV-2 antibody, SARS-CoV-2 viral RNA clearance, and disease progression were evaluated in the early stages of infection in this study. The viral antigens were persistent in cases after less than 5 days infection with high viral load.

Molecular-based approaches are the first-line methods for diagnosis of SARS-CoV-2 acute infection. RT-qPCR assay of respiratory samples is the currently recommended method to confirm suspected cases

(*11*). However, this method is not efficient in rapidly screening a large number of individuals in places where thousands of people transit per hour. In addition, the accuracy of RT-qPCR depends on many factors, such as the sample type, stage of infection, skill of sample collection, and quality and consistency of the PCR assay (*12,13*). A new type of rapid diagnostic test (RDT) has been recently developed. It detects the presence of SARS-CoV-2 viral antigens in a respiratory tract sample, it is simple and can be completed typically within 30 minutes. However, recent research in Belgium showed that the poor sensitivity of the SARS-CoV-2 Ag Respi-Strip leads to false negative results, and suggested that SARS-CoV-2 Ag Respi-Strip should not be used alone for COVID-19 diagnosis (*14*). Viral antigen(s) are expressed only when the virus is in an actively replicating stage; thus, such tests are best for identification of acute or early infection (*15*), especially in the first 5 days after disease onset. In comparison with molecular techniques, antigen detection has several advantages such as ease, speed, low cost and non-requirement of special equipment or skills (*24*), and meets the need to rapidly screen positive patients at early infection.

Viral antigen clearance is earlier than viral RNA clearance after SARS-CoV-2 infection. In this study, we found that hospitalized patients of confirmed COVID-19 in Shanghai were at different stages of disease, mostly because all of them were diagnosed by viral nucleic acid screening after disembarking. Some of them had viral antibodies in their serum, while others did not. We found that the median negative turning time for virus nucleic acid in nasopharyngeal swab was about 16 days of hospitalization and 20 days after onset in the viral antibody negative group who showed longer virus clearance than those in the antibody positive group (12 days of hospitalization). Viral antigen can be detected in 52.63% (30/57) patients with anti-SARS-CoV-2 antibody negative from nasopharyngeal swabs in the first 5 days of hospitalization. When the CT value of viral nucleic acid RT-qPCR was less than 30, the positive rate of viral antigen was high either for gene ORF-1ab or for gene N. When the CT value was more than 30, the positive rate of antigen was significantly decreased. The grades of disease course and CT value in gene ORF-1ab may help to predict viral antigen detection. The continuous detection of viral antigen in nasopharyngeal swabs suggests that the antigen may disappear in about 6.5 days of hospitalization and 8 days after onset. According to the follow-up of 17 cases with antigen positive patients, the virus antigen disappeared earlier than both the nucleic acid and antibody disappearance. All of these tests may be helpful to estimate the stage of the disease.

Positive viral antigen detection suggests disease in progression. We found that nine cases with antigen positive (9/30, 30.0%) progressed, in contrast with only two cases with negative antigen (2/27, 7.40%) (p = 0.0444), which probably related to the strong immune response of B cells in the early stage of the disease, which is consistent with previous reports (*16,17*). An analysis of the correlation among factors such as CT value, disease course and detection of virus antigen in the two target genes showed that the disease course (less than 5 days) and CT value(less than 30) may help predict viral antigen detection, respectively, and the disease course was strongly correlated with antigen detection, that suggests the importance of early viral antigens detection. However, there was no significant difference in these immune indexes between antigen positive and negative groups, suggesting no significant change in cellular immune status during the disappearance of virus antigen. During the outbreak of SARS-CoV-2 infection, serum levels of TSH, T3 and T4 in COVID-19 patients were significantly lower than those in controls, and levels of T3 were a positive correlation with the severity of the disease (*22*). In our study, we found a negative correlation between TSH and virus antigen clearance, however, positive antibody detection indicates recovery from illness. The levels of $CD4^+$ T cells, $CD8^+$ T cells and $CD19^+$ B cells in the antibody negative group were also lower than those in antibody positive group. The age and the thyroid stimulating hormone (TSH) level in antibody negative group were higher than antibody negative group. This suggests that the existence of antibody indicates the recovery of immune function.

In summary, the viral antigens were persistent in the nasopharyngeal place less than 5 days in early stages of infection and is related to high viral load, Viral antigen detection may be helpful to screen the positive patients early and rapidly. However, the small amount of samples and loss of quantitative detection of viral antigen and virus nucleic acid in this study limited its value in clinic application, further multi-center studies are needed in the future to validate its clinical significance.

Acknowledgements

We would like to thank all the participants whose data were used in this study. We are most grateful for the assistance and support of Shanghai Public Health Clinical Center for providing clinical data.

Funding: The work was supported by Guangdong Province Science and Technology Project (2018B020241002) Shanghai Science and Technology Innovation Action Plan, Medical Innovation Research Special Project (20Z11900900), National Natural Science Foundation of China (82072260) and Shanghai "Medical Garden Rising Star" Youth Medical Talent Training Funding Program in 2021.

Conflict of Interest: The authors have no conflicts of interest to disclose.

References

1. World Health Organization. WHO Coronavirus Disease (COVID-19) Dashboard. Available at: *https://covid19.who.int* (accessed Jan 31, 2021).
2. Liu X, Liu C, Liu G, Luo W, Xia N. COVID-19: Progress in diagnostics, therapy and vaccination. Theranostics. 2020; 10:7821-7835.
3. Wu Z, McGoogan JM. Characteristics of and Important Lessons From the Coronavirus Disease 2019 (COVID-19) Outbreak in China: Summary of a Report of 72 314 Cases From the Chinese Center for Disease Control and Prevention. JAMA. 2020; 323:1239-1242.
4. Chang D, Lin M, Wei L, Xie L, Zhu G, Dela Cruz CS, Sharma L. Epidemiologic and Clinical Characteristics of Novel Coronavirus Infections Involving 13 Patients Outside Wuhan, China. JAMA. 2020; 323:1092-1093.
5. Li JW, Shao J, Wang CD, Li WM. The epidemiology and therapeutic options for the COVID-19. Precision Clinical Medicine. 2020; 3:71-84,
6. Huang C, Wang Y, Li X, *et al*. Clinical features of patients infected with 2019 novel coronavirus in Wuhan, China. Lancet. 2020; 395:497-506.
7. Petherick A. Developing antibody tests for SARS-CoV-2. Lancet. 2020; 395:1101-1102.
8. National Health Commission.Interpretation of the Seventh Edition of the Guidance for COVID-19: Prevention, Control, Diagnosis, and Management Guideline for COVID-19 (version8.0). *http://www.nhc.gov.cn/cms-search/downFiles/a449a3e2e2c94d9a856d5faea2ff0f94.pdf* (accessed Jan 31, 2021). (in Chinese)
9. Philippe G, Jean-Christophe L, Philippe P, *et al*. Hydroxychloroquine and azithromycin as a treatment of COVID-19: results of an open-label non-randomized clinical trial. Int J Antimicrob Agents. 2020; 56:105949.
10. Fei Z, Ting Y, Ronghui D, *et al*. Clinical course and risk factors for mortality of adult inpatients with COVID-19 in Wuhan, China: a retrospective cohort study. Lancet. 2020; 395:1054-1062.
11. Corman VM, Landt O, Kaiser M, *et al*. Detection of 2019 novel coronavirus (2019-nCoV) by real-time RT-PCR. Euro Surveill. 2020; 25:2000045.
12. Zou L, Ruan F, Huang M, *et al*. SARS-CoV-2 Viral Load in Upper Respiratory Specimens of Infected Patients. N Engl J Med. 2020; 382:1177-1179.
13. Chan JF, Yuan S, Kok KH, *et al*. A familial cluster of pneumonia associated with the 2019 novel coronavirus indicating person-to-person transmission: a study of a family cluster. Lancet. 2020; 395: 514-523.
14. Scohy A, Anantharajah A, Bodéus M, Kabamba-Mukadi B, Verroken A, Rodriguez-Villalobos H. Low performance of rapid antigen detection test as frontline testing for COVID-19 diagnosis. J Clin Virol. 2020; 129:104455.
15. Sheridan C. Fast, portable tests come online to curb coronavirus pandemic. Nat Biotechnol. 2020; 38:515-518.
16. Suthar MS, Zimmerman MG, Kauffman RC, *et al*. Rapid generation of neutralizing antibody responses in COVID-19 patients. Cell Rep Med. 2020; 1:100040.
17. Mathew D, Giles JR, Baxter AE, *et al*. Deep immune profiling of COVID-19 patients reveals distinct immunotypes with therapeutic implications. Science. 2020; 369:eabc8511.
18. Tan C, Huang Y, Shi F, Tan K, Ma Q, Chen Y, Jiang X, Li X. C-reactive protein correlates with computed tomographic findings and predicts severe COVID-19 early. J Med Virol. 2020; 92:856-862.
19. Cai Q, Chen F, Wang T, Luo F, Liu X, Wu Q, He Q, Wang Z, Liu Y, Liu L, Chen J, Xu L. Obesity and COVID-19 Severity in a Designated Hospital in Shenzhen, China. Diabetes Care. 2020; 43:1392-1398.
20. Petrilli CM, Jones SA, Yang J, Rajagopalan H, O'Donnell L, Chernyak Y, Tobin KA, Cerfolio RJ, Francois F, Horwitz PI. Factors associated with hospitalization and critical illness among 4,103 patients with COVID-19 disease in New York City. MedRxiv. 2020; https://www.medrxiv.org/content/10.1101/2020.04.08.20057794v1
21. Hamer M, Gale CR, Kivimäki M, Batty GD. Overweight, obesity, and risk of hospitalization for COVID-19: A community-based cohort study of adults in the United Kingdom. Proc Natl Acad Sci U S A. 2020; 117:21011-21013.
22. Wang W, Ye YX, Yao H. Evaluation and observation of serum thyroid hormone and parathyroid hormone in patients with severe acute respiratory syndrome. J Chin Antituberculous Assoc. 2003; 25:232-234
23. Zhang W, Zhao Y, Zhang F, Wang Q, Li T, Liu Z, Wang J, Qin Y, Zhang X, Yan X, Zeng X, Zhang S. The use of anti-inflammatory drugs in the treatment of people with severe coronavirus disease 2019 (COVID-19): The Perspectives of clinical immunologists from China. Clin Immunol. 2020; 214:108393.
24. Berlin DA, Gulick RM, Martinez FJ. Severe Covid-19. N Engl J Med. 2020; 383:2451-2460.

Received March 7, 2021; Revised March 19, 2021; Accepted March 22, 2021.

[§]These authors contributed equally to this work.

*Address correspondence to:
Tiefu Liu, Scientific Department, Shanghai Public Health Clinical Center, Fudan University, Shanghai 201508, China.
E-mail: liutiefu@shphc.org.cn

Yun Ling and Hongzhou Lu, Department of Infectious Disease, Shanghai Public Health Clinical Center, Shanghai 201508, China.
E-Mail: yun.ling@shphc.org.cn (YL), luhongzhou@fudan.edu.cn (HL)

Released online in J-STAGE as advance publication March 26, 2021.

Original Article

DOI: 10.5582/bst.2021.01016

MCM4 in human hepatocellular carcinoma: a potent prognostic factor associated with cell proliferation

Yan Xu, Xueling Yang, Tongguo Si, Haipeng Yu, Yong Li, Wenge Xing, Zhi Guo*

Department of Interventional Therapy, Tianjin Medical University Cancer Institute and Hospital, National Clinical Research Center for Cancer, Key Laboratory of Cancer Prevention and Therapy, Tianjin's Clinical Research Center for Cancer, Tianjin, China.

SUMMARY Hepatocellular carcinoma (HCC) remains a major public health problem. MCM4, a constitutive member of the minichromosomal maintenance protein family, has been reported to play a vital role in cancer malignancy behavior. However, the function of MCM4 in HCC remains largely unknown. The present study explored the specific role of MCM4 in HCC. The data from public datasets including TCGA and GTEx showed that MCM4 was overexpressed in HCC and significantly associated with poor prognosis. Immunohistochemistry results from 102 HCC patients suggested that high-level expression of MCM4 was correlated with tumor size. Then a series of *in vivo* and *in vitro* experiments were performed to investigate the function of MCM4 in HCC tumor cells. MCM4 silencing suppressed the cell proliferation and sphere formation of hepatoma cells. Moreover, silencing MCM4 significantly decreased the growth of tumors in a xenograft tumor model. In conclusion, the results of the present study indicated that MCM4 was a potential prognostic predictor associated with poor outcomes of HCC patients and even a therapeutic target for HCC.

Keywords MCM4, minichromosomal maintenance protein family, hepatocellular carcinoma, prognostic marker, tumor proliferation

1. Introduction

The minichromosomal maintenance (MCM) protein family consists of six related proteins that have essential roles in the initiation of DNA replication, elongation of DNA replication, and other chromosome transactions (*1-4*). MCM4 is part of the MCM2-7 heterohexameric complex, that has ATPase activity and serves as the core of the replicative helicase that unwinds duplex DNA and drives the progression of the replication fork (*5*). It has been recently reported that deregulation of MCM4 can contribute to cell proliferation and tumorigenesis. Therefore, aberrant expression of MCM4 may be applied as a promising prognostic marker in several malignancies (*4,6-10*). However, there is still a shortage of studies exploring the correlation between MCM4 and HCC. The role of MCM4 in HCC remains unclear.

In this study, we systematically investigated the roles of MCM4 in HCC. We demonstrated that the expression level of MCM4 was negatively associated with the clinical stage and prognosis of HCC patients. Furthermore, we also revealed the functions of MCM4 in tumor behavior including tumor proliferation.

2. Materials and Methods

2.1. Bioinformatics analysis

The data from GTEx database and TCGA database were used for differential genetic analysis. Differential gene expression and survival analysis were measured using the GEPIA website (*http://gepia.cancer-pku.cn*) (*11*). One-way ANOVA was applied for gene expression analysis between cancer and non-cancerous liver tissues. The disease-free survival time and overall survival time were obtained from the TCGA public database.

2.2. Patients and samples

Following Institutional Review Board approval, 102 patients with hepatocellular carcinoma who have been proved by pathology were incorporated into the study. Fresh samples were collected just after surgery and fixed in 10% formalin before embedding in paraffin wax. Patients' clinical and pathological data including age, gender, number of tumor nodes, tumor sizes and AFP levels were identified. All samples used were analyzed by experienced pathologists to ensure they were diagnosed as HCC. Written informed consent was obtained from patients before the study. We have also complied with the World Medical Association

Declaration of Helsinki involving the ethical conduct of research involving human subjects.

2.3. Immunohistochemistry

A standard immunoperoxidase staining procedure was performed. The paraffin-embedded tissues were sliced into 4um sections and baked at 70°C for 45 minutes. The sections were de-waxed in xylene and rehydrated in graded ethanol. Then, 0.01M citrate buffer was applied to repair the antigen, 3% H_2O_2 in methanol was added to the slices for 10 minutes. The tissues were incubated with primary anti-MCM4 antibodies (rabbit, Sigma-Aldrich) at a 1:500 dilution overnight. After washing with phosphate buffered saline, the tissues were incubated with goat anti-rabbit IgG at room temperature for 40 minutes. After DAB staining, the sections were counterstained with hematoxylin, dehydrated in ethanol, and cleared with xylene. For the results analysis, semiquantitative H-score was computed for each sample by multiplying the staining intensities (0: negative, 1: weak staining, 2: moderate staining, 3: strong staining) and distribution areas (0-100%). All samples were classified as high expression and low expression groups, respectively, according to the distribution of H-score.

2.4. Cell culture and transfection

Both human hepatocellular carcinoma cell lines (Hep3B and SNU-475) used in this study were purchased from the Cell Bank of the Chinese Academy of Sciences (Shanghai, China). SNU-475 was cultured in RPMI-1640 medium while Hep3B was cultured in Dulbecco's modified Eagle's medium (DMEM), both contained 1% penicillin streptomycin and 10% fetal bovine serum. Cells were cultured at 37°C with 5% CO_2. Both cell lines were maintained in our institution. For *in vitro* studies, both Hep3B and SNU-475 cells were transfected with shRNA to silence MCM4 according to the manufacturer's instructions. Short hairpin RNA (Target sequence: AAATGCATTCTTCAGCTATCCCT and AAATGTTGGCATAGATATTACTG) was obtained from the National Core Facility for Manipulation of Gene Function by RNAi, miRNA, miRNA sponges, and CRISPR/Genomic Research Center, Academia Sinica, Taipei, Taiwan. The stable cell lines were verified by RT-qPCR and Western blot before proceeding to the next experiment.

2.5. RT-PCR

The total RNA derived from cells were isolated using TRIzol® reagent (Invitrogen; Thermo Fisher Scientific, Inc.) according to protocols. After measuring the content by ultraviolet analysis, cDNA was synthesized from total RNA applying Fast Reverse Transcriptase (Tiangen Biotech Co., Ltd.). Quantitative PCR was performed on a Smart Cycler using SGExcel FastSYBR Mixture (With Low ROX) Plus (Sango biotech, China). To further analyze the real-time PCR data, we applied a comparative threshold cycle (Ct) method that compares differences in CT values between target RNA and common control (*12*). The forward and reverse primers are shown below (MCM4, F, 5′-TTGAAGCCATTGATGTGGAA-3′ and R, 5′-GGCACTCATCCCCGTAGTAA-3′; GAPDH, F, 5′-GAGTCAACGGATTTGGTCGT-3′ and R, 5′-TTGATTTTGGAGGGATCTCG-3′).

2.6. Western blot

Cell samples were lysed in RIPA lysis buffer, and protein concentrations were determined using a BCA Protein Assay kit (Beijing Solarbio Science & Technology Co., Ltd.). Then the denatured protein (~30 μg) was loaded and separated in SDS-PAGE gels and transferred to a wet polyvinylidene membrane. After blocking with 5% dry milk for 1h at 37°C, primary antibodies including MCM4 (1:1,500 dilution, ab4461, Abcam), mouse anti-β-actin (1:1,000 dilution, ab8226, Abcam plc, Cambridge, UK) were added and incubated at 4°C overnight. After washing with TBS with Tween-20, the membranes were further incubated with HRP-conjugated goat anti-rabbit IgG antibody (Abcam, cat. no. ab181662, 1:2,000) at room temperature for 1h. The blots were visualized using an enhanced chemiluminescence detection kit (Thermo Fisher Scientific, Inc.).

2.7. Colony formation array

Hep3B and SNU-475 cells were seeded and cultured on 60mm^2 plates at an initial density of 800/well, and each group was measured in 3 parallel wells. After 2 weeks, cells were washed and fixed with 10% formaldehyde for 15 min at room temperature. The cells were then stained with Giemsa for 15 min. Colony numbers were counted by using an optical microscope.

2.8. MTT assay

Both Hep3B and SNU-475 cells were seeded and cultured on 96-well plates at a density of 3500 cells/well. The cell's proliferation capacity was measured by MTT (methyl thiazolyl tetrazolium) assay. 0.02mL of 5mg/mL MTT reagent was added into each well for 24 hours at 37°C. The medium was replaced by 0.15mL of dimethyl sulfoxide (DMSO, Sigma) for 10min incubation. A microplate spectrophotometer (Thermo Scientific, Franklin, MA) was used to measure the optical density at 570 nm. All experiments were performed in triplicate.

2.9. Tumorigenicity assay

For *in vivo* xenograft studies, 1×10^7 Hep3B cells transfected with MCM4 shRNA and controls were

subcutaneously injected into the left flank of 8week-old BALB/c nude mice (Slac Laboratory Animal Co. Ltd, Shanghai, China). The mice were euthanized 4 weeks postinjection, and the tumors were excised and fixed for subsequent histopathological examination and analysis. Meanwhile, tumor volumes were measured twice a week after two weeks, tumor volume = 1/2 (length × width^2). All animal experiments were approved by the Animal Care and Use Committee of Tianjin Medical University Cancer Institute & Hospital.

2.10. Statistical analyses

SPSS.22.0 statistic software (IBM Corp.) was applied to analyze the data. All data are presented as the mean ± SD. Student's *t*-test was used for continuous variables, χ^2 tests were applied to analyze categorical variables. Survival of patients was plotted using Kaplan-Meier method. *P*-value was two-sided and $p < 0.05$ was considered to indicate a statistically significant difference.

3. Results

3.1. MCM4 was highly expressed in hepatocellular carcinoma

To explore the potential roles of MCM4 in hepatocellular carcinoma, we first compared the mRNA expression of MCM4 in hepatocellular carcinoma and normal liver tissues by Bioinformatics analysis. Differential gene expression analysis was conducted from GTEx and TCGA database and 369 primary HCC samples and 160 normal liver tissues were analyzed. As Figure 1A shows, MCM4 was significantly overexpressed in HCC. Moreover, we further explored the expression of MCM4 in serval HCC cell lines through public dataset (CCLE). As Figure 1B shows, MCM4 represented a high expression level in all five HCC cell lines. Next, we investigated the expression of MCM4 protein in HCC and normal liver tissues from 102 patients *via* IHC. Similar to mRNA expression, the expression of MCM4 protein was significantly overexpressed in HCC (Figure 1). Moreover, the positive signal of MCM4 was mainly expressed in the nuclei of tumor cells and showed typical strong and weak staining (Figurer 1C). In contrast, normal liver tissues barely expressed MCM4 (Figure 1D).

3.2. High expression of MCM4 correlated with clinicopathological variables and prognosis of HCC

To investigate the correlation between MCM4 protein expression status and clinical pathological characteristics of HCC patients, we divided HCC patients into two groups according to the expression of MCM4 protein. The associations between MCM4 protein expression

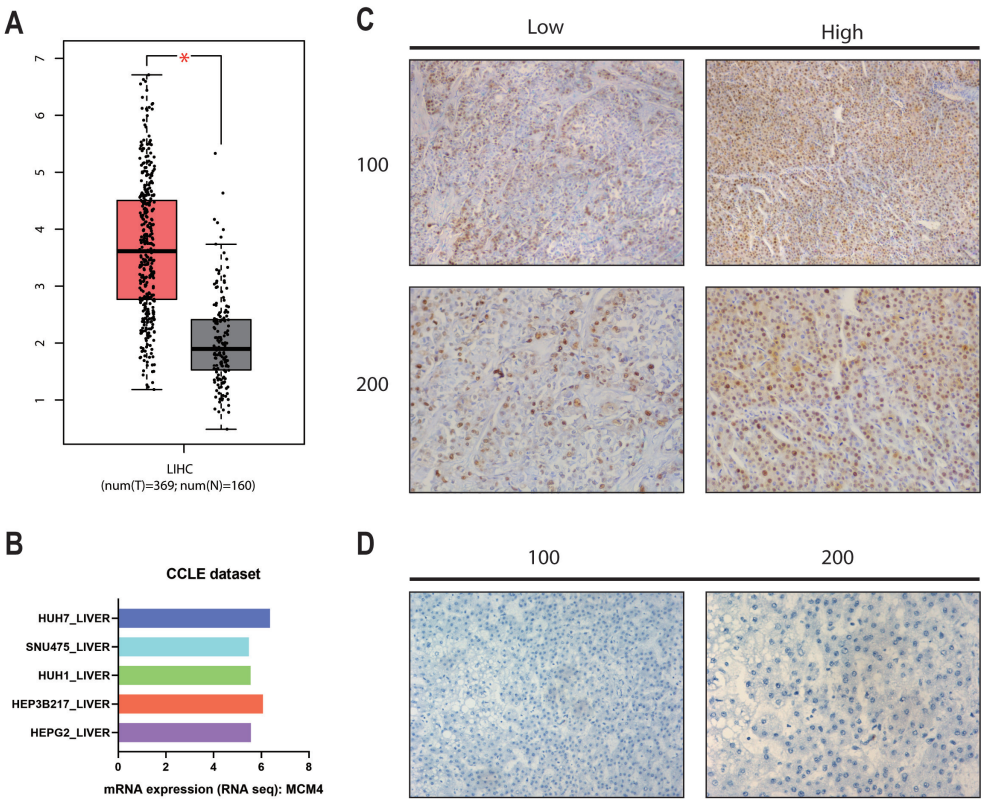

Figure 1. The expression of MCM4 in human HCC cell lines and tissues. (A) The expression of MCM4 mRNA level in HCC and normal liver tissues. **(B)** MCM4 mRNA expression in the CCLE dataset. **(C)** Immunostaining showed high and low expression of MCM4 in HCC tissues. **(D)** Immunostaining showed negative or weak expression of MCM4 in adjacent benign liver tissues.

and clinicopathological features are shown in Table 1. High expression of MCM4 protein was significantly correlated with larger tumor size ($p = 0.043$). As for other clinicopathological features including age, gender, number of tumor nodes, and AFP level, no associations were found (all $p > 0.05$). On the other hand, we assessed the association between MCM4 expression and prognosis to identify the prognostic value of MCM4 for HCC. Overall survival (OS) and disease-free survival (DFS) information were obtained from TCGA database. A significant correlation was found between MCM4 expression and adverse clinical outcomes including short OS and DFS of HCC patients (Figure 2A and 2B).

3.3. MCM4 promotes the proliferation of HCC cancer cells

To understand the potential roles of MCM4 in malignant behavior of HCC, we inhibited the expression of MCM4 in HCC cancer cells. MCM4 expression was knocked down in both Hep3B and SNU-475 cells using shRNA. Both RT-PCR and Western blot results showed that shRNA worked as we expected, the expression of MCM4 was dramatically decreased in the shRNA group (Figure 3A and 3B).

Next, we tested whether loss-of-function of MCM4 is correlated with the proliferation of HCC cells by MTT assay and colony formation arrays. We found that downregulated expression of MCM4 significantly inhibits the proliferation of Hep3B and SNU-475 cells compared to controls ($p < 0.05$), manifested as decreased cell proliferation rate and colony formation (Figure 4A and 4B).

3.4. Downregulated expression of MCM4 suppressed the tumorigenicity of HCC cells *in vivo*

To further explore whether the role of MCM4 was

Table 1. Relationships of MCM4 and clinicopathological characteristics in 102 patients with hepatocellular carcinoma

Feature	All ($n = 102$)	MCM4 expression		χ^2	p
		Low ($n = 46$)	High ($n = 56$)		
Age (year)					
< 60	64	25	39	2.527	0.112
≥ 60	38	21	17		
Gender					
Male	56	29	27	2.243	0.134
Female	46	17	29		
Number of tumor nodes					
Single	44	20	24	0.004	0.950
Multiple ≥ 2	58	26	32		
Tumor size					
< 5 cm	40	23	17	4.088	0.043*
≥ 5 cm	62	23	39		
AFP (ng/mL)					
< 50	34	15	19	0.020	0.888
≥ 50	68	31	37		

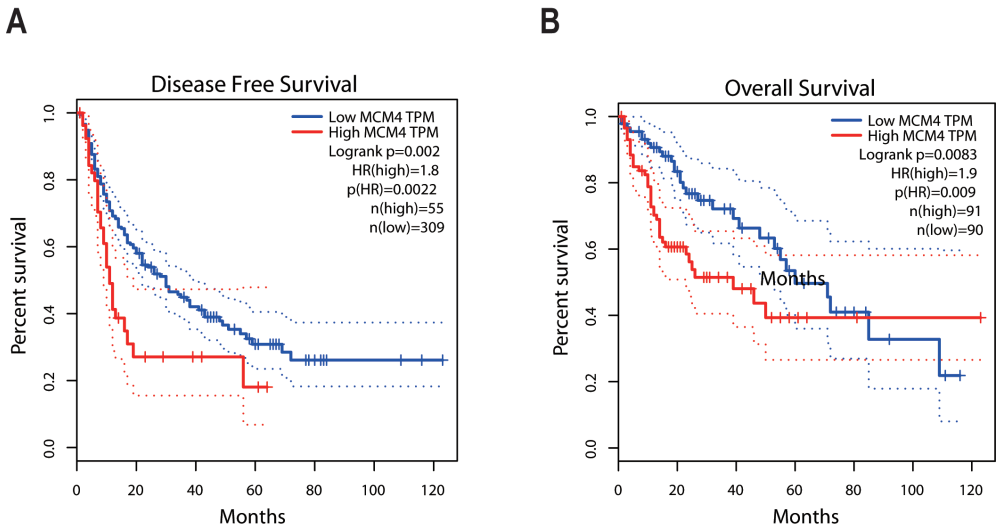

Figure 2. High expression of MCM4 as a prognostic factor of human HCC. (A) Kaplan-Meier survival analysis of disease-free survival for MCM4 expression in HCC. **(B)** Kaplan-Meier survival analysis of overall survival for MCM4 expression in HCC.

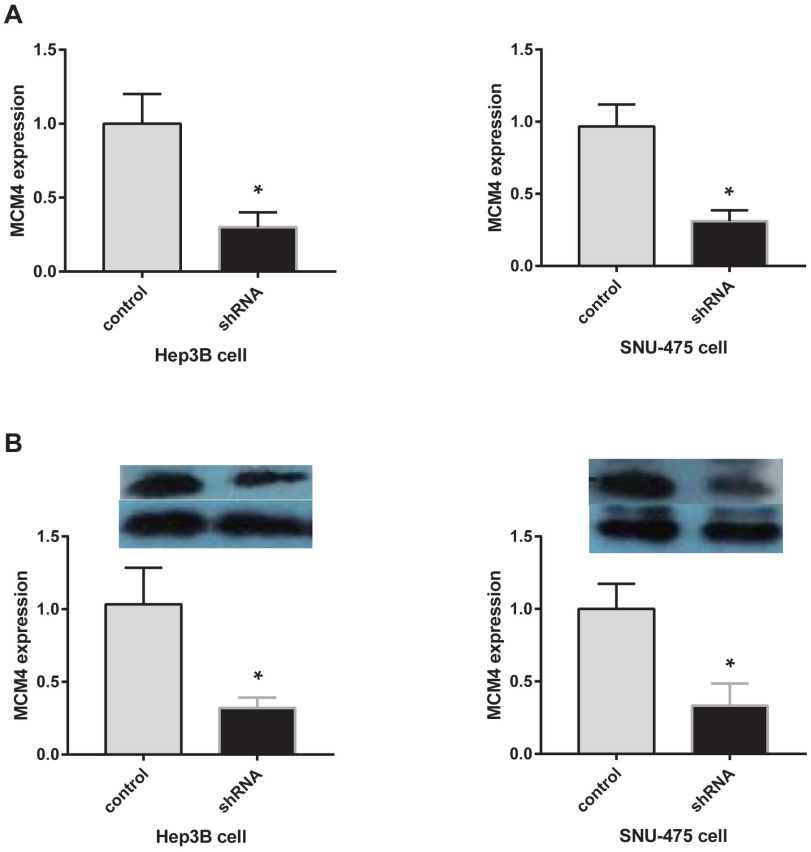

Figure 3. Stably knock down of MCM4 by shRNA in both Hep3B and SNU-475 cells. (A, B) RT-PCR and Western blot showed lower expression level of MCM4 in shRNA group ($p < 0.05$), compared to the control group. (*$p < 0.05$)

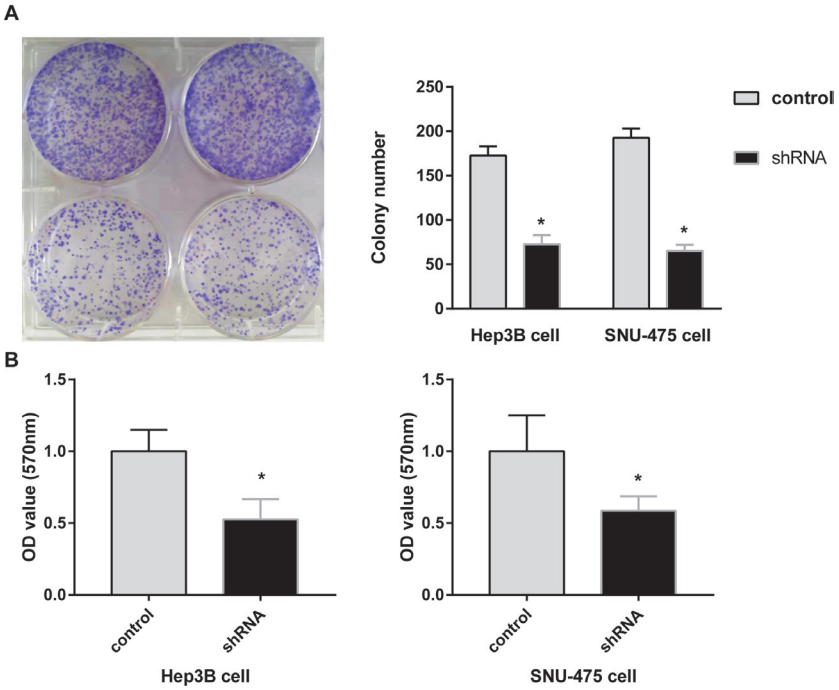

Figure 4. Knock down MCM4 in HCC cancer cells inhibited tumor cell proliferation. (A) Typical images of colony-forming assay and its quantification demonstrated that colony rate of shRNA group was significantly lower than control group in both cancer cell lines ($p < 0.05$). **(B)** OD value of MTT assay suggested that cell proliferation rate of shRNA group was lower than control group in both cancer cell lines ($p < 0.05$). shRNA, short hairpin RNA. (*$p < 0.05$)

associated with abnormal *in vitro* behavior and could translate into abnormal tumorigenesis *in vivo*, cells from the MCM4 shRNA group and control group were injected subcutaneously into athymic mice respectively. The tumor volumes were measured twice a week after two weeks. As the growth curve shown in Figure 5A, tumor growth of the shRNA group was significantly slower than that of the control group ($p < 0.05$). Meanwhile, we also performed IHC to detect the expression of MCM4 in subcutaneous tumors. Consistently, MCM4 expression was dramatically decreased in the shRNA group, which indicated that an effective and stable knock-down of MCM4 was expressed in mouse tumors (Figure 5B).

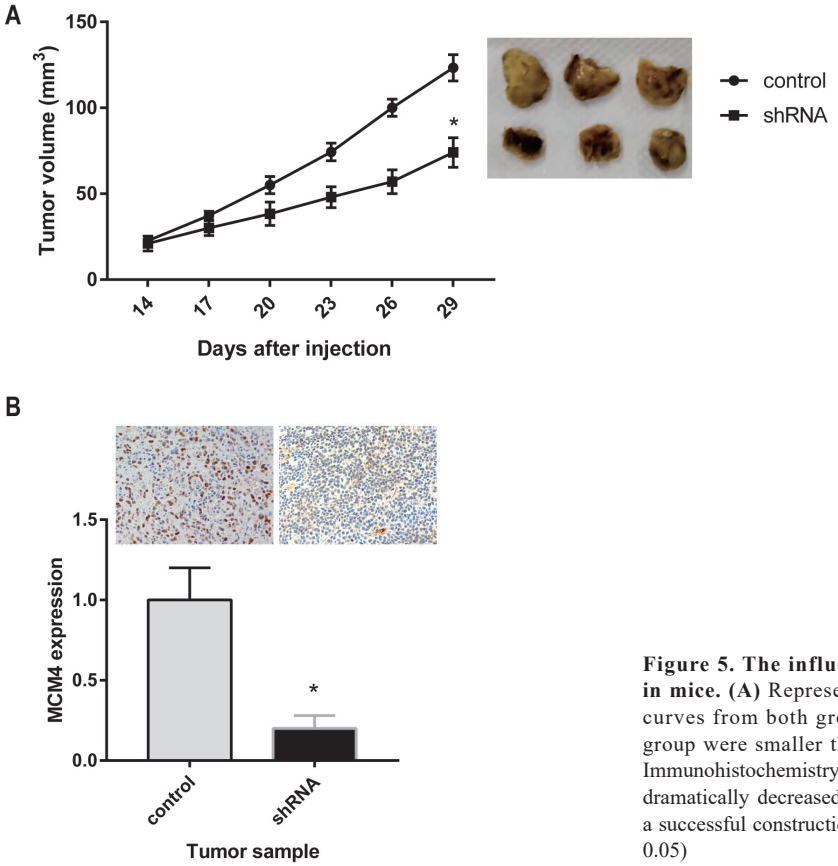

Figure 5. The influence of MCM4 on tumor growth of HCC in mice. (A) Representative images of tumors and tumor growth curves from both groups are shown. Tumor volumes of shRNA group were smaller than that of the control group ($p < 0.05$). **(B)** Immunohistochemistry demonstrated that the expression of MCM4 was dramatically decreased in mouse tumors ($p < 0.05$), which suggested a successful construction of MCM4 knock down model in mice. (*$p < 0.05$)

4. Discussion

In this study, we explored the potential role of MCM4 in HCC. We first showed that MCM4 was overexpressed in HCC tissues and high MCM4 expression represents a poor clinical outcome. Furthermore, we investigated the function of MCM4 in HCC aggression. Consistent with previous reports, MCM4 may be an effective marker and probably even a potential therapeutic target for malignant tumors, including HCC.

MCM4 is part of the MCM2–7 heterohexameric complex that is involved in origins of DNA replication prior to S phase (*8*). Improper replication fork progression can lead to stalled forks, the potential for incomplete DNA replication and even fork collapse which may lead to double strand break (DSB) formation (*8,13*). Therefore, the MCM proteins play important roles in maintaining genomic integrity. Deregulation of MCM proteins including MCM4 may contribute to cell proliferation and tumorigenesis. In our study, we demonstrated that MCM4 plays an important role in HCC cell proliferation. Knocking down MCM4 significantly decreased HCC cell proliferation rate and colony formation. Consistent with our findings, Choy B *et al.* investigated the correlation between MCM4 and MCM7 expression and Ki-67, Bmi1, and cyclin E expression in serval tumor types. They found that the percentage of MCM4 expression to be significantly correlated with Ki-67, Bmi1, and cyclin E expression in esophageal carcinoma and precancerous lesions (*3*). Bagley *et al.* (*8*) identified a mutant allele of MCM4 in a spontaneous mouse model for dominantly inherited T-cell leukemia/lymphoma, and this MCM4 allele promoted the accumulation of focal chromosomal gains and losses, including aberration at the Notch1 locus that drives the formation of T-cell leukemia/lymphoma. Shima *et al.* (*9*) isolated a hypomorphic mutation of MCM4 in a phenotype-based screen for chromosome instability in mice and the mutation caused exclusively mammary adenocarcinoma in approximately 80% of homozygous females. They (*14*) also found that hypomorphic alleles of the genes encoding the subunits of the MCM2-7 complex may increase breast cancer risk.

The current status of HCC diagnosis and treatment urgently requires us to investigate more underlying mechanisms. Plenty of studies have reported that aberrant expression of MCM4 can be a promising prognostic marker and even a therapeutic target in a number of malignancies (*4,6-10*). In our study, the data from public databases suggested that high expression of MCM4 was correlated with clinical pathological characters such as tumor size. Moreover, a high level of MCM4 was associated with poorer OS and DFS of HCC patients. All these results indicated that MCM4 may be a potential prognostic predictor, which plays a great role in tumor progression. Similar to our results, Huang *et al.* reported that increased expression of MCM4 might

be associated with pathological staging and it may be a valuable molecular marker involved in the development and/or genesis of esophageal cancer (*10*). Using public databases including TCGA and The Protein Atlas (TPA) database, Ahluwalia P *et al.* identified a novel 4 gene prognostic signature with clinical utility in colorectal cancer containing MCM4 (*15*). Moreover, a study also developed a four-gene predictive model of clinical responses to aromatase inhibitors in breast cancer patients by applying MCM4 (*16*).

In conclusion, we first showed the roles of MCM4 in HCC. Though more research is still needed to explore and verify the exact underlying mechanisms of HCC development and progression, we speculate that MCM4 can be a prognostic marker and even a therapeutic target for HCC.

Funding: This work was supported by the National Natural Science Foundation of China (No. 81471761, No.81501568) and the National Key Clinical Specialist Construction Programs of China (No. 2013-544).

Conflict of Interest: The authors have no conflicts of interest to disclose.

References

1. Yardimci H, Walter JC. Prereplication-complex formation: a molecular double take? Nat Struct Mol Biol. 2014; 21:20-25.
2. Forsburg SL. Eukaryotic MCM proteins: beyond replication initiation. Microbiol Mol Biol Rev. 2004; 68:109-131.
3. Choy B, LaLonde A, Que J, Wu T, Zhou Z. MCM4 and MCM7, potential novel proliferation markers, significantly correlated with Ki-67, Bmi1, and cyclin E expression in esophageal adenocarcinoma, squamous cell carcinoma, and precancerous lesions. Hum Pathol. 2016; 57:126-135.
4. Bochman ML, Schwacha A. The Mcm complex: unwinding the mechanism of a replicative helicase. Microbiol Mol Biol Rev. 2009; 73:652-683.
5. Giaginis C, Vgenopoulou S, Vielh P, Theocharis S. MCM proteins as diagnostic and prognostic tumor markers in the clinical setting. Histol Histopathol. 2010; 25:351-370.
6. Kikuchi J, Kinoshita I, Shimizu Y, Kikuchi E, Takeda K, Aburatani H, Oizumi S, Konishi J, Kaga K, Matsuno Y, Birrer MJ, Nishimura M, Dosaka-Akita H. Minichromosome maintenance (MCM) protein 4 as a marker for proliferation and its clinical and clinicopathological significance in non-small cell lung cancer. Lung Cancer. 2011; 72:229-237.
7. Ladstein RG, Bachmann IM, Straume O, Akslen LA. Ki-67 expression is superior to mitotic count and novel proliferation markers PHH3, MCM4 and mitosin as a prognostic factor in thick cutaneous melanoma. BMC Cancer. 2010; 10:140.
8. Bagley BN, Keane TM, Maklakova VI, Marshall JG, Lester RA, Cancel MM, Paulsen AR, Bendzick LE, Been RA, Kogan SC, Cormier RT, Kendziorski C, Adams DJ, Collier LS. A dominantly acting murine allele of Mcm4 causes chromosomal abnormalities and promotes tumorigenesis. PLoS Genet. 2012; 8:e1003034.
9. Shima N, Buske TR, Schimenti JC. Genetic screen for chromosome instability in mice: Mcm4 and breast cancer. Cell Cycle. 2007; 6:1135-1140.
10. Huang XP, Rong TH, Wu QL, Fu JH, Yang H, Zhao JM, Fang Y. MCM4 expression in esophageal cancer from southern China and its clinical significance. J Cancer Res Clin Oncol. 2005; 131:677-682.
11. Tang Z, Li C, Kang B, Gao G, Li C, Zhang Z. GEPIA: a web server for cancer and normal gene expression profiling and interactive analyses. Nucleic Acids Res. 2017; 45:W98-W102.
12. Livak KJ, Schmittgen TD. Analysis of relative gene expression data using real-time quantitative PCR and the 2(-Delta Delta C(T)) Method. Methods. 2001; 25:402-408.
13. Allen C, Ashley AK, Hromas R, Nickoloff JA. More forks on the road to replication stress recovery. J Mol Cell Biol. 2011; 3:4-12.
14. Shima N, Alcaraz A, Liachko I, Buske TR, Andrews CA, Munroe RJ, Hartford SA, Tye BK, Schimenti JC. A viable allele of Mcm4 causes chromosome instability and mammary adenocarcinomas in mice. Nat Genet. 2007; 39:93-98.
15. Ahluwalia P, Mondal AK, Bloomer C, Fulzele S, Jones K, Ananth S, Gahlay GK, Heneidi S, Rojiani AM, Kota V, Kolhe R. Identification and clinical validation of a novel 4 gene-signature with prognostic utility in colorectal cancer. Int J Mol Sci. 2019; 20.
16. Turnbull AK, Arthur LM, Renshaw L, Larionov AA, Kay C, Dunbier AK, Thomas JS, Dowsett M, Sims AH, Dixon JM. Accurate prediction and validation of response to endocrinetherapy in breast cancer. J Clin Oncol. 2015; 33:2270-2278.

Received January 10, 2021; Revised February 25, 2021; Accepted March 3, 2021.

**Address correspondence to:*
Zhi Guo, Department of Interventional Therapy, Tianjin Medical University Cancer Institute & Hospital, Huanhuxi Road, Hexi District, Tianjin 300060, China.
E-mail: guozhi9960@sina.com

Released online in J-STAGE as advance publication March 12, 2021.

Original Article

DOI: 10.5582/bst.2021.01017

Role of circulating tumor cell detection in differentiating tumor recurrence from treatment necrosis of brain gliomas

Faliang Gao[1,2,3,§], Wenyan Zhao[4,§], Mingxiao Li[2,3], Xiaohui Ren[2,3], Haihui Jiang[2,3], Yong Cui[2,3], Song Lin[2,3,*]

[1] Department of Neurosurgery, Zhejiang Provincial People's Hospital, People's Hospital of Hangzhou Medical College, Hangzhou, China; Key Laboratory of Endocrine Gland Diseases of Zhejiang Province, China.
[2] Department of Neurosurgery, Beijing Tiantan Hospital, Capital Medical University, Beijing, China;
[3] China National Clinical Research Center for Neurological Diseases, Beijing, China;
[4] General Practice Department, Zhejiang Provincial People's Hospital, People's Hospital of Hangzhou Medical College, Hangzhou, Zhejiang, China.

SUMMARY Differentiating treatment necrosis from tumor recurrence poses a diagnostic conundrum for many clinicians in neuro-oncology. To investigate the potential role of circulating tumor cells (CTCs) detection in differentiating tumor recurrence and treatment necrosis in brain gliomas, we retrospectively analyzed the data of 22 consecutive patients with tumor totally removed and new enhancing mass lesion(s) showed on MRI after initial radiotherapy. The 22 patients were finally classified into tumor recurrence group (n = 10) and treatment necrosis group (n = 12), according to evidence from the clinical course (n = 11) and histological confirmation (n = 11). All 22 patients received CTCs detection, and DSC-MRP and 11C-MET-PET were performed on 20 patients (90.9%) and 17patients (77.3%) respectively. The data of the diagnosis efficacy to differentiate the two lesions by CTC detection, MPR and PET were analyzed by ROC analysis. The mean CTCs counts were significantly higher in the tumor recurrence group (6.10 ± 3.28) compared to the treatment necrosis group (1.08 ± 2.54, $p < 0.001$). The ROC curve showed that an optimized cell count threshold of 2 had 100% sensitivity and 91.2% specificity with AUC = 0.933 to declare tumor recurrence. The diagnostic efficacy of CTC detection was superior to rCBV of DSC-MRP and $rSUV_{max}$ in MET-PET. Furthermore, we observed that CTCs detection could have a potential role in predicting tumor recurrence in one patient. Our research results preliminarily showed the potential value of CTC detection in differentiating treatment necrosis from tumor recurrence in brain gliomas, and is worthy of further confirmation with large samples involved.

Keywords glioma, circulating tumor cell, tumor recurrence, treatment response, radionecrosis

1. Introduction

The current treatment regimen for patients with brain gliomas includes a combination of maximal safe tumor resection, radiation therapy, and chemotherapy after surgery (*1*). This combinatory therapy has prolonged patient life spans, but the increasing use of radiation therapy carries the risk of side effects on the surrounding tissues, resulting in radiation necrosis, while the adjuvant use of temozolomide can exacerbate this side effect (*2*). This treatment response, named "treatment necrosis", is difficult to differentiate from tumor recurrence, as these two outcomes often manifest with similar clinical symptoms and image appearance that characterizes a new contrast-enhancing lesion appearing on a patient's follow-up imaging (*3*). Furthermore, it has also been found that a new contrast-enhancing lesion observed *via* imaging is neither solely necrotic tissue or tumor, but rather a mixture of both lesions, which adds to the complexity of lesion determination (*4*). Given that the treatment for these two lesions differs significantly from one another, differentiating treatment necrosis from tumor recurrence poses a diagnostic conundrum for many clinicians in neuro-oncology.

To date, histological confirmation by biopsy or surgical resection is still the most reliable approach for differentiating treatment necrosis from tumor recurrence. However, both methods are expensive and invasive, and pose an unnecessary risk that negatively impacts patients' lives (*5*). Currently, an increased interest has arisen in development of numerous noninvasive functional imaging modalities, such as Diffusion-

weighted Imaging (DWI), MRI resonance Spectroscopy (MRS), MRP, PET, single-photon emission computed tomography (SPECT) and CT perfusion (CTP), to help differentiate these two lesions (*6*); however, the diagnosis efficiency is not perfect. According to a systematic review study, the diagnostic sensitivity for the two most commonly used imaging modalities, DSC-MRP and 11C-MET-PET, is 79.8% and 76.8% respectively, with a diagnostic specificity of 76.8% and 82.4% respectively (*6*). It is also reported that even with the same imaging modality, the results are not always consistent (*7*). Unfortunately, a noninvasive and reliable method with high diagnostic specificity and sensitivity to distinguish these two lesions is still unavailable.

In recent years, as a major component of "liquid biopsies", circulating tumor cell (CTC) detection has been applied in monitoring treatment response in diverse types of solid tumors (*8-10*), but its application in brain glioma monitoring systems is quite limited. This was mainly due to the traditional concept that CTCs most originally came from the primary tumor and then reached the vascular compartment, but the specific brain environment prevented glioma cells from descending into the blood (*11*). However, this misconception has been corrected by several studies in the past three years. By using different CTCs detection approaches, researchers have successfully identified CTCs in high-grade brain gliomas (*12-14*). Furthermore, in our previous study we demonstrated that CTCs could be detected in all seven common pathological subtypes of brain gliomas, and to some extent, showed its superiority to rCBV of MRP in differentiating treatment necrosis from tumor recurrence in five patients (*15*). The previous studies have given us greater interest in CTC application in differentiating these two lesions, and we postulated that CTCs detection could provide a new perspective towards the diagnosis of treatment necrosis and tumor recurrence in brain gliomas.

In this regard, for the present study, a series of 22 patients with tumor totally removed and afflicted with new enhancing lesions formed after radiotherapy (combined with or without temozolomide) on conventional-contrast MRI imaging were enrolled. Data of CTCs count, rCBV of DSC-MRP and $rSUV_{max}$ of 11C-MET-PET before treatment planning were collected and the diagnosis efficacy of CTC, DSC-MPR and 11C-MET-PET to differentiate treatment necrosis from tumor recurrence were compared by receiver operating characteristic (ROC) analysis. To our knowledge, this is one of the few systematic studies to evaluate the application value of CTC detection and traditional imaging in distinguishing radiation necrosis from tumor recurrence in brain gliomas.

2. Materials and Methods

2.1. Patients and ethics

To perform this study, a series of consecutive patients were retrospectively screened to be included in our study based on all the following criteria: *i*) histologically proven primary brain glioma at first presentation, prior gross total resection of tumor, and prior treatment with radiotherapy, with or without concurrent and adjuvant temozolomide treatment; *ii*) suspicion of new tumor recurrence or treatment necrosis having a new enhancing mass lesion(s) on the initial post-radiotherapy MRI as compared to the pre- radiotherapy MRI; *iii*) proof of tumor recurrence on the basis of direct histology (presence of as any amount of tumor), and proof of treatment necrosis on the basis of either direct histology (complete absence of tumor) or stability of imaging (substantial regression or stability of the enhancing lesions on serial follow-up MRI scans without additional treatment for at least 4 months) (*16,17*), and *iv*) all patients received CTCs detection, and at least one functional imaging modality (DSC-MRP or 11C-MET-PET) before the operation, biopsy or arranged next follow-up period; the interval between CTCs detection, DSC-MRP and 11C-MET-PET exams was within 30 days.

A total of 33 patients with new enhanced mass lesion(s) on the initial post- radiotherapy MRI were screened, including 6 patients with tumor sub-totally removed, 4 patients without any functional imaging modality preformation and 1 patient lost to follow up. Finally, 22 patients who met the above criterial were included in this study.

In our daily clinical work, surgical operations or biopsies were preferred for patients suspicious of tumor recurrence under the following situations: *i*) Evidence supported by at least one functional imaging (MRP or PET); *ii*) Clinical symptoms could not be relieved by steroids or mannitol; *iii*) Family members' willingness and doctors' experience (especially when MRP and PET inspection results are inconsistent). In our study, for patients suspicious of treatment necrosis and were arranged for observation, if their image features got worse in the next follow-up and then received additional chemotherapy, these patients were excluded. Since this is a retrospective study, CTC detection results were not used as a consideration for subsequent treatment of patients.

Patients in our study were all from Beijing Tiantan hospital. This study was approved by the Medical Ethics Committee of Beijing Tiantan hospital (2017-2021) and written informed consent was obtained from all patients and healthy volunteers. To avoid bias, different experimental procedures in CTCs detection, including blood sample collection, enrichment, SE-iFISH and results interpretation were performed by different personnel. Results of DSC-MRP and 11C-MET-PET were analyzed by consensus interpretation of two board-certified neuro-radiologists who were blinded to the tissue diagnosis. The histological result of all specimens

was independently evaluated by three neuro-pathologists, with the diagnosis adhering to the WHO classification of CNS tumors. In our study, all patients underwent chest X-ray examination and blood tests routinely in our clinic, and those with abnormal results were not enrolled in our study.

2.2. CTC Subtraction enrichment and Immunostaining-FISH

The experimental procedures for CTC subtraction enrichment and immunostaining-FISH were mainly performed as previously described (*15,18*), with the procedure for CTCs images identification and collection improved. In CTC subtraction enrichment procedures, briefly, 7.5 mL peripheral blood was collected and centrifuged. Solutions above RBCs were collected and incubated with 150 μl of anti-WBC and endothelial cell immunomagnetic beads for 15 min and were centrifuged. The resulting pellet containing monolayer rare cells was thoroughly mixed with 100 μl cell fixative, followed by application to the formatted and coated CTC slide (Cytelligen). Next the immunostaining-FISH experimental procedure was performed. At first, samples on the coated CTC slides were subjected to Vysis Centromere Probe (CEP8) SpectrumOrange (Abbott Laboratories, Abbott Park, IL, USA) hybridization for 90 min using a S500 StatSpin ThermoBrite Slide Hybridization/Denaturation System (Abbott Molecular, Des Plaines, IL, USA), followed by incubation with Alexa Fluor 594 conjugated monoclonal anti-CD45, anti-GFAP (BD, USA). CTC is defined as $DAPI^+$, $CD45^-$, and heteroploidy CEP8 signal.

In our previous study, images of the CTCs were collected using a fluorescence microscope and visually identified by a pathologist. In this study, this procedure was improved so that images of the tumor cells were identified by a Zeiss Metafer-iFISH automated CTCs scanning system (Zeiss and MetaSystems, Germany, Cytelligen, USA).

2.3. DSC-MRP

MRI scans (n = 20) were performed using 3.0-T magnets (Trio, SIEMENS, Germany). DSC sequences were acquired using 5-mm slice thickness and 1.5-mm gap, and were obtained using gradient-echo echo-planar images (repetition time/echo time = 1400/32 ms, matrix 320 × 320, flip angle 90°, number of slices 19). A standard dose (0.2 mL/kg of body weight, maximum dose 20 mL) of gadopentetate dimeglumine (BEILU Pharmaceutical CO. LTD, Beijing, China) contrast was injected though a peripheral Angiocath (22 gauge) using 5 mL/s and immediately followed by a 20-ml saline flush at the same rate. Then multi-section image data were acquired every second for a total of 75 s, with the bolus contrast injection occurring after 10 s.

The axial DSC images were transferred to an offline commercially available workstation (MAGNETOM Trio. A Tim System, SIEMENS, Germany) and processed using commercially available software (NUMARIS/4, syngo MRB17, SIEMENS). To analyze the cerebral blood volume (CBV), ROI analysis for CBV was performed as follows: A single contrast section containing the maximum diameter of the enhancing lesion was selected, and an ROI was manually drawn around the entire enhancing lesion. Areas of hemorrhage, blood vessels, susceptibility artifacts, and cystic or necrotic change were excluded. Control ROI was placed over the contralateral normal-appearing white matter (CBV_{NL}) to calculate relative cerebral blood volume (rCBV). The rCBV measurements were recorded as CBV_{ROI} / CBV_{NL} as previously described (*16*). Negative enhancement integral perfusion maps were reconstructed using standard algorithms; blood vessels, cystic/necrotic changes, and areas of susceptibility from hemorrhage, bone, or air were excluded from the ROIs.

2.4. 11C-MET-PET

11C-MET-PET images (n = 17) were performed using a previously described methodology (*19*). Briefly, PET imaging was performed parallel to the orbit meatal line. A molded plastic facemask was used to restrict head motion. Images were obtained by intravenous bolus injection of 200-550 MBq of MET. All images were reconstructed using a conventional filtered back-projection algorithm, and were corrected for non-uniformity of detector response, dead time, random coincidences, and scattered radiation. After fusing the PET and contrast-enhanced T1-weighted images using commercial software (Xeleris 3 Functional Imaging Workstation, GE, USA), each ROI was manually placed on the lesion (including the pixel with the highest accumulation), using the contralateral region of the normal gray matter as a reference. The uptake lesion-to-normal tissue (L_{max}/N_{max}) ratios $rSUV_{max}$ were calculated from the maximum uptake of lesions and the reference area as visible in11C-MET-PET.

2.5. Statistical analysis

SPSS version 22.0 and MedCalc Version 16.8.4 (a statistical software package for biomedical research. including ROC curve analysis, method comparison and quality control tools, *https://www.medcalc.org/index.php*) were used for statistical analyses. Data were presented as the mean ± standard deviation (data obeyed normal distribution) or median with range (data that did not obey normal distribution). Comparisons between treatment necrosis and tumor recurrence groups were performed using Wilcoxon rank sum tests. Diagnosis efficacy of CTC, MPR and PET to differentiate treatment

necrosis from tumor recurrence were evaluated by ROC analysis. Optimal threshold values of CTCs count, rCBV and $rSUV_{max}$ were obtained by AUC analysis derived from ROC curves, to maximize the sum of sensitivity and specificity. In this study, $p < 0.05$ was considered statistically significant.

3. Results

3.1. Clinical characteristics, final diagnosis and grouping of these 22 patients

The authors identified 22 patients (12 males and 10 females, median age: 41 years, range from 31 to 55) who fulfilled the study criteria. All 22 patients received CTCs detection, and DSC-MRP and 11C-MET-PET were performed on 20 patients (90.9%) and 17 patients (77.3%) respectively. These 22 patients were divided into two groups, a tumor recurrence group (n = 10) and a treatment necrosis group (n = 12), according to evidence from the clinical course (n = 11) or histological confirmation (n = 11). Typical images of these two patient groups are shown in Figure 1.

In these two groups, no significant difference of the patients' baseline was observed. The mean age in the tumor recurrence and treatment necrosis group was 45.1 ± 5.28 and 39.8 ± 7.51 years respectively, and no significant difference (p = 0.073) was found. The sex distribution (male/female) of tumor recurrence and treatment necrosis group was 1.5:1 and 1:1 respectively, with no significant difference observed (p = 0.639). The ratio of high/low grade gliomas was 8:2 and 8:4 in tumor recurrence and treatment necrosis group respectively, which also revealed no significant difference (p = 0.481). The mean interval from radiotherapy was 12.2 ± 8.95 months (range: 3-29 months) in the tumor recurrence group and 13.9 ± 14.5 months (range: 3-37 months) in the treatment necrosis group, and no significance was observed (p = 0.748). Details on the patients' clinical characteristics are summarized in Table 1.

3.2. CTCs detection

Figure 2 A-E shows a CTC enriched from peripheral blood in one patient with GFAP positively expressed. A large strong polyploidy (≥ 5 copies) chromosome 8+ and CD45- CTC was observed, with GFAP positively expressed. WBCs surrounding CTC were diploid in chromosome 8, and stained positively for CD45. Figure

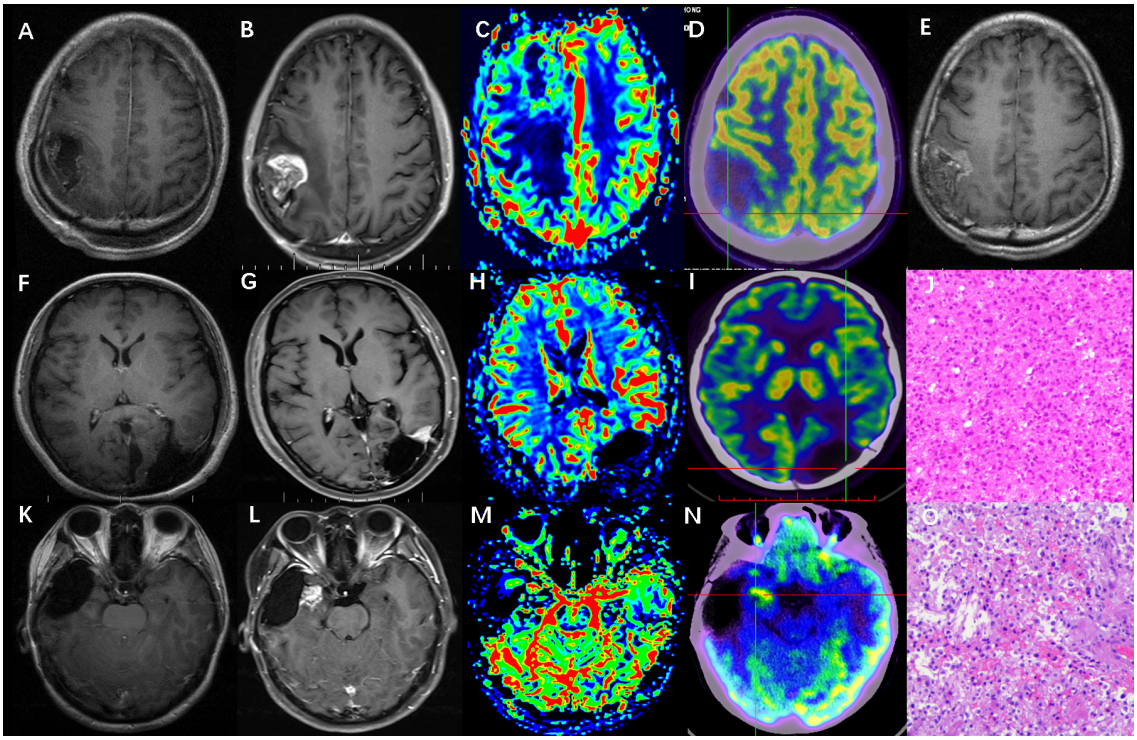

Figure 1. Typical images of 3 patients finally diagnosed as TN and TR. (A-E): 1 patient (No. 3 in table 1, CTC counts was 0) was finally diagnosed as treatment necrosis. (A) Enhancing MR image after gross total resection. **(B)** Enhancing MR image after completion of first radio-chemotherapy. **(C)** Simultaneous DSC-MRP showed hypoperfusion in the enhancing lesion. **(D)** Simultaneous 11C-MET-PET showed hypo metabolism in the enhancing lesion. **(E)** Enhancing MR image after 9 months' follow-up period, the enhancing lesion was significantly decreased. **(F-O)**:1 patient (No. 4 in table 1, CTC counts was 3) was finally diagnosed as tumor recurrence **(F-J)** and 1 patient (No. 12 in table 1, CTC counts was 1) was diagnosed as treatment necrosis **(K-O)** respectively. **(F, K)** Enhancing MR image after gross total resection. **(G, L)** Enhancing MR image after completion of first radio-chemotherapy. **(H, M)** Simultaneous DSC-MRP showed hyperperfusion in the enhancing lesion. **(I, N)** Simultaneous 11C-MET-PET showed hyper metabolism in the enhancing lesion. **(J, O)** Pathological findings of tumor recurrence **(J)** and treatment necrosis **(O)** after the subsequent surgery (HE, 10×10).

Table 1. Characteristics and diagnosis of 22 patients who underwent CTCs detection, DSC-MRP and 11C-MET-PET

No.	Age (years)/Sex	Primary diagnosis	Adjuvant Thera-py/Interval from RT(month)	KPS	CTC counts	DSC	MEG-PET	TR or TN by Cl/ Pa (Bio/Res)
						$rCBV_{ROI}$	$rSUV_{max}$	
1	55/F	OA	TMZ/17	90	0	0.66	no exam	TN(Cl)
2	45/M	GBM	TMZ/13	90	2	2.38	3.00	TR(Pa, Res)
3	41/M	GBM	TMZ/3	90	0	0.52	0.76	TN(Cl)
4	45/F	GBM	TMZ/6	70	3	2.27	3.83	TR(Pa. Res)
5	41/F	GBM	TMZ/7	90	3	2.07	3.80	TR(Pa, Res)
6	31/M	AOA	TMZ/4	80	0	2.67	1.82	TN(Cl)
7	41/M	OA	None/21	80	5	2.43	3.70	TR(Pa, Res)
8	53/M	AO	TMZ/3	90	0	0.85	1.71	TN(Cl)
9	46/F	AA	TMZ/29	80	8	0.65	1.93	TR(Pa, Res)
10	40/M	A	None/20	90	5	2.01	4.00	TR(Pa, Res)
11	40/F	GBM	TMZ/37	90	0	0.61	3.94	TN(Cl)
12	34/F	AA	TMZ/10	90	1	2.44	3.29	TN(Pa, Res)
13	31/F	AOA	TMZ/21	90	9	no exam	2.20	TN(Cl)
14	36/M	A	None/4	90	0	0.48	no exam	TN(Cl)
15	41/M	OA	AVM/7	90	1	0.57	no exam	TN(Cl)
16	39/F	OA	None/47	90	1	0.44	no exam	TN(Cl)
17	39/M	AA	None/11	90	1	0.48	2.50	TN(Cl)
18	47/M	GBM	TMZ/3	80	10	2.18	no exam	TR(Pa, Res)
19	37/F	GBM	TMZ/3	90	0	no exam	2.61	TN(Cl)
20	40/M	GBM	TMZ/15	70	8	2.58	4.80	TR(Pa, Bio)
21	55/F	GBM	TMZ/6	70	12	0.86	2.43	TR(Pa, Bio)
22	53/M	GBM	TMZ/5	80	5	0.55	5.70	TR(Pa, Bio)

Abbreviations: A, astrocytoma; AA, anaplastic astrocytoma; AO, anaplastic oligodendroglioma; AOA, anaplastic oligoastrocytoma; AVM, nimustine, vincristine and methotrexate; Bio, biopsy; Cl, clinically diagnosed; GBM, glioblastoma multiforme; KPS, Karnofsky performance scale; OA, oligoastrocytoma; Pa, pathologically diagnosed; Res, surgical resection; RT, radiotherapy; TMZ, temozolomide; TN, treatment necrosis; TR, tumor recurrence.

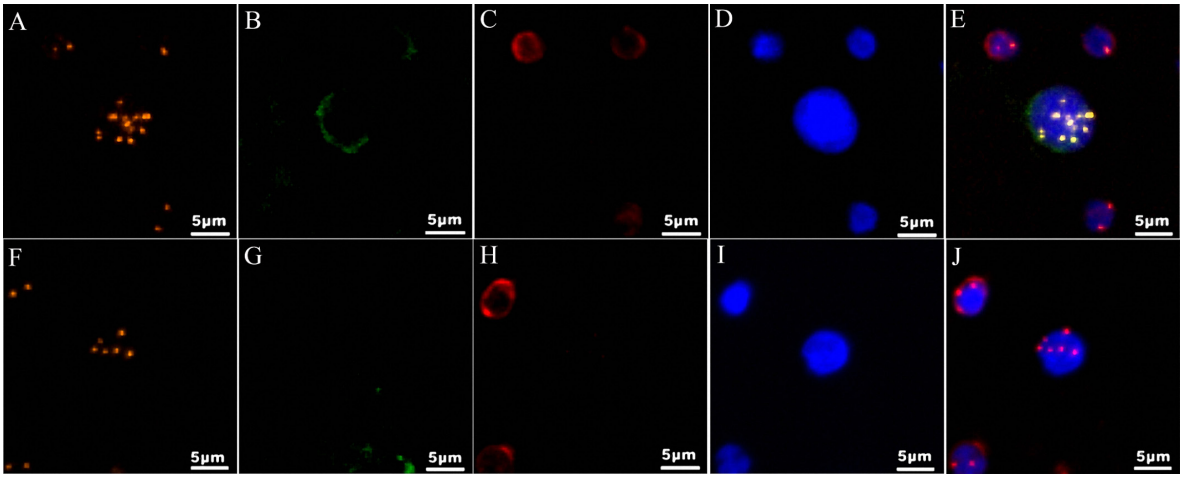

Figure 2. Characteristics of a CTC with GFAP expressed in the peripheral blood of one glioma patient. (A-D) CTC observed was $FISH^+$ (polyploidy chromosome 8, orange, A) /$GFAP^+$(green, B) / $CD45^-$ (red, C) and $DAPI^+$ (blue, D). **(E)** Four images emerged. WBCs surrounding CTC were diploid in chromosome 8, and stained positively for CD45, without GFAP expressed. **(F-J)** Image of a CTC without GFAP expressed in another patient.

2 F-J shows 1 CTC detected with GFAP negative expressed from the same patient. In our study, CTCs were found with GFAP positively expressed in only 1 patient (total 5 cells, 1 cell with GFAP positively expressed and 4 cells with GFAP negatively expressed), similar to our previous results.

No CTC was detected in 20 healthy volunteers. In 22 patients, results of CTCs detection revealed that the mean CTCs count were significantly higher in tumor recurrence group (6.10 ± 3.28), compared to treatment necrosis group (1.08 ± 2.54, $p < 0.001$), as shown in Figure 3. An optimized CTCs count threshold of 2 had 100% sensitivity and 91.2% specificity with AUC = 0.933 to declare tumor recurrence. ROC curves are shown in Figure 4A; the diagnostic results of ROC are shown in Table 2.

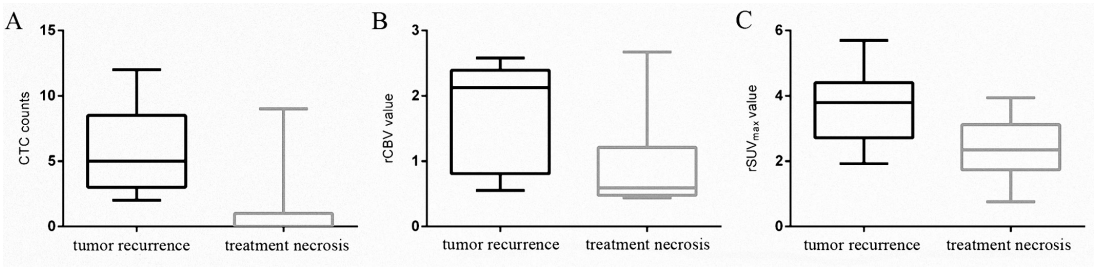

Figure 3. Box-and-whisker plots for CTCs counts, rCBV value and $rSUV_{max}$ value in TR (tumor recurrence) and TN (treatment necrosis) group.

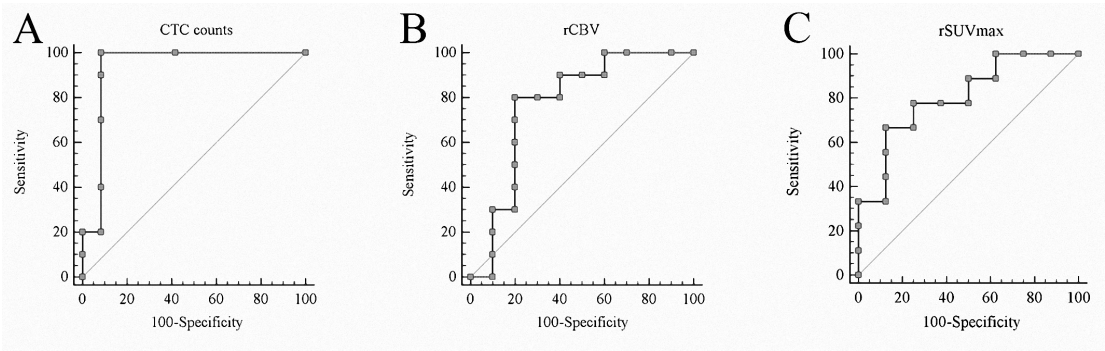

Figure 4. Roc curve associated with CTCs detection, DSC-MRP and 11C-MET-PET to differentiate tumor recurrence from treatment necrosis.

Table 2. Comparison of diagnostic results of CTCs detection, DSC-MRP, 11C-MET-PET in diagnosis of tumor recurrence in 22 patients

variables	CTCs counts (n = 22)	rCBV (n = 20)	$rSUV_{max}$ (n = 17)
Sensitivity (%)	100. 0	80. 0	66.7
Specificity (%)	91.7	80. 0	87.5
Positive predictive value (%)	90.9	80. 0	85.7
Negative predictive value (%)	100. 0	80. 0	70. 0
Accuracy (%)	95.5	80. 0	76.5

3.3. DSC-MRP

Results of DSC-MRP showed that the mean $rCBV_{ROI}$ was higher in tumor recurrence group (1.80 ± 0.79), compared to treatment necrosis group (0.96 ± 0.82, p = 0.031). An optimized $rCBV_{ROI}$ threshold of > 0.85 had 80% sensitivity and 80% specificity with AUC = 0.770 to declare tumor. ROC curves are shown in Figure 4B; the diagnostic results of ROC are shown in Table 2.

3.4. 11C-MET-PET

Results of 11C-MET-PET showed that the mean $rSUV_{max}$ was higher in tumor recurrence group (3.69 ± 1.15), compared to treatment necrosis group (2.35 ± 0.98, p = 0.022). An optimized $rSUV_{max}$ threshold of > 3.29 had 66.7% sensitivity and 87.5% specificity with AUC = 0.806 to declare tumor. ROC curves are shown in Figure 4C; and the diagnostic results of ROC are shown in Table 2.

3.5. CTCs detection could predict tumor recurrence in one of these 22 patients

A 40-year-old male suffering from a severe headache was admitted to our hospital and MR imaging showed an enhanced mass lesion in his left temporal lobe. The patient received surgical resection and was diagnosed with glioblastoma multiform (GBM) through histology. The tumors were completely removed and no enhancing lesion was observed on MRI imaging after the operation was complete (Figure 5A). After surgery, the patient was arranged to undergo radio-chemotherapy, with a total radiation dose of 6000 cGy to the extended local zone using the hyper-fractionated method. Follow-up MR imaging revealed a new enhancing lesion in the left hippocampus six months later (Figure 5B). Although a chemotherapy plan was suggested, the patient did not experience any clinical discomfort, and refused to receive any anti-tumor treatment. During the follow-up periods no obvious symptoms were detected, and

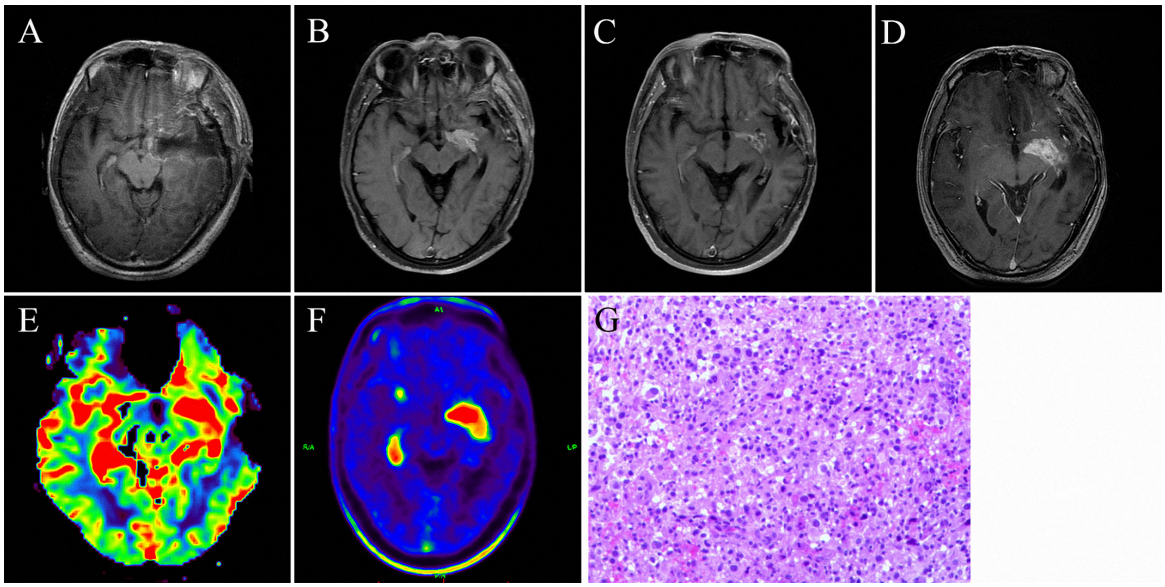

Figure 5. An illustrative case indicating the predictive role of CTCs detection in tumor recurrence. (A-D) Contrast axial T1-weighted image: **(A)** After gross total resection, there is a surgical cavity without enhancement. **(B)** After completion of radio-chemotherapy, there is a new enhancing mass lesion on the initial post- radiotherapy MRI. **(C)** Nine months later, MR imaging revealed that the enhancing lesion decreased. **(D)** Three months later, MR imaging showed that the enhancing lesion finally significantly increased. **(E)** Simultaneous DSC-MRP showed hyper perfusion in the enhancing lesion. **(F)** Simultaneous 11C-MET-PET showed hyper metabolism in the enhancing lesion. **(G)** Pathological findings of tumor recurrence of GBM after biopsy (HE, 10×10).

nine months later, the next MR imaging revealed that the enhancing lesion had significantly decreased (Figure 5C). This development suggested a diagnosis of treatment necrosis. To our surprise however, four CTCs were detected in his blood, which was higher than our previous experience in the treatment necrosis group. Given that no clinical symptoms were observed with better features on MRI imaging, the patient did not receive any anti-tumor treatment but was asked to follow up. Unfortunately, three months later, the patient was once again admitted to our hospital for memory loss and a continuous headache. MR imaging showed that the enhancing lesion had significantly increased (Figure 5D). Simultaneous DSC-MRP and 11C-MET-PET demonstrated the higher rCBV (Figure 5E) and $rSUV_{max}$ (Figure 5F) in the enhancing lesion, and CTCs detection showed that the CTCs counts increased to eight (patient No. 20 in Table 1). A biopsy was performed and histological examination resulted in a diagnosis of tumor recurrence (Figure 5G).

4. Discussion

Numerous studies have investigated the roles of different functional imaging modalities in differentiating treatment necrosis from tumor recurrence (*6,20,21*). In 2013, Komotar conducted a systematic review to explore the value of a variety of functional imaging modalities, including MRS, ASL MRI (arterial spin-labeled MR imaging), DSC-MRP, CTP, SPECT, 18F-FDG-PET and 11C-MET-PET, in the diagnosis of treatment necrosis and tumor recurrence, but most of the results were disappointing because a high sensitivity and specificity could not be achieved concurrently in one modality. Of the explored modalities, SPECT has the potential to be the best modality, but low spatial resolution and tracer uptake in normal tissues of the choroid plexus and pituitary gland have limited its clinical application (*6*). More importantly, reported results achieved by the same modality are sometimes inconsistent. For example, Tsuyuguchi reported that the sensitivity and specificity of 11C-MET-PET in differentiating treatment necrosis from tumor recurrence were 100% and 60%, respectively (*22*). While Kim's study, in contrast, reported that the sensitivity and specificity of 11C-MET-PET were 75% and 100%, respectively (*19*). Concerning another commonly used parameter, rCBV in MRP, the diagnostic efficacy in differentiating treatment necrosis from tumor recurrence is also quite variable. Sugahara and Huang reported the sensitivity of rCBV for detecting tumor recurrence was 50% and 56%, respectively (*23,24*), while Matsusue and Mitsuya reported sensitivity of 90% and 100% respectively *(25,26)*. A variety of reasons could explain this phenomenon: the inherent limitation of each functional imaging modality, the usual overlap imaging features of the two lesions, and the subjective bias involved in data analysis procedures. Thus far, insufficient and inconsistent diagnostic efficacy, together with high operational costs and low insurance coverage, has limited their clinical application, which needs further evaluation to establish their reliability and robustness in differentiating these two lesions.

In our study, 22 patients were divided into tumor

recurrence group (n = 10) and treatment necrosis group (n = 12), according to evidence from the clinical course (n = 11) or histological confirmation (n = 11). Only half of these patients' diagnoses were proven by histological confirmation, because treatment necrosis was mostly proven by clinical course (11 patients), with only 1 patient proven by histological result after surgery. This is mainly due to the very strict and complex surgical indications for these patients (described in material and methods section below); but even to do this, there was still one patient who was operated on and diagnosed with treatment necrosis finally, suffering left hemiplegia after. Another reason is that although biops were performed in many neurosurgery centers, in our institute this was not widely used.

It has been demonstrated in recent years that CTCs detection in the blood *via* so-called "liquid biopsies" has an important clinical translational value for its direct biological reflection of tumor microenvironments, without the need for repeated neurosurgical procedures with inherent risk of patient morbidity (*8-10,27-30*). But related studies of CTCs application in CNS malignancies are quite limited. In the recent three years, a few studies have successfully isolated CTCs in patients of both primary and recurrent GBM and diffuse glioma, which initiated related studies in brain gliomas (*12-14*). In 2014, Dorsey noticed that sequential CTCs counts increased and decreased in 2 patients later diagnosed with "tumor recurrence" and "Pseudo recurrence", respectively. Our previous study further confirmed that CTCs could be detected in all 7 common subtypes of primary brain gliomas, and to some extent, has superiority to MRP in identification of treatment necrosis or tumor recurrence in 5 patients (*15*). Due to the quite distinct tumor microenvironment of treatment necrosis and tumor recurrence, we postulated that CTCs counts of these 2 lesions could be significantly different, which should be proven by in a systematic study with a larger sample size and include common functional imaging modalities for comparison purposes.

Since the detection of CTCs in the blood of glioma patients was initiated recently, the technology adopted in each institution was different. The earliest method used to find CTCs was based on the detection of tumor cell surface specific markers such as GFAP. Muller *et al.* identified CTCs in blood from 29 of 141 (20.6%) GBM patients by immunostaining of GFAP and stated that CTCs are an "intrinsic property" of GBM biology (*14*). However, GFAP expression is not totally restricted to glial cells (*31,32*), and more importantly, some tumor cell markers lost their expression in blood. For example, it was reported that CK18, the dual epithelial marker and tumor biomarker, was positive in only 14% of lung and 24% of esophageal CTCs, respectively (*18*). In this study, the methodology we applied for CTCs detection was similar to our previous study, which was initially reported by Ge *et al.* in 2015, who has first detected glioma tumor cells in CSF, based on polyploidy of chromosome 8 examination by CEP8-FISH (*18*). We choose this protocol because compared to surface markers, aneuploidy, or abnormal chromosome content, could be the more common and stable marker of human solid tumors, for its characteristics that contribute to, or even drive, tumor development (*33*). Numerous studies have demonstrated the aneuploidy chromosome in many solid tumors; concerning brain glioma, it is also reported that polysomy of chromosome 8 could be found in CGH array results of 172 patients with GBM in a TCGA dataset, with a highest frequency of about 30-40% in one subgroup (*34*). In our previous study, we also demonstrated that chromosome 8 polyploidy cells generally existed in glioma specimens (*15*), providing the feasibility of CTCs detection based on aneuploidy chromosome.

Different from our previous study with CTCs detection in brain gliomas not treated, CTCs detection were performed in 10 recurrent gliomas after radiotherapy, and results showed that the CTC incidence was 100%, higher than our previous results (with CTC incidence of 77%). We speculated that the high incidence could be mainly due to the blood-brain barrier disruption after radio-chemo therapy (this is also the mechanism of the enhancing features of MRI), which could facilitate tumor cells entering the circulation. However, immunostaining results showed that only one patient was found with GFAP positive expressed, which was consistent with our previous results (*15*). Although the mechanisms of how GFAP expression was lost in the blood is still unknown, the present study has demonstrated the higher feasibility of CTCs detection in gliomas after radiotherapy, which could yield great potential for brain gliomas monitoring and treatment planning.

In our results, the sensitivity and specificity of rCBV and 11C-MET-PET in differentiating treatment necrosis from tumor recurrence were consistent with the findings of previous studies. CTCs counts were significantly different in the treatment necrosis and tumor recurrence groups, and by setting a cut-off value of 2, the ROC curve results showed that CTCs detection had a superior diagnostic efficacy compared to DSC-MRP and 11C-MET-PET. The different CTCs counts in treatment necrosis and tumor recurrence groups did meet our expectations because it is reasonable to suppose that the tumor burdens of these two lesions are quite different. However, the result obtained using the cut-off value of 2, rather than a cut-off of 0, was quite surprising. In this study, tumors were gross totally removed in all patients, and those patients with sub-totally removed tumors were not included, due to the unclear assumption about the difference in CTCs counts between recurrent tumor and residual tumors after surgery. Our results showed that even with visible surgical total resection on MRI imaging, CTCs were

still positive in four patients (with CTCs counts of 1). The results were consistent with the phenomenon that a new contrast-enhancing lesion observed *via* imaging is neither solely necrotic tissue nor tumor, but rather a mixture of both lesions. The present results demonstrate an advantage of CTCs detection in effective diagnosis of treatment necrosis and tumor recurrence, which is largely due to its direct reflection of the brain tumor environment after combined clinical treatment, rather than the indirect manifestation and computational results used by imaging modalities.

Beyond its application in differentiating treatment necrosis from tumor recurrence, our results could have additional illuminating indications. At first we wonder whether CTCs counts could have some prognostic effects in brain gliomas recurrence. In our study, we noticed that one patient (case 20) had 4 CTCs, but the enhancing lesion on MRI imaging decreased compared to the first enhancing lesion after radiotherapy. However, the enhancing lesion increased subsequently and tumor recurrence was finally confirmed three months later. The most likely explanation of this phenomenon is the usual overlap features of treatment necrosis and tumor recurrence on imaging, and the different evolution of treatment necrosis and tumor recurrence in the same enhancing lesion. Since several studies have shown a predictive role of CTCs count in tumor recurrence in other non-CNS tumors (*10,35,36*), we supposed that even in the same treatment necrosis group, those patients with different CTCs counts could have different prognoses, which would be proven during the next follow-up. Furthermore, we believe that the essential goal of differentiating treatment necrosis from tumor recurrence is not the "diagnosis" itself, but developing a "treatment plan" for the patient. Therefore, whether sequential CTCs detection in those patients should be performed and whether the treatment should be individually modified according to the sequential CTCs count still needs further study. Since this is the first step toward investigating the translational value of CTCs detection in brain gliomas, these interesting questions might be even more meaningful than the diagnostic result itself.

To date, histological confirmation is still the gold standard for differentiating treatment necrosis from tumor recurrence, but its sampling error and observer variability limitations make it an imperfect method. Furthermore, even in the case of treatment-related necrosis, areas with tumor cells are often present between large areas with necrosis, and it is very difficult to verify whether these tumor cells are still viable (*37*). Compared to histology, CTCs detection could reflect the invisible tumor status directly, and its continuous value could provide more information than the very rigid 2-group division used in histology. Besides its accurate diagnostic efficacy, CTCs detection has other advantages over imaging modalities. First, only a 7.5 mL blood sample was collected, and the experimental time requirement for patients was much shorter. Second, in our study, CTCs were identified by an automated CTC scanning system, which made our results more objective and reproducible. Lastly, compared to most functional imaging modalities, CTCs count is an absolute number, not a relative ratio, which could make the monitoring process more accessible. Considering the above advantages, we believe, as a new biomarker that directly comes from brain tumors (visible or invisible on imaging), CTCs detection could be a reliable tool for differentiating treatment necrosis from tumor recurrence, which both have very different tumor burdens.

Additionally, in our study, some patients' intervals from radiation therapy had a value of within 6 months. In a popular opinion, for the gliomas after radiation therapy, the radionecrosis often occurs in the late stage of radiation damage, which is over 6 months' after radiation therapy, and pseudo progression often occurs within 3 months after radiation therapy. Therefore, it is relatively easy to cause conceptual confusion of the generalized term "treatment necrosis". In fact, we initially wanted to change "treatment necrosis" to "treatment response" or "treatment effect". After serious consideration, we decided to proceed with the term "treatment necrosis." The underlying reasons are: on the one hand, compared with "treatment response" and "treatment effect" – which are too wide in scope – "treatment necrosis" describes our research purpose more accurately; on the other hand, from a pathophysiological point of view, according to certain studies, pseudo progression can be broadly considered as a period of "acute or sub-acute necrosis" with symptoms that are usually recoverable. Radiation necrosis, in this regard, can be broadly interpreted as "the late stage of necrosis" with a predominantly irreversible course of disease (*37*). Therefore, considering the above mentioned reasons, we preferred using "treatment necrosis" (not radiation necrosis).

There are, inevitably, some shortcomings in our study, including the relatively small size of the final analysis cohort and the retrospective design. Our study only focused on the situation after the first radiotherapy, and did not follow up the CTC examination in most patients and compare it with the clinical course. Therefore, the diagnosis of CTC cannot be clarified after multiple treatments in this study. Most of these patients did not receive continuous CTC detection, and since this is not a prospective study, the prognostic potential of CTCs detection in these cases cannot be disclosed at present. At last, patients with subtotal and partial resection of tumors are not included, and this may account for a large part of clinical work. A prospective, larger sample size study would provide more information about the application value of CTCs detection. These efforts are currently being pursued in our ongoing studies.

Funding: This study was supported by Natural Science Foundation of Zhejiang Province (No. LY19H160035), and Zhejiang Province Public Welfare Technology Application Research Project (No. LGF20G030011), and National Natural Science Foundation of China (81771309).

Conflict of Interest: The authors have no conflicts of interest to disclose.

References

1. Stupp R, Mason WP, Van Den Bent MJ, *et al.* Radiotherapy plus concomitant and adjuvant temozolomide for glioblastoma. N Engl J Med. 2005; 352:987-996.
2. Peca C, Pacelli R, Elefante A, De Caro MDB, Vergara P, Mariniello G, Giamundo A, Maiuri F. Early clinical and neuroradiological worsening after radiotherapy and concomitant temozolomide in patients with glioblastoma: tumour progression or radionecrosis? Clin Neurol Neurosurg. 2009; 111:331-334.
3. Wen PY, Macdonald DR, Reardon DA, *et al.* Updated response assessment criteria for high-grade gliomas: response assessment in neuro-oncology working group. J Clin Oncol. 2010; 28:1963-1972.
4. Melguizo-Gavilanes I, Bruner JM, Guha-Thakurta N, Hess KR, Puduvalli VK. Characterization of pseudoprogression in patients with glioblastoma: is histology the gold standard? J Neurooncol. 2015; 123:141-150.
5. Strauss SB, Meng A, Ebani EJ, Chiang GC. Imaging glioblastoma posttreatment: progression, pseudoprogression, pseudoresponse, radiation necrosis. Neuroimaging Clin N Am. 2021; 31:103-120.
6. Shah AH, Snelling B, Bregy A, Patel PR, Tememe D, Bhatia R, Sklar E, Komotar RJ. Discriminating radiation necrosis from tumor progression in gliomas: a systematic review what is the best imaging modality? J Neurooncol. 2013; 112:141-152.
7. Verma N, Cowperthwaite MC, Burnett MG, Markey MK. Differentiating tumor recurrence from treatment necrosis: a review of neuro-oncologic imaging strategies. Neuro Oncol. 2013; 15:515-534.
8. Riethdorf S, Müller V, Zhang L, *et al.* Detection and HER2 expression of circulating tumor cells: prospective monitoring in breast cancer patients treated in the neoadjuvant GeparQuattro trial. Clin Cancer Res. 2010; 16:2634-2645.
9. Pachmann K, Camara O, Kavallaris A, Krauspe S, Malarski N, Gajda M, Kroll T, Jörke C, Hammer U, Altendorf-Hofmann A, Rabenstein C, Pachmann U, Runnebaum I, Höffken K. Monitoring the response of circulating epithelial tumor cells to adjuvant chemotherapy in breast cancer allows detection of patients at risk of early relapse. J Clin Oncol. 2008; 26:1208-1215.
10. Cristofanilli M, Budd GT, Ellis MJ, Stopeck A, Matera J, Miller MC, Reuben JM, Doyle GV, Allard WJ, Terstappen LW, Hayes DF. Circulating tumor cells, disease progression, and survival in metastatic breast cancer. N Engl J Med. 2004; 351:781-791.
11. Terheggen HG, Müller W. Extracerebrospinal metastases in glioblastoma. Eur J Pediatr. 1977; 124:155-164.
12. Sullivan JP, Nahed BV, Madden MW, *et al.* Brain tumor cells in circulation are enriched for mesenchymal gene expression. Cancer Discov. 2014; 4:1299-1309.
13. MacArthur KM, Kao GD, Chandrasekaran S, Alonso-Basanta M, Chapman C, Lustig RA, Wileyto EP, Hahn SM, Dorsey JF. Detection of brain tumor cells in the peripheral blood by a telomerase promoter-based assay. Cancer Res. 2014; 74:2152-2159.
14. Müller C, Holtschmidt J, Auer M, *et al.* Hematogenous dissemination of glioblastoma multiforme. Sci Transl Med. 2014; 6:247ra101.
15. Gao F, Cui Y, Jiang H, Sui D, Wang Y, Jiang Z, Zhao J, Lin S. Circulating tumor cell is a common property of brain glioma and promotes the monitoring system. Oncotarget. 2016; 7:71330-71340.
16. Prager AJ, Martinez N, Beal K, Omuro A, Zhang Z, Young RJ. Diffusion and perfusion MRI to differentiate treatment-related changes including pseudoprogression from recurrent tumors in high-grade gliomas with histopathologic evidence. AJNR Am J Neuroradiol. 2015; 36:877-885.
17. Minniti G, Clarke E, Lanzetta G, Osti MF, Trasimeni G, Bozzao A, Romano A, Enrici RM. Stereotactic radiosurgery for brain metastases: analysis of outcome and risk of brain radionecrosis. Radiat Oncol. 2011; 6:48.
18. Ge F, Zhang H, Wang DD, Li L, Lin PP. Enhanced detection and comprehensive in situ phenotypic characterization of circulating and disseminated heteroploid epithelial and glioma tumor cells. Oncotarget. 2015; 6:27049-27064.
19. Kim YH, Oh SW, Lim YJ, Park CK, Lee SH, Kang KW, Jung HW, Chang KH. Differentiating radiation necrosis from tumor recurrence in high-grade gliomas: assessing the efficacy of 18 F-FDG PET, 11 C-methionine PET and perfusion MRI. Clin Neurol Neurosurg. 2010; 112:758-765.
20. Alexiou GA, Tsiouris S, Kyritsis AP, Voulgaris S, Argyropoulou MI, Fotopoulos AD. Glioma recurrence versus radiation necrosis: accuracy of current imaging modalities. J Neurooncol. 2009; 95:1-11.
21. Caroline I, Rosenthal MA. Imaging modalities in high-grade gliomas: pseudoprogression, recurrence, or necrosis? J Clin Neurosci. 2012; 19:633-637.
22. Tsuyuguchi N, Takami T, Sunada I, Iwai Y, Yamanaka K, Tanaka K, Nishikawa M, Ohata K, Torii K, Morino M, Nishio A, Hara M. Methionine positron emission tomography for differentiation of recurrent brain tumor and radiation necrosis after stereotactic radiosurgery – in malignant glioma. Ann Nucl Med. 2004; 18:291-296.
23. Sugahara T, Korogi Y, Tomiguchi S, Shigematsu Y, Ikushima I, Kira T, Liang L, Ushio Y, Takahashi M. Posttherapeutic intraaxial brain tumor: the value of perfusion-sensitive contrast-enhanced MR imaging for differentiating tumor recurrence from nonneoplastic contrast-enhancing tissue. AJNR Am J Neuroradiol. 2000; 21:901-909.
24. Huang J, Wang AM, Shetty A, Maitz AH, Yan D, Doyle D, Richey K, Park S, Pieper DR, Chen PY, Grills IS. Differentiation between intra-axial metastatic tumor progression and radiation injury following fractionated radiation therapy or stereotactic radiosurgery using MR spectroscopy, perfusion MR imaging or volume progression modeling. Magn Reson Imaging. 2011; 29:993-1001.
25. Matsusue E, Fink JR, Rockhill JK, Ogawa T, Maravilla KR. Distinction between glioma progression and post-radiation change by combined physiologic MR imaging.

Neuroradiology. 2010; 52:297-306.
26. Mitsuya K, Nakasu Y, Horiguchi S, Harada H, Nishimura T, Bando E, Okawa H, Furukawa Y, Hirai T, Endo M. Perfusion weighted magnetic resonance imaging to distinguish the recurrence of metastatic brain tumors from radiation necrosis after stereotactic radiosurgery. J Neurooncol. 2010; 99:81-88.
27. Pantel K, Brakenhoff RH, Brandt B. Detection, clinical relevance and specific biological properties of disseminating tumour cells. Nat Rev Cancer. 2008; 8:329-340.
28. Pierga JY, Bidard FC, Mathiot C, Brain E, Delaloge S, Giachetti S, de Cremoux P, Salmon R, Vincent-Salomon A, Marty M. Circulating tumor cell detection predicts early metastatic relapse after neoadjuvant chemotherapy in large operable and locally advanced breast cancer in a phase II randomized trial. Clin Cancer Res. 2008; 14:7004-7010.
29. Maheswaran S, Haber DA. Circulating tumor cells: a window into cancer biology and metastasis. Curr Opin Genet Dev. 2010; 20:96-99.
30. Pantel K, Alix-Panabières C. Circulating tumour cells in cancer patients: challenges and perspectives. Trends Mol Med. 2010; 16:398-406.
31. Danielyan L, Tolstonog G, Traub P, Salvetter J, Gleiter CH, Reisig D, Gebhardt R, Buniatian GH. Colocalization of glial fibrillary acidic protein, metallothionein, and MHC II in human, rat, NOD/SCID, and nude mouse skin keratinocytes and fibroblasts. J Invest Dermatol. 2007; 127:555-563.
32. Lim MC, Maubach G, Zhuo L. Glial fibrillary acidic protein splice variants in hepatic stellate cells – expression and regulation. Mol Cells. 2008; 25:376-384.
33. Kops GJ, Weaver BA, Cleveland DW. On the road to cancer: aneuploidy and the mitotic checkpoint. Nat Rev Cancer. 2005; 5:773-785.
34. Kim YW, Koul D, Kim SH, Lucio-Eterovic AK, Freire PR, Yao J, Wang J, Almeida JS, Aldape K, Yung WK. Identification of prognostic gene signatures of glioblastoma: a study based on TCGA data analysis. Neuro Oncol. 2013; 15:829-839.
35. Mejean A, Vona G, Nalpas B, Damotte D, Brousse N, Chretien Y, Dufour B, Lacour B, Bréchot C, Paterlini-Bréchot P. Detection of circulating prostate derived cells in patients with prostate adenocarcinoma is an independent risk factor for tumor recurrence. J Urol. 2000; 163:2022-2029.
36. Morgan TM, Lange PH, Porter MP, Lin DW, Ellis WJ, Gallaher IS, Vessella RL. Disseminated tumor cells in prostate cancer patients after radical prostatectomy and without evidence of disease predicts biochemical recurrence. Clin Cancer Res. 2009; 15:677-683.
37. Brandsma D, Stalpers L, Taal W, Sminia P, van den Bent MJ. Clinical features, mechanisms, and management of pseudoprogression in malignant gliomas. Lancet Oncol. 2008; 9:453-461.

Received January 10, 2021; Revised April 2, 2021; Accepted April 17, 2021.

[§]These authors contributed equally to this work.

*Address correspondence to:
Song Lin, Department of Neurosurgery, Beijing Tiantan Hospital, Capital Medical University; China National Clinical Research Center for Neurological Diseases, Beijing 100160, China.
E-mail: linsong2005@126.com

Released online in J-STAGE as advance publication April 29, 2021.

Original Article

DOI: 10.5582/bst.2021.01052

Vasa previa: Perinatal outcomes in singleton and multiple pregnancies

Na Liu[1,2], Qing Hu[1,2], Hua Liao[1,2], Xiaodong Wang[1,2], Haiyan Yu[1,2,*]

[1] Department of Obstetrics and Gynecology, West China Second University Hospital, Sichuan University; Chengdu, China;
[2] Key Laboratory of Birth Defects and Related Diseases of Women and Children (Sichuan University), Ministry of Education, Chengdu, China.

SUMMARY Vasa previa (VP) is a rare and life-threatening condition for the fetus. It is associated with increased perinatal mortality rates. The current study sought to retrospectively analyze the perinatal outcomes of VP in singleton and multiple pregnancies between January 1, 2013 and December 31, 2019 at a tertiary hospital in west China. One hundred and fifty-seven cases of VP were identified, including 131 singletons, 23 twins and 3 triplets. VP in 20 cases was diagnosed at delivery. There were 183 live births. Neonatal mortality was significantly higher in cases with no prenatal diagnosis (9.7% *vs.* 1.3%, $p = 0.035$). There was a significantly higher rate of NICU admission, premature infant and neonatal pneumonia in cases with prenatal diagnosis ($p < 0.05$). Among twin pregnancies with VP as a prenatal diagnosis, there were significantly earlier gestational age at admission (31.1 *vs.* 34.1 weeks, $p = 0.000$) and delivery age (33.4 *vs.* 35.3 weeks, $p = 0.000$) than those among singleton pregnancies. The neonatal mortality in twins with prenatal diagnosis was significantly higher than that in singletons (0% *vs.* 6.9%, $p = 0.037$). Early hospitalization of VP in the third trimester may be reasonable. The data suggest that the timing of elective delivery at 34-36 weeks in singletons and 32-34 weeks in twins may be suitable. It should be emphasized to make corresponding optimal delivery time according to individual differences for the women, especially in twin pregnancy.

Keywords vasa previa (VP), prenatal diagnosis, no prenatal diagnosis, singleton and multiple pregnancies, perinatal outcomes

1. Introduction

Vasa previa (VP) is a rare condition in which the umbilical vessels, unprotected by either placental tissue or Wharton's jelly, run through the membranes over the internal cervical os and under the fetal presenting part. The estimated incidence varies from 0.2 to 0.60 per 1,000 pregnancies (*1-3*). Previa vessels laceration may result in blood loss and catastrophic fetal distresses or stillbirth/neonatal death (*4,5*), which is associated with increased perinatal mortality.

Risk factors for VP are velamentous cord insertion, second-trimester low-lying placenta or placenta praevia, conception by assisted reproductive technologies, bilobed and succenturiate lobe placentas situated in the lower uterine segment, and multiple pregnancies (*3,6,7*).

Antenatal diagnosis of VP and delivery by planned cesarean section before the rupture of the membranes is recommended with the survival rate increased to 97-99%; however, survival rates in cases without antenatal diagnosis are poor, even in cases with emergency cesarean section, the neonatal survival rate is less than 50% (*2*).

According to the image of VP by color Doppler ultrasound, two varieties have been described (*8*): Type 1, in which there was a single placental lobe with a velamentous cord insertion, and Type 2, in which the vessels over the cervix were connecting between lobes of a placenta with multiple lobes. Recently, Suekane highlighted a new type of VP as Type 3, which is with a boomerang orbit and without velamentous insertion nor bilobed/accessory placenta (*9*).

The aims of this study were to *i*) analyze the outcomes of VP in singleton and multiple pregnancies; *ii*) investigate the clinical characteristics of patients with prenatal diagnosed VP or VP diagnosed at delivery.

2. Patients and Methods

A retrospective cohort study was conducted in patients with VP, which delivered between January 1, 2013 and December 31, 2019 at a tertiary hospital in west China. The study was approved by the Ethics committee of West China Second University Hospital (No. 2020129).

Informed consent was not required because the study was conducted retrospectively. Medical records of pregnant women were reviewed by the authors.

2.1. Diagnosis of VP

Prenatal diagnosis of VP were evaluated by transabdominal or transvaginal ultrasound (*10*) and suspected VP in ultrasonography confirmed by MRI.

Patients with antenatal diagnosis of VP or diagnosis at delivery *via* clinical and/or pathologic investigation were reviewed. Placental pathological examination was performed to confirm the diagnosis of VP (*11*). Cases with antenatal diagnosis of VP but not verified at delivery were excluded.

According to the image of VP by color Doppler ultrasound, VP was diagnosed as follows: Type 1 VP, in which there was a single placental lobe and the fetal vessels run freely through the membranes over the cervix or within 2 cm from the internal cervical os; Type 2 VP, in which the vessels were connected between lobes of a placenta with multiple lobes over the cervix or within 2 cm from the internal cervical os (*8,12*); Type 3 VP, in which fetal vessels were boomerang orbit and without velamentous insertion nor bilobed/accessory placenta (*9*).

2.2. Data collection

Maternal collected data included demographic characteristics, gestational age at diagnosis, delivery age, obstetric history, complications, indications of delivery, mode of delivery, delivery documents, pathologic reports, and blood loss at delivery. Neonatal data included gestational age at delivery, birth weight, Apgar scores, neonatal death, admission to the NICU, and major neonatal conditions.

2.3. Statistical analysis

Descriptive statistics, such as frequency, percentage, and mean, standard deviation (SD), and the range were used for the presentation of variables. Parameters were analyzed using two-tailed student's *t*-test , Chi-squared test or Fisher's exact probability test, and Spearman test. Statistical analyses were performed with SPSS version19.0 (SPSS Inc, Chicago, IL). A p value < 0.05 was considered statistically significant.

3. Results

3.1. Study participants

During the study period, 79,647 pregnant women were delivered at our institution. One hundred and fifty-seven patients had VP, and 26 cases (16.56%) were multiple pregnancies, as 10 monochorionic diamniotic (MCDA) twin pregnancy, 13 dichorionic diamniotic (DCDA) twin pregnancy, 2 dichorionic triamniotic (DCTA) triplet pregnancy, and 1 trichorionic triamniotic (TCTA) triplet pregnancy. The incidence of VP was 1.97 per 1,000 pregnancies. Maternal age was 31.7 ± 4.9 years.

The classifications of VP were: Type 1 141cases (89.8%) (Figure 1), Type 2 12 cases (7.6%) (Figure 2), and Type 3 4 cases (2.6%) (Figure 3). Among the cases, 137 cases (87.3%) were diagnosed antenatally, 20 cases (12.7%) were diagnosed at delivery.

In prenatal diagnosis cases, there were 120 singleton pregnancies, 16 twin pregnancies (MCDA 7, DCDA 9) and 1 triplet pregnancy (TCTA 1). One hundred thirty-two cases (96.4%) were diagnosed by ultrasound and 5 cases were diagnosed by MRI.

In cases without prenatal diagnosis , there were 11 singleton pregnancies, 7 twin pregnancies (MCDA 3, DCDA 4) and 2 triplet pregnancies (DCTA 2).

One hundred and fifty-one cases (96.2%) had one or more identifiable placental and/or maternal risk indications. Velamentous cord insertion (70.1%) and low-lying placenta or placenta previa (59.2%) were two of the most prevalent. Maternal demographics and pregnancy characteristics are presented in Table 1.

3.2. Management during pregnancy in prenatal diagnosis group

Among the prenatal diagnosis cases, 22 cases were conceived by assisted reproduction technology, as 7 twins, 14 singletons and 1 triplet pregnancy. The diagnosis gestational age (GA) in singletons was 26.6 ± 4.9 weeks, 66.7% in the second trimester, and 33.3% in the third trimester. In twins, GA at diagnosis was 24.4 ± 4.1 weeks, 81.2% in the second trimester of pregnancy, 18.8% in the third trimester. In twin pregnancies, selected termination of abnormal fetus was performed at 17+3 weeks in one DCDA twin; one fetus death (not with VP) presented at 28+6 weeks in one MCDA twin; one fetus (not with VP) was dead at 27 weeks due to severe fetal growth retardation in one DCDA twin.

One hundred and thirty-seven cases were monitored closely until delivery. The gestational age at admission

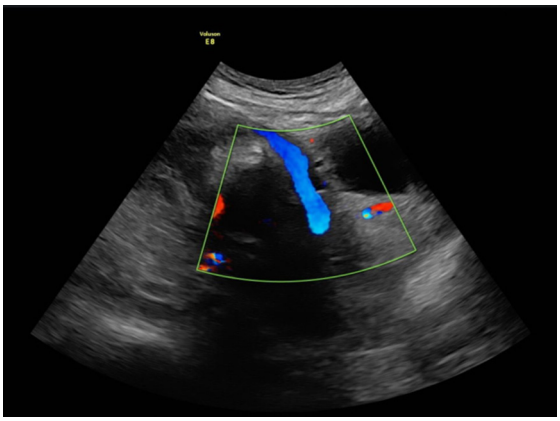

Figure 1. Images of Type 1 vasa previa.

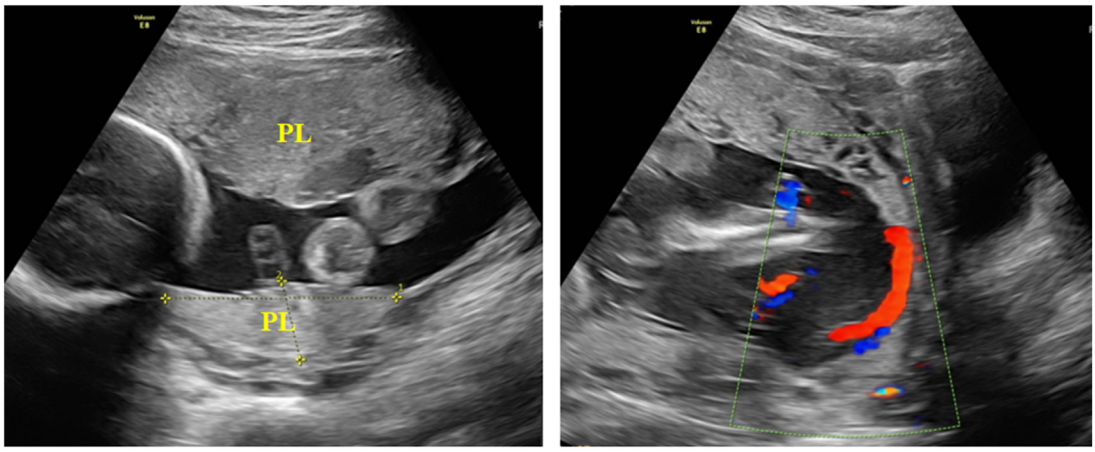

Figure 2. Images of Type 2 vasa previa.

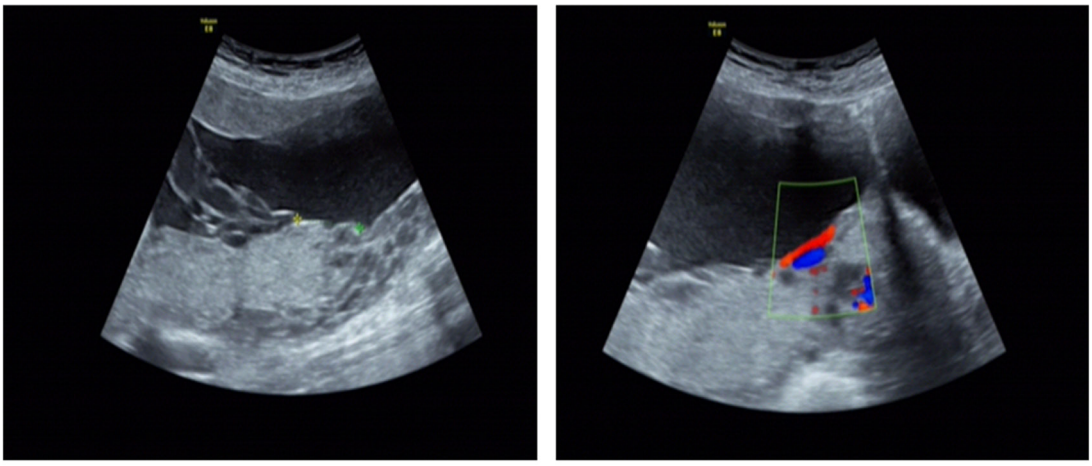

Figure 3. Images of Type 3 vasa previa.

Table 1. Maternal demographics and pregnancy characteristics of vasa previa

Variables	All cases (n = 157)	Prenatal diagnosis (n = 137)	No prenatal diagnosis (n = 20)	p value
Maternal age (y)	31.7 ± 4.9	31.7 ± 4.8	31.2 ± 5.3	0.642
≥ 35 years old, n (%)	39 (24.8)	33 (24.1)	6 (30.0)	0.768
BMI (kg/m^2)	25.7 ± 2.5	25.6 ± 2.5	26.3 ± 2.5	0.248
Gravidity	2 (1-8)	3 (1-8)	2 (1-5)	0.031
Primipara, n (%)	100 (63.7)	84 (61.3)	16 (80.0)	0.105
Singleton, n (%)	131 (83.4)	120 (87.6)	11 (55.0)	0.001
Risk factor				
Multiple pregnancy, n (%)	26 (16.6)	17 (12.4)	9 (45.0)	0.001
ART, n (%)	28 (17.8)	25 (18.2)	3 (15.0)	0.967
Low-lying placenta or placenta previa, n (%)	93 (59.2)	88 (64.2)	5 (25.0)	0.001
Velamentous cord insertion, n (%)	110 (70.1)	100 (73.0)	10 (50.0)	0.036
Bilobate or succenturiate placenta, n (%)	12 (7.6)	12 (8.8)	0 (0.0)	0.354
At least one risk factor[#], n (%)	151 (96.2)	134 (97.8)	17 (85.0)	0.028[*]

Data are presented as mean ± standard deviation or proportion (%). BMI: Body Mass Index; ART: assisted reproduction technology. [#]includes multiple pregnancy, ART pregnancy and placental factor. [*]Fisher's Exact Test.

was 33.7 ± 2.3 weeks with delivery age 35.1 ± 1.6 weeks. All were performed as cesarean section (CS), 35 cases with emergency CS, and 102 cases with planned CS. There were 15.3% cases before 34 weeks, 72.3% between 34 and 36 weeks, and 12.4% at term. A total of 120 cases (87.6%) received either 1 or 2 courses of antenatal steroids.

In 120 singleton cases, 83 (69.2%) patients were hospitalized with no symptoms, which included 33 cases of hospitalization at 32.6 ± 1.4 weeks (range 29-34 weeks) with delivery at 34.7 ± 1.5 weeks (range 30-38 weeks), 50 cases of hospitalization at 35.4 ± 1.3 weeks

(range 34-40 weeks) with delivery at 36.1 ± 1.2 weeks (range 34-40 weeks of gestation). Thirty-seven cases had emergency admissions due to premature rupture of membranes (PROM), vaginal bleeding, abnormal fetal monitoring and threatened premature labor, with delivery at 34.7 ± 1.2 weeks (range 32-39 weeks).

Among 16 twin cases, 7 patients were hospitalized with no symptoms at 32.6 ± 1.3 weeks (range 30-35 weeks) with delivery at 33.9 ± 1.0 weeks (range 32-36 weeks). Nine cases had emergency admissions due to vaginal bleeding, abnormal fetal monitoring and threatened premature labor, with delivery at 33.0 ± 1.1 weeks (range 31-35 weeks).

In singleton pregnancies, emergency caesarean delivery was performed in 28 cases due to PROM (3 cases), vaginal bleeding (3 cases), abnormal fetal monitoring (2 cases), severe preeclampsia (1 case), in labor (19 cases). In twin pregnancies, emergency caesarean section was performed due to vaginal bleeding (2 cases), abnormal fetal monitoring (2 cases) and in labor (2 cases). In a triplet pregnancy an emergency caesarean section was performed for severe preeclampsia.

The management in cases with prenatal diagnosis is shown in Table 2 and Table 3.

3.3. Management during pregnancy in not prenatal diagnosis group

Among the cases diagnosed at delivery, the admission age was 35.6 ± 3.6 weeks (range 27-40 weeks), with delivery at 36.3 ± 3.0 weeks (range 28-40 weeks), and 12 cases with delivery at term.

Seventeen cases had CS, 12 cases with planned CS, 5 cases with emergency CS due to PROM with velamentous cord insertion, PROM with twin pregnancy, intrahepatic cholestasis of pregnancy with twin pregnancy, twin-twin transfusion syndrome and severe preeclampsia.

Vaginal delivery was performed in 3 cases, including 2 singleton pregnancies with velamentous cord insertion delivery at term and 1 DCTA triplet pregnancy in labor at 28+1 weeks with PROM.

3.4. Perinatal outcomes between type1 and type 2 VP

Among the cases of Type 1 VP, one hundred twenty-one cases were diagnosed prenatally. Gestational age at diagnosis was 26.1 ± 4.8 weeks, 71.1% in the second trimester, and 28.9% in the third trimester. The gestational age at admission was 33.9 ± 2.6 weeks with delivery age 35.2 ± 1.9 weeks. 138 cases (97.9%) had cesarean section.

Among the cases of Type 2 VP, they were all diagnosed prenatally. The gestational age at admission was 33.7 ± 1.5 weeks with delivery age 35.0 ± 1.6 weeks. All cases had cesarean section.

Except for 4 cases of Type 3 VP, perinatal outcomes between Type 1 and Type 2 VP cases are shown in detail in Table 4.

Table 2. Perinatal outcomes in cases with vasa previa

Variables	Prenatal diagnosis (*n* = 137)	No prenatal diagnosis (*n* = 20)	*p* value
Prenatal hemorrhage, *n* (%)	21 (15.3)	1 (5.0)	0.369
GA at admission (wks)	33.7 ± 2.3	35.6 ± 3.6	0.002
Corticosteroids for fetal lung maturity, *n* (%)	120 (87.6)	12 (60.0)	0.005
GA at delivery (wks), *n* (%)	35.1 ± 1.6	36.3 ± 3.0	0.004
28-31 6/7	3 (2.2)	2 (10.0)	0.000*
32-33 6/7	18 (13.1)	0 (0.0)	
34-36 6/7	99 (72.3)	6 (30.0)	
≥ 37	17 (12.4)	12 (60.0)	
Mode of delivery, *n* (%)			
Vaginal delivery	0 (0.0)	3 (15.0)	0.002*
Cesarean delivery	137 (100.0)	17 (85.0)	
Planning cesarean delivery	102 (74.5)	12 (70.6)	0.961
Emergency cesarean delivery	35 (25.5)	5 (29.4)	
Neonatal outcomes			
Number of fetus			
Live births, *n*	152	31	-
5 min Apgar < 7, *n* (%)	2 (1.3)	2 (6.5)	0.134*
Premature infant, *n* (%)	135 (88.8)	17 (54.8)	0.000
Birth weight (g)	2,374.5 ± 439.2	2,380.7 ± 665.6	0.961
NICU, *n* (%)	85 (55.9)	11 (35.5)	0.038
NICU LOS (days)	8 (1-49)	6 (5-50)	0.503
Neonatal mortality, *n* (%)	2 (1.3)	3 (9.7)	0.035*
RDS, *n* (%)	19 (12.5)	2 (6.5)	0.513
Pneumonia, *n* (%)	53 (34.9)	5 (16.1)	0.041
IVH, *n* (%)	14 (9.2)	2 (6.5)	0.883
Anemia, *n* (%)	19 (12.5)	3 (9.7)	0.891

GA: gestational age; RDS: Respiratory distress syndrome; IVH: Intraventricular hemorrhage; LOS: Length of stay. *Fisher's Exact Test.

Table 3. Perinatal outcomes between singleton and twin pregnancies in antenatal diagnosed cases

Variables	Singleton	Twin	*p* value
Total	120	16	-
Age	32.0 ± 5.0	30.1 ± 3.4	0.136
≥ 35, *n* (%)	32 (26.7)	1 (6.3)	0.139
ART, *n* (%)	16 (13.3)	8 (50.0)	0.001
GA at diagnosis (wks), *n* (%)	26.6 ± 4.9	24.4 ± 4.1	0.097
Second trimester of pregnancy	80 (66.7)	13 (81.2)	0.272
Third trimester of pregnancy	40 (33.3)	3 (18.8)	
GA at admission (wks)	34.1 ± 2.0	31.1 ± 2.6	0.000
Irregular vaginal bleeding at early pregnancy, *n* (%)	43 (35.8)	5 (31.3)	0.788
Antenatal hospital LOS (day)	8 (1-47)	10 (2-52)	0.029
Indication for hospitalization, *n* (%)			
Asymptomatic	83 (69.2)	7 (43.8)	0.004*
Vaginal bleeding	20 (16.7)	1 (6.3)	
Premature rupture of membrane	3 (2.5)	0 (0.0)	
Threatened premature labor	13 (10.8)	6 (37.5)	
Abnormal fetal monitoring	1 (0.8)	2 (12.5)	
Corticosteroids for fetal lung maturity, *n* (%)	104 (86.7)	15 (93.8)	0.687
Tocolysis, *n* (%)	32 (26.7)	11 (68.8)	0.001
Length of tocolysis (days)	3 (1-21)	3 (2-14)	0.945
GA at delivery (wks), *n* (%)	35.3 ± 1.5	33.4 ± 1.1	0.000
28-31 6/7	2 (1.7)	1 (6.3)	0.000*
32-33 6/7	9 (7.5)	8 (50.0)	
34-36 6/7	92 (76.7)	7 (43.8)	
≥ 37	17 (14.2)	0 (0.0)	
Planning cesarean, *n* (%)	92 (76.7)	10 (62.5)	0.357
Emergency cesarean, *n* (%)	28 (23.3)	6 (37.5)	
Live births	120	29	
Neonatal mortality, *n* (%)	0 (0.0)	2 (6.9)	0.037*
Preterm, *n* (%)	103 (85.8)	29 (100.0)	0.068
Birth weight (g)	2,495.2 ± 385.5	1,909.5 ± 331.8	0.000
Birth weight < 2500g, *n* (%)	63 (52.5)	28 (96.6)	0.000
NICU, *n* (%)	59 (49.2)	23 (79.3)	0.003

ART: Assisted reproduction technology; GA: gestational age; LOS: Length of stay; NICU: neonatal intensive care unit. *Fisher's Exact Test.

3.5. Neonatal outcomes

Except for one twin death due to selected termination, sudden death and severe fetal growth retardation in twin pregnancies, there were 183 live births in 157 cases.

In prenatal diagnosis cases, there were 152 live births with mean birth weight 2,374.5 ± 439.2g and 88.8% were preterm infants. Over half of neonates (55.9%) were transferred to NICU with length of stay about 8 days (1-49 days). Nineteen neonates had respiratory distress syndrome, twelve of them were treated with pulmonary surfactant; 19 neonates were diagnosed with anemia and nine of them required blood transfusions. The neonatal mortality was 1.3% (2/152). Perinatal outcomes between singleton and twin pregnancies in antenatal diagnosed cases are shown in detail in Table 3.

There were 31 live births in cases with no antenatal diagnosis, mean birth weight 2,380.7 ± 665.6g and 54.8% were preterm infants. Eleven neonates (35.5%,) were transferred to NICU with length of stay about 6 days (5-50 days), 2 neonates were complicated with respiratory distress syndrome, and 3 (9.7%) with anemia. The neonatal mortality was 9.7% (3/31).

Compared with cases with prenatal diagnosis of VP, neonatal mortality was significantly higher in cases with no prenatal diagnosis (9.7% *vs.* 1.3%, $p = 0.035$). There was no difference in neonatal respiratory distress syndrome between the prenatal diagnosis cases and no prenatal diagnosis cases ($p = 0.513$). Meanwhile, there was a significantly higher rate of NICU admission, premature infant and neonatal pneumonia in cases with prenatal diagnosis. All surviving newborns were followed up and in good health.

4. Discussion

VP is a rare and life-threatening condition for the fetus. The incidence in this study was higher due to our hospital being the regional tertiary referral center in west China.

In this study, 96.2% cases of VP had one or more identifiable placental and/or maternal risk indications, velamentous cord insertion (70.1%) and placenta previa or low-lying placenta (59.2%) are most prevalent among them, the same as published reports (*3,6,7*).

Some authors put forward that velamentous insertion of the cord is a prerequisite for VP (*13*). In this study, 4 cases were difficult to classify into either type1 or type2 VP, in which the umbilical cord showed no velamentous insertion and some vessel branches went out of the placental surface and subsequently returned to the

Table 4. Perinatal outcomes between type1 and type 2 vasa previa

Variables	Type 1	Type 2	*p* value
Total	141	12	-
Age	31.5 ± 4.8	33.8 ± 5.1	0.111
≥ 35, *n* (%)	32 (22.7)	6 (50.0)	0.079
Singleton, *n* (%)	116 (82.3)	11 (91.7)	0.666
ART, *n* (%)	28 (19.9)	0 (0.0)	0.187
Prenatal diagnosis, *n* (%)	121 (85.8)	12 (100.0)	0.340
GA at diagnosis (wks), *n* (%)	26.1 ± 4.8	27.5 ± 5.7	0.366
Second trimester of pregnancy	86 (71.1)	6 (50.0)	0.238
Third trimester of pregnancy	35 (28.9)	6 (50.0)	
Antenatal hospital LOS (day)	7 (1-52)	6 (1-25)	0.788
GA at admission (wks)	33.9 ± 2.6	33.7 ± 1.5	0.693
Irregular vaginal bleeding at early pregnancy, *n* (%)	44 (31.2)	7 (58.3)	0.111
Indication for Hospitalization, *n* (%)			
Asymptomatic	89 (63.1)	7 (58.3)	0.554*
Vaginal bleeding	18 (12.8)	3 (25.0)	
Premature rupture of membrane	7 (5.0)	0 (0.0)	
Threatened premature labor	4 (2.8)	1 (8.3)	
Abnormal fetal monitoring	20 (14.2)	1 (8.3)	
Corticosteroids for fetal lung maturity, *n* (%)	120 (85.1)	8 (66.7)	0.211
Tocolysis, *n* (%)	46 (32.9)	3 (25.0)	0.813
GA at delivery (wks), *n* (%)	35.2 ± 1.9	35.0 ± 1.6	0.693
28-31 6/7	5 (3.5)	0 (0.0)	0.725*
32-33 6/7	16 (11.3)	2 (16.7)	
34-36 6/7	92 (65.2)	9 (75.0)	
≥ 37	28 (19.9)	1 (8.3)	
Mode of delivery, *n* (%)			
Vaginal delivery	3 (2.1)	0 (0.0)	1.000*
Cesarean delivery	138 (97.9)	12 (100.0)	
Planning cesarean delivery	100 (72.5)	11 (91.7)	0.187*
Emergency cesarean delivery	38 (27.5)	1 (8.3)	
Neonatal outcomes			
Live births, n	166	13	-
5 min Apgar < 7, *n* (%)	2 (1.2)	2 (15.4)	0.027*
Premature infant, *n* (%)	136 (81.9)	12 (92.3)	0.567
Birth weight (g)	2,355.4 ± 488.4	2,490.8 ± 385.5	0.331
NICU, *n* (%)	86 (51.8)	9 (69.2)	0.261
NICU LOS (days)	8 (1-50)	7 (3-10)	0.001
Neonatal mortality, *n* (%)	3 (1.8)	2 (15.4)	0.043*
RDS, *n* (%)	19 (11.4)	2 (15.4)	0.653*
Pneumonia, *n* (%)	5 (32.5)	4 (30.8)	1.000
IVH, *n* (%)	16 (9.6)	0 (0.0)	0.504
Anemia, *n* (%)	21 (12.7)	1 (7.7)	0.932

ART: Assisted reproduction technology; GA: gestational age; LOS: Length of stay; NICU: neonatal intensive care unit; RDS: Respiratory distress syndrome; IVH: Intraventricular hemorrhage. *Fisher's Exact Test.

placental cotyledons. Kanda *et al.* (*14*) and Suekane *et al.* (*9*) reported the same conditions and Suekane highlighted this new type as Type3. We agreed with the suggestion and classified the four cases as Type 3 VP. Based on these data, careful observation of fetal vessels running around the internal cervix by color Doppler imaging should be performed whether cases had velamentous cord insertion or not. At present, there is no evidence to prove that different forms of VP have different perinatal outcomes. The essence of VP classification is based on the variation of fetal blood vessels. It has no clear clinical significance in the current classification without considering the mechanism of developmental biology.

The ultrasonic signs of VP could be described as linear or tubular structures in front of the cervix inner os, and pulsed wave color Doppler demonstrates the fetus's umbilical artery blood flow and a rate consistent with the fetal heart rate (*10*). VP should be confirmed by examining the placenta membrane during labor and postpartum (*15*).

Transvaginal ultrasound using colour and pulse-wave Doppler to evaluate the internal os and lower uterine segment is the most accurate means to diagnose VP (*16*). Prenatal diagnosis of VP was made most frequently during the second trimester of pregnancy. Although two prospective studies showed that the sensitivity of VP detection was 100% with a specificity of 99-99.8%, the prenatal detection rate of VP varied from 53% to 100% in retrospective studies (*17*). It should be known that not all cases of VP can be diagnosed antenatally (*18*).

In published guidelines, universal screening for VP in singleton pregnancies by ultrasound is not recommended. However, targeted screening should be considered in high risk pregnant women during the midtrimester scan using a transvaginal ultrasound probe with color and pulsed Doppler (*3,16,17,20*), which can reduce perinatal loss. Whereas, screening all twin pregnancies for VP with transvaginal ultrasound is cost-effective (*20*).

Some VP may be undiagnosed. The American Institute of Ultrasound in Medicine (AIUM) and Society for Maternal-Fetal Medicine (SMFM) recommend that the "placental position, appearance and relationship with the cervix" should be used as part of the standard parameters for routine ultrasound evaluation in obstetrics (*21,22*). Furthermore, the multiplanar imaging capability of magnetic resonance imaging (MRI) is more useful to identify the exact position of placenta and the area adjacent to the internal cervix os (*23,24*). In this study, five VP were diagnosed antenatally using MRI, one case with central placenta previa and bilobed placentas, three cases with placental implantation abnormality, and one case with marginal placental previa. It should be noted that MRI cannot be used in most obstetric practices due to its expensiveness and applicable conditions.

Hospitalization of VP was suggested at 30-32 gestational weeks by RCOG, SOGC and RANZCOG (*11,16,19*), 30-34 weeks by SMFM (*22*). Administration of corticosteroids in patients with VP was recommended at 28-32 weeks by SOGC and SMFM (*19,22*), around 30-32 weeks by RANZCOG (*16*), and at 32 weeks by RCOG (*11*).

To minimize the impact of prematurity and adverse outcomes due to VP, optimal gestational age at delivery is of vital importance. Gestational age at delivery was proposed to be 34-36 weeks by RCOG and RANZCOG(11,16), 34-37 weeks by SMFM (*22*), and the guidelines recommend that emergency cesarean delivery should be performed if bleeding or rupture of membranes occurs in cases with suspected VP (*11,16,19,22*). Swank (*25*) suggested elective delivery at 33-34 weeks. A decision analysis suggested that delivery at 34-35 weeks may balance the risk of perinatal death, risks related to prematurity as respiratory distress syndrome, mental retardation, and cerebral palsy (*26*).

Based on our findings, we concur with the delivery timing recommendations in singletons with antepartum VP at 34-36 weeks, and corticosteroids administration at 28-32 weeks. Whether advanced admission should be a combination of kinds of factors, including multiple pregnancy, prenatal bleeding and premature birth risk (*11,27*).

Although the perinatal mortality in VP is reduced with improved prenatal diagnosis, catastrophes also still happen (*7*). In Oyelese's report, prenatal diagnosed VP had a higher infant survival rate than cases with no prenatal diagnosis (97% *vs.* 44%) (*2*). In this study the neonatal mortality in cases without prenatal diagnosis was significantly higher (9.7% *vs.* 1.3%).

Because of fear of stillbirth, preterm delivery in VP is high. In this study, the rate of preterm delivery in prenatal diagnosis cases was significantly higher than that with no prenatal diagnosis cases (87.6% *vs.* 40%). The neonatal complications are always related to iatrogenic preterm birth and a good perinatal outcome can be obtained after treatment (*28*).

In published papers, there are few cases of VP in multiple pregnancies. Rupture of the vessels in VP can cause acute hemorrhage and acute fetal exsanguination, which occur in the corresponding twin in dichorionic twin pregnancy, and in both fetuses in monochorionic twin pregnancy.

No consensus suggested delivery age for twins with VP. In Jauniaux's systematic review of VP diagnosed prenatally in twin pregnancies, delivery age was 32+6 (3+5) weeks (*29*). Catanzarite suggests timing of elective delivery for singletons at 34-35 weeks and delivery at 32-34 weeks in twins may be risk-beneficial (*30*). Based on our findings, we think that in twin pregnancies with antepartum VP, optimal delivery timing is at 32-34 weeks.

The strengths of this study are that perinatal outcomes were compared in VP cases with prenatal diagnosis and with no prenatal diagnosis; there is a larger number of DC and MC twin pregnancy; and the perinatal outcomes between singleton and twin pregnancies in antenatal diagnosed cases were investigated. The limitation in this study lies in the retrospective study. Definitely, a prospective study in VP is not feasible due to its rarity.

5. Conclusion

Prenatal diagnosis of VP should be highlighted. Our results confirm that the fetal and neonatal outcomes either in singletons or in twins are better in cases with VP diagnosed antenatally. Early hospitalization of VP in the third trimester may be reasonable. The timing of elective delivery at 34-36 weeks in singletons and at 32-34 weeks in twins may be suitable. It should be emphasized to make a corresponding optimal delivery time according to individual differences for the women, especially in twin pregnancy.

Acknowledgements

We feel grateful for the doctors and staff who have been involved in this work.

Funding: This study was supported by the Academic and Technical Leader's Foundation of Sichuan Province (No.2017-919-25).

Conflict of Interest: The authors have no conflicts of interest to disclose.

References

1. Oyelese Y, Smulian JC. Placenta previa, placenta accreta, and vasa previa. Obstet Gynecol. 2006; 107:927-941.
2. Oyelese Y, Catanzarite V, Prefumo F, Lashley S, Schachter M, Tovbin Y, Goldstein V, Smulian JC. Vasa previa: the impact of prenatal diagnosis on outcomes. Obstet Gynecol. 2004; 103:937-942.
3. Ruiter L, Kok N, Limpens J, Derks JB, de Graaf IM, Mol B, Pajkrt E. Incidence of and risk indicators for vasa praevia: a systematic review. BJOG. 2016; 123:1278-1287.
4. Silver RM. Abnormal placentation: placenta previa, vasa previa, and placenta accreta. Obstet Gynecol. 2015; 126: 654-668.
5. Jauniaux E, Savvidou MD. Vasa praevia: more than 100 years in preventing unnecessary fetal deaths. BJOG. 2016; 123:1287.
6. Pirtea LC, Grigoraş D, Sas I, Ilie AC, Stana LG, Motoc AG, Jianu AM, Mazilu O. *In vitro* fertilization represents a risk factor for vasa praevia. Rom J Morphol Embryol. 2016; 57:627- 632.
7. Tsakiridis I, Mamopoulos A, Athanasiadis A, Dagklis T. Diagnosis and management of vasa previa: a comparison of 4 national guidelines. Obstet Gynecol Surv. 2019; 74:436-442.
8. Catanzarite V, Maida C, Thomas W, Mendoza A, Stanco L, Piacquadio KM. Prenatal sonographic diagnosis of vasa previa: ultrasound findings and obstetric outcome in ten cases. Ultrasound Obstet Gynecol. 2001; 18:109-115.
9. Suekane T, Tachibana D, Pooh RK, Misugi T, Koyama M. Type-3 vasa previa: normal umbilical cord insertion is not enough to exclude vasa previa in cases with abnormal placental location. Ultrasound Obstet Gynecol. 2020; 55:556-557.
10. D'Antonio F, Bhide A. Ultrasound in placental disorders. Best Pract Res Clin Obstet Gynaecol. 2014; 28:429-442.
11. Jauniaux E, Alfirevic Z, Bhide AG, Burton GJ, Collins SL, Silver R, Royal College of Obstetricians and Gynaecologists. Vasa praevia: diagnosis and management. Green-top Guideline No. 27b. BJOG. 2019; 126:e49-e61.
12. Kelley BP, KlochkoCL, Atkinson S, Hillman D, Craig BM, Sandberg SA, Gaba AR, Halabi SS. Sonographic diagnosis of velamentous and marginal placental cord insertion. Ultrasound Q. 2020; 36:247-254.
13. Stafford IP, Neumann DE, Jarrell H. Abnormal placental structure and vasa previa: confirmation of the relationship. J Ultrasound Med. 2004; 23:1521-1522.
14. Kanda E, Matsuda Y, Kamitomo M, Maeda T, Mihara K, Hatae M. Prenatal diagnosis and management of vasa previa: a 6-year review. J Obstet Gynaecol Res. 2011; 37:1391-1396.
15. Derbala Y, Grochal F, Jeanty P. Vasa previa. J Prenat Med. 2007; 1: 2-13.
16. The Royal Australian and New Zealand College of Obstetricians and Gynaecologists Excellence in Women's Health. Vasa Praevia (C-Obs-47). *https://ranzcog.edu.au/RANZCOG_SITE/media/RANZCOG-MEDIA/Women%27s%20Health/Statement%20and%20guidelines/Clinical-Obstetrics/Vasa-Praevia-(C-Obs-47).pdf?ext=.pdf* (accessed November 30, 2020)
17. Ruiter L, Kok N, Limpens J, Derks JB, de Graaf IM, Mol BWJ, Pajkrt E. Systematic review of accuracy of ultrasound in the diagnosis of vasa previa. Ultrasound Obstet Gynecol. 2015; 45:516-522.
18. Nishtar A, Wood PL. Is it time to actively look for vasa praevia? J Obstet Gynaecol. 2012; 32:413-418.
19. Gagnon R. No. 231-guidelines for the management of vasa previa. J Obstet Gynaecol Can. 2017; 39: e415-e421.
20. Cipriano LE, Barth WH Jr, Zaric GS. The cost-effectiveness of targeted or universal screening for vasa praevia at 18-20 weeks of gestation in Ontario. BJOG. 2010; 117:1108-1118.
21. American Institute of Ultrasound in Medicine. AIUM practice guideline for the performance of obstetric ultrasound examinations. J Ultrasound Med. 2013; 32:1083-1101.
22. Society of Maternal-Fetal (SMFM) Publications Committee, Sinkey RG, Odibo AO, Dashe JS. #37: Diagnosis and management of vasa previa. Am J Obstet Gynecol. 2015; 213: 615-619.
23. Kikuchi A, Uemura R, Serikawa T, Takakuwa K, Tanaka K. Clinical significances of magnetic resonance imaging in prenatal diagnosis of vasa previa in a woman with bilobed placentas. J Obstet Gynaecol Res. 2011; 37:75-78.
24. Oppenheimer DC, Mazaheri P, Ballard DH, Yano M, Fowler KJ. Magnetic resonance imaging of the placenta and gravid uterus: a pictorial essay. Abdom Radiol (NY). 2019; 44:669-684.
25. Swank ML, Garite TJ, Maurel K, Das A, Perlow JH, Combs CA, Fishman S, Vanderhoeven J, Nageotte M, Bush M, Lewis D. Vasa previa: diagnosis and management. Am J Obstet Gynecol. 2016; 215:223.e1-e6.
26. Robinson BK, Grobman WA. Effectiveness of timing strategies for delivery of individuals with vasa previa. Obstet Gynecol. 2011; 117:542-549.
27. Yerlikaya-Schatten G, Chalubinski KM, Pils S, Springer S, Ott J. Risk-adapted management for vasa praevia: a retrospective study about individualized timing of caesarean section. Arch Gynecol Obstet. 2019; 299:1545-1550.
28. Sullivan EA, Javid N, Duncombe G, Li Z, Safi N, Cincotta R, Homer CSE, Halliday L, Oyelese Y. Vasa previa diagnosis, clinical practice, and outcomes in Australia. Obstet Gynecol. 2017; 130:591- 598.
29. Jauniaux E, Melcer Y, Maymon R. Prenatal diagnosis and management of vasa previa in twin pregnancies: a case series and systematic review. Am J Obstet Gynecol. 2017; 21:568-575.
30. Catanzarite V, Cousins L, Daneshmand S, Schwendemann W, Casele H, Adamczak J, Tith T, Patel A. Prenatally diagnosed vasa previa: a single-institution series of 96 cases. Obstet Gynecol. 2016; 128:1153-1161.

Received January 30, 2021; Revised March 7, 2021; Accepted March 17, 2021.

**Address correspondence to:*
Haiyan Yu, Department of Obstetrics and Gynecology, West China Second University Hospital, Sichuan University, No. 20, 3rd section, South Renmin Road, Chengdu, Sichuan 610041, China.
E-mail: fanjy422@163.com

Released online in J-STAGE as advance publication March 21, 2021.

Communication

DOI: 10.5582/bst.2021.01092

New challenges to fighting COVID-19: Virus variants, potential vaccines, and development of antivirals

Jun Chen, Hongzhou Lu*

Department of Infectious Diseases and Immunology, Shanghai Public Health Clinical Center, Fudan University, Shanghai, China.

SUMMARY Despite strict control measures implemented worldwide, the COVID-19 pandemic continues to rage. Several drugs, including lopinavir/ritonavir, hydroxychloroquine, dexamethasone, and remdesivir, have been evaluated for the treatment of COVID-19 during the past year. While most of the drugs failed to display efficacy in treating COVID-19, scientists have encouraged herd immunity to control the pandemic. Immunity generated after natural infection with SARS-CoV-2 is precarious, as indicated by real-world evidence in the form of epidemiological data from Manaus, Brazil. Vaccines using different platforms are therefore the most promising approach to help us return to normality. Although several vaccines have been authorized for emergency use, there are still many concerns regarding their accessibility, the vaccination rate, and most importantly, their efficacy in preventing infection with emerging virus variants. Continued virus surveillance and rapid redesign of new vaccines to counter new variants are crucial to fighting COVID-19. Rapid production and extensive vaccination are also essential to preventing the emergence of new variants. Nevertheless, antivirals including monoclonal antibodies and oral medicines need to be developed in light of uncertainties with regard to vaccination. In the battle between humans and SARS-CoV-2, the speed with which we fight the virus, and especially its emerging variants, is the key to winning.

Keywords COVID-19, SARS-CoV-2, vaccine, variants

The COVID-19 pandemic has infected more than 100 million people and caused 2 million deaths as the end of February 2021. Since its outbreak, China implemented various interventions, including a complete lockdown of the population, mandated wearing of masks outside the home, and handwashing during the first wave of the disease. Public participation in and adherence to control measures helped the Chinese Government to quickly control the epidemic. Although cases have been imported and contaminated imports have caused recent COVID-19 outbreaks in several cities, these outbreaks were stamped out thanks to China's disease control system, which involves quarantine upon entry, rapid case diagnosis, active case surveillance, strict follow-up, and quarantine of close contacts. Unlike China, many countries implemented an incomplete lockdown. More importantly, people failed to fully adhere to control measures. The number of the infected fluctuated depending on the strength of the control measures but never declined to zero.

These measures have been at the expense of the economy. More importantly, these strict control measures alone are not effective enough to stop the COVID-19 pandemic. Even in China, where the strictest control measures were implemented, sporadic cases of COVID-19 have still been reported. The world is, therefore, looking forward to effective medicines and vaccines to prevent or treat COVID-19. During the past year, several drugs to treat COVID-19 were investigated, most of which were repurposed. While most of the drugs including lopinavir/ritonavir and hydroxychloroquine failed to display efficacy in clinical trials, dexamethasone has been found to decrease mortality among some patients with COVID-19, and especially those with severe or critical disease (*1,2*). However, the role of remdesivir in treating COVID-19 is still controversial. Although several clinical trials indicated that remdesivir was superior to a placebo in reducing the time to recovery in adults who were hospitalized with COVID-19, the WHO has recommended against its use in inpatients, regardless of disease severity, as there is currently no evidence that it improves survival (*3,4*).

Herd immunity, achieved either by natural infection or by vaccination, is therefore being pursued to prevent the spread of disease and to control the pandemic. However, mounting evidence suggests that natural infection is not able to achieve herd immunity as expected. Dozens of reinfections with SARS-CoV-2

have been reported, indicating that immunological memory generated by natural infection may not strong or last long enough to protect people from reinfection. More importantly, epidemiological data from the city of Manaus, Brazil, have indicated the precarious state of natural herd immunity in the real world. The rate of infection with SARS-CoV-2 was estimated to increase from 66% in June to 76% in October in Manaus based on seroprevalence data (*5*). The high seroprevalence indicates that natural herd immunity has been achieved, given a basic reproduction number of 3 (*6*). However, the number of hospitalizations for COVID-19 in Manaus increased sharply in January 2021. Several possible explanations have been put forward, including overestimated seroprevalence before the second wave and a rapid decline in immunological memory post-infection, but the most pressing concern is new variants of the virus (*7*). In a preliminary study, the new virus variant P.1 was identified in 42% (13/31) of samples from patients reported in Manaus in December 2020, though it was absent in 26 samples collected between March and November 2020 (*8*). Indeed, the new variant has been linked to increased infectivity in mouse models (*9*). Reinfection with the P.1 lineage in Manaus was also reported in January 2021 (*10*). This evidence suggests that the high transmission of P.1 may require a higher seroprevalence to achieve herd immunity and that P.1 may evade immunological memory generated post-infection (*11*). Therefore, herd immunity from an infection should not be an option either from an ethical or scientific point of view (*12*).

A host of potential COVID-19 vaccines is currently being developed based on different platforms, from conventional inactivated and live attenuated vaccines to more creative message RNA (mRNA) and DNA technologies including viral vector and subunit vaccines. Most potential COVID-19 vaccines target the spike protein of SARS-CoV-2. Several vaccines have been authorized for emergency use with varied efficacy in preventing COVID-19 and in decreasing disease severity. In a real-world study, the BNT162b2 mRNA COVID-19 vaccine was effective for a wide range of COVID-19–related outcomes (*13*). With the high rate of protection from infection after vaccination, herd immunity could theoretically be achieved. However, the use of vaccines to control the pandemic still faces many challenges. The most serious concern is the availability of vaccines. As of March 5, 2021, only around 291 million people have been vaccinated (*14*). A shortage of vaccines, especially in developing countries, is one of the main reasons for the low vaccination rate worldwide. Another explanation might be the limited willingness of people to be vaccinated. According to a recent survey, around half of respondents would not take a vaccine even if it was available (*14*). Moreover, there are still several questions about vaccines that remain unanswered. These include the duration of the protective effect of a vaccine and cross-protection against virus variants, and especially emerging mutations. A most recent study examined immunogenicity 119 days after initial vaccination with mRNA-1273 and noted high levels of binding and neutralizing antibodies against SARS-CoV-2 even though those levels were expected to decline over time (*15*). The study in question indicated that immunity generated by a vaccine, or at least mRNA-1273, has the potential to provide sustained protection against SARS-CoV-2. However, virus variants also diminish the efficacy of vaccines. Although most researchers believe that the D614G variant and the B.1.1.7 strain will not affect the efficacy of vaccines, the B.1.351 variant was found to be partially resistant to neutralizing antibodies induced by most of the common vaccines used worldwide, including the Pfizer mRNA vaccine, the Moderna mRNA vaccine, and the Novavax protein vaccine (*16,17*).

As the vaccination rate increases, new cases of COVID-19 are now declining. However, there is still much uncertainty, given emerging new variants, the unknown duration and efficacy of protection, and questions about efficacy against new variants. There are several strategies that could be adopted now to control the pandemic and eventually eliminate the disease. The most important approach is to continue viral surveillance and rapid design of vaccines against new variants. We cannot predict whether virus variants will emerge in the future. Therefore, viral surveillance and rapid evaluation of vaccine efficacy against new viral variants are extremely important. Indeed, under the current threat of new variants and B.1.351 in particular, all leading vaccine companies are now redesigning their vaccines to counter new variants. The development of a broad-spectrum vaccine against SARS-CoV-2 by retaining the conserved amino acids in the receptor-binding domain region also offers promise (*18*).

Rapid production of vaccines and extensive vaccination are also essential to winning the battle. Virus variants can only emerge when a large number of people are infected. While herd immunity is generated by vaccination, the number of the infected would decrease sharply, thus limiting the emergence of virus variants. However, mutations that evade the vaccine might appear when immunity wanes or in the event of incomplete vaccination (*e.g.*, taking only one dose of a vaccine that requires two doses). Therefore, rapid and complete vaccination and monitoring of the immune response should be implemented.

Until vaccine-induced herd immunity is achieved, another favorable strategy would be to develop new medicines that are effective against SARS-CoV-2. The FDA has authorized the emergency use of two monoclonal antibodies for the treatment of COVID-19 as they were able to limit SARS-CoV-2 replication in the nasopharynx and therefore prevent disease progression if administered early (*19*). However, the efficacy of

monoclonal antibodies against viral variants, and B.1.351 in particular, has raised concern. In a recent study, binding of the REGN-COV2 cocktail to B.1.351 variants was nine times lower than that to other prevalent SARS-CoV-2 strains (*20*). Therefore, the combination of several different monoclonal antibodies should be tested in future clinical trials. More importantly, new monoclonal antibodies or spectrum neutralizing antibodies should be developed faster than new variants emerge.

Besides vaccines and monoclonal antibodies, the development of antivirals to treat COVID-19 should not be ruled out. Given the uncertainty of vaccines, affordable and convenient medicines (*e.g.* oral preparations) for the treatment of COVID-19 may not only help to limit the spread of the pandemic but more importantly alleviate the fears of the general public. In developing countries, the best strategies are to social distance, wash one's hands, and wear a mask while awaiting vaccines and affordable drugs. These countries need to control the epidemic as much as they can, though vaccines and drugs should be provided as early as possible. In this battle between humans and viruses, the slower the process, the more likely we are to lose.

Funding: This work was supported by the Shanghai Science and Technology Committee (grant nos. 20411950200 and 20Z11900900), the fund to foster personnel in Shanghai (grant no. 2020089), and the Shanghai "Rising Stars in Medicine" program to foster young medical personnel (grant no. 2019-72).

Conflict of Interest: The authors have no conflicts of interest to disclose.

References

1. Cao B, Wang Y, Wen D, *et al*. A trial of lopinavir-ritonavir in adults hospitalized with severe Covid-19. N Engl J Med. 2020; 382:1787-1799.
2. RECOVERY Collaborative Group, Horby P, Lim WS, *et al*. Dexamethasone in hospitalized patients with Covid-19. N Engl J Med. 2021; 384:693-704.
3. Beigel JH, Tomashek KM, Dodd LE, *et al*. Remdesivir for the treatment of Covid-19 - Final report. N Engl J Med. 2020; 383:1813-1826.
4. World Health Orgnization. Therapeutics and COVID-19: Living guideline. 2020. *https://www.who.int/publications/i/item/therapeutics-and-covid-19-living-guideline* (accessd March 7, 2021).
5. Buss LF, Prete CA, Jr., Abrahim CMM, *et al*. Three-quarters attack rate of SARS-CoV-2 in the Brazilian Amazon during a largely unmitigated epidemic. Science. 2021; 371:288-292.
6. Fontanet A, Cauchemez S. COVID-19 herd immunity: Where are we? Nature Reviews Immunology. 2020; 20:583-584.
7. Sabino EC, Buss LF, Carvalho MPS, *et al*. Resurgence of COVID-19 in Manaus, Brazil, despite high seroprevalence. Lancet. 2021; 397:452-455.
8. Faria NR, Claro IM, Candido D, *et al*. Genomic characterisation of an emergent SARS-CoV-2 lineage in Manaus: Preliminary findings. *https://virological.org/t/genomic-characterisation-of-an-emergent-sars-cov-2-lineage-in-manaus-preliminary-findings/586* (accessd March 7, 2021).
9. Rambaut A, Loman N, Pybus O, Barclay W, Barrett J, Carabelli A, Connor T, Peacock T, Robertson DL, Volz E, on behalf of COVID-19 Genomics Consortium UK (CoG-UK). Preliminary genomic characterisation of an emergent SARS-CoV-2 lineage in the UK defined by a novel set of spike mutations. *https://virological.org/t/preliminary-genomic-characterisation-of-an-emergent-sars-cov-2-lineage-in-the-uk-defined-by-a-novel-set-of-spike-mutations/563* (accessd March 7, 2021).
10. Naveca F, Costa CD, Nascimento V, *et al*. SARS-CoV-2 reinfection by the new Variant of Concern (VOC) P.1 in Amazonas, Brazil. *https://virological.org/t/sars-cov-2-reinfection-by-the-new-variant-of-concern-voc-p-1-in-amazonas-brazil/596* (accessd March 7, 2021).
11. Taylor L. Covid-19: Is Manaus the final nail in the coffin for natural herd immunity? BMJ. 2021; 372:n394.
12. Sridhar D, Gurdasani D. Herd immunity by infection is not an option. Science. 2021; 371:230-231.
13. Dagan N, Barda N, Kepten E, Miron O, Perchik S, Katz MA, Hernan MA, Lipsitch M, Reis B, Balicer RD. BNT162b2 mRNA Covid-19 vaccine in a nationwide mass vaccination setting. N Engl J Med. 2021.
14. Data OWi. Coronavirus (COVID-19) Vaccinations. *https://ourworldindata.org/covid-vaccinations* (accessd March 7, 2021).
15. Widge AT, Rouphael NG, Jackson LA, *et al*. Durability of responses after SARS-CoV-2 mRNA-1273 vaccination. N Engl J Med. 2021; 384:80-82.
16. Wu K, Werner AP, Koch M, *et al*. Serum neutralizing activity elicited by mRNA-1273 vaccine - Preliminary report. N Engl J Med. 2021.
17. Liu Y, Liu J, Xia H, *et al*. Neutralizing activity of BNT162b2-elicited serum - Preliminary report. N Engl J Med. 2021. doi: 10.1056/NEJMc2102017.
18. Ma C, Su S, Wang J, Wei L, Du L, Jiang S. From SARS-CoV to SARS-CoV-2: Safety and broad-spectrum are important for coronavirus vaccine development. Microbes Infect. 2020; 22:245-253.
19. Chen P, Nirula A, Heller B, *et al*. SARS-CoV-2 Neutralizing antibody LY-CoV555 in outpatients with Covid-19. N Engl J Med. 2021; 384:229-237.
20. Tada T, Dcosta BM, Zhou H, Vaill A, Kazmierski W, Landau NR. Decreased neutralization of SARS-CoV-2 global variants by therapeutic anti-spike protein monoclonal antibodies. bioRxiv. 2021; 2021.02.18.431897. doi: 10.1101/2021.02.18.431897.

Received March 8, 2021; Revised March 13, 2021; Accepted March 15, 2021.

**Address correspondence to:*
Hongzhou Lu, Department of Infectious Diseases and Immunology, Shanghai Public Health Clinical Center, Fudan University, 2901 Caolang Road, Shanghai 201508, China.
E-mail: luhongzhou@fudan.edu.cn

Released online in J-STAGE as advance publication March 19, 2021.

Communication

DOI: 10.5582/bst.2021.01099

Burnout in nurses during the COVID-19 pandemic in China: New challenges for public health

Lin Zhang[§], Ling Chai[§], Yihong Zhao, Lin Wang, Wenxiu Sun, Lingqing Lu, Hongzhou Lu[*], Jianliang Zhang[*]

Shanghai Public Health Clinical Center, Fudan University, Shanghai, China.

SUMMARY During the COVID-19 pandemic, frontline nurses have faced extraordinary personal and professional challenges. These challenges have had mental health consequences, and concerning reports of burnout have emerged globally. We conducted a cross-sectional survey at a designated COVID-19 hospital in Shanghai at the peak of the pandemic, *i.e*. about 2 months after the onset of the outbreak from February to April 2020. Findings revealed burnout in 6.85% of nurses. Of 336 respondents, 87 (25.89%) had a high level of emotional exhaustion, 61 (18.15%) had a high level of depersonalization, and 100 (29.76%) had a low level of personal accomplishment. Burnout can be prevented by offering more support from families and supervisors, paying attention to health monitoring and personal protection, and creating a rational human resource allocation and shift management system. Specific training on infection control and self-protection, mental health guidance, and stress coping techniques must be implemented. As the current health crisis ultimately abates, moving the focus from mental health issues to public health issues, more attention and support at the national and organizational levels are needed to reduce occupational discrimination, nurse autonomy and status need to be promoted, and public health emergency teams need to be created. A positive and fair working environment is essential to effective healthcare delivery.

Keywords COVID-19, Chinese nurses, burnout, workload, Shanghai

1. Introduction

The spread of the novel coronavirus SARS-CoV-2 and the disease it causes (COVID-19) has resulted in an unprecedented global health crisis. This unfolding healthcare emergency has placed nurses under increasing pressure (*1*), with broad repercussions for their mental health. In specific terms, burnout has emerged as a significant concern, affecting both quality of life and workplace performance (*2,3*). In China, nurses have played a critical role in the treatment of COVID-19 and they constitute the largest subset of healthcare workers (*4*). Unlike in Hubei Province where approximately 28,600 nurses were deployed to assist local healthcare teams in the fight against COVID-19, Shanghai depended on a combination of support nurses from the top three hospitals in Shanghai, together with nurses at a designated COVID-19 hospital. Moving the focus from patient care to caregiver health, the current authors conducted a cross-sectional survey at a designated COVID-19 hospital in Shanghai at the peak of the pandemic, *i.e*. about 2 months after the onset of the outbreak from February to April 2020. Findings revealed burnout in 6.85% of nurses. Out of 336 respondents, 87 (25.89%) had a high level of emotional exhaustion, 61 (18.15%) had a high level of depersonalization, and 100 (29.76%) had a low level of personal accomplishment (Supplementary Table S1-3, *http://www.biosciencetrends.com/action/getSupplementalData.php?ID=72*). Accordingly, burnout poses not just a risk to Chinese nurses but also to the Chinese healthcare system. To highlight the issue of burnout, the current authors explored the factors influencing burnout in this cohort and suggested corresponding countermeasures to assist Chinese nurses in adjusting to public health emergencies. Future pandemics may occur more frequently, so public health officials and policymakers must act to protect the mental health of healthcare workers.

2. Tackling burnout among nurses: Efforts are underway

Burnout is an under-recognized and under-reported problem. Burnout is characterized by a state of emotional exhaustion (EE) and/or depersonalization (DP) and a low sense of personal accomplishment (PA). In the

current study, 92.56% of the nurses working in a front-line care setting were women and 46.43% had children; burnout in this cohort is likely related to marital status and age, so family responsibilities should be considered to reassure frontline nurses. The Department of Nursing has proposed family-based support programs, evaluated every nurse's level of family and social support and mental health before starting frontline work, arranged for visits home, provided necessary assistance to relieve nurses' concerns when entered frontline wards, and encouraged an hour-long video or voice call with family members every day.

A previous study found that younger and less experienced staff members had a higher level of DP than nurses over the age of 30 (*5*), which is consistent with the current findings. Continuous guidance and psychological assistance should be offered to this vulnerable group of nurses. The Department of Nursing established a series of training courses, including orientation to general emergency ward work and nursing responsibilities, infection control and self-protection, and mental health guidance to orient younger less experienced nurses during the pandemic response. In terms of nurses' own health and personal protection, daily self-health monitoring is promoted, and anti-viral sprays and thymus injections to enhance immunity are offered and vaccination is encouraged. To improve mental health care, the Department of Nursing engaged psychiatrists and psychologists to provide online counseling, advice hotlines, and online chat rooms for frontline nursing staff. Involvement of mental health care professionals may allow for earlier intervention and improved ability to cope with negative emotions.

As the pandemic continues, an important consideration is that frontline nurses work in a specific work environment, facing a heavy workload while combating a highly contagious disease (*6,7*). When nurses care for grievously suffering patients and patients with multiple requirements, they are more likely to experience burnout (*8*). This is typically how Chinese nurses work on the frontline, in addition to providing basic treatment and nursing, serving food to patients, preparing their daily necessities, and meeting the special needs of patients of different nationalities. They also disinfect items, transport specimens, and supervise infection control.

Interestingly, nurses who cared for mildly ill patients reported a higher level of EE, a higher level of DP, and a lower level of PA than those who cared for severely ill patients. This may be related to differences in human resource allocation where, relatively speaking, nurses caring for mildly ill patients cared for more patients. Other researchers have also reported that when nurses care for a higher number of patients, they are more likely to experience burnout (*9*). In this context, nurses' work cycles and shifts were adjusted based on the work experience of nursing administrators and the bed-to-care ratio in general wards. A rational human resource allocation and shift management system should be created within the Department of Nursing. This system would adjust human resource allocation based on the number of patients admitted, their condition, and the overall workload intensity. At the authors' hospital, most of the support measures considered were implemented for frontline nurses. Comfortable living conditions, sufficient materials, and sufficient nutrients were considered the most necessary measures. In addition, benefits such as incentives and promotions should be provided to encourage frontline nurses.

3. Burnout: Moving the focus from mental health issues to public health issues

Paying attention to early burnout among nurses on the frontline can help to provide timely solutions to prevent further worsening of this problem. As the current health crisis ultimately abates, China has transitioned to the mitigation phase. Given the burnout seen among frontline nurses, has enough been done? Is it too little, too late? And how can China better prepared for future pandemics that may occur more frequently? The current study was conducted at a designated COVID-19 hospital in Shanghai and countermeasures for burnout were proposed. In-depth interviews may help to identify important issues and may be a topic of further study. Research has shown that nursing professionals nationwide were already experiencing burnout and subsequent turnover during the COVID-19 pandemic, indicating that the mental health of healthcare workers and insufficient human resources are serious issues that public health officials and policymakers need to address. In order to deal with the shortage of nurses with multiple specialties in the emergency response to public health emergencies, the current authors' hospital committed to creating “special nursing teams” to prepare and train for both peacetime and wartime while improving their overall clinical competence and efficiency. For the government, the urgent task is to create and prepare public health and epidemic prevention teams to respond to outbreaks of infectious diseases and deal with human turnover. Healthcare professionals may also face extra hardships during a pandemic due to the discrimination and lack of understanding faced by individuals and their families. A positive working environment should be created, nurse autonomy should be promoted, and the status of nurses should be improved. The government should actively promote positive news reports, improve the population's awareness of infectious disease control, and reduce "secondary psychological harms and panic" caused by discrimination against medical personnel combating infectious diseases.

Funding: The work was supported by grants from Fudan University's Project to Create First-class Universities

and First-class Disciplines (grant no. IDF162005), the Shanghai Public Health Clinical Center's Special Scientific Research Project on COVID-19 (grant no. 2020YJKY01), a Fudan University Project (grant no. FNF202042), and the Shanghai Shenkang Hospital Development Center Project (grant no. 2020SKMR-10).

Conflict of Interest: The authors have no conflicts of interest to disclose.

References

1. Bradley M, Chahar P. Burnout of healthcare providers during COVID-19. Cleve Clin J Med. 2020. doi: 10.3949/ccjm.87a.ccc051.
2. Chen Q, Liang M, Li Y, Guo J, Fei D, Wang L, He L, Sheng C, Cai Y, Li X, Wang J, Zhang Z. Mental health care for medical staff in China during the COVID-19 outbreak. Lancet Psychiatry. 2020; 7:e15-e16.
3. Joshi G, Sharma G. Burnout: A risk factor amongst mental health professionals during COVID-19. Asian J Psychiatr. 2020; 54:102300.
4. Smith GD, Ng F, Ho Cheung Li W. COVID-19: Emerging compassion, courage and resilience in the face of misinformation and adversity. J Clin Nurs. 2020; 29:1425-1428.
5. Gomez-Urquiza JL, Vargas C, De la Fuente EI, Fernandez-Castillo R, Canadas-De la Fuente GA. Age as a risk factor for burnout syndrome in nursing professionals: A meta-analytic study. Res Nurs Health. 2017; 40:99-110.
6. Perez-Francisco DH, Duarte-Climents G, Del Rosario-Melian JM, Gomez-Salgado J, Romero-Martin M, Sanchez-Gomez MB. Influence of workload on primary care nurses' health and burnout, patients' safety, and quality of care: Integrative review. Healthcare (Basel). 2020; 8:12.
7. Li W, Frank E, Zhao Z, Chen L, Wang Z, Burmeister M, Sen S. Mental health of young physicians in China during the novel coronavirus disease 2019 outbreak. JAMA Netw Open. 2020; 3:e2010705.
8. Rizo-Baeza M, Mendiola-Infante SV, Sepehri A, Palazon-Bru A, Gil-Guillen VF, Cortes-Castell E. Burnout syndrome in nurses working in palliative care units: An analysis of associated factors. J Nurs Manag. 2018; 26:19-25.
9. Morgantini LA, Naha U, Wang H, Francavilla S, Acar O, Flores JM, Crivellaro S, Moreira D, Abern M, Eklund M, Vigneswaran H, Weine SM. Factors contributing to healthcare professional burnout during the COVID-19 pandemic: A rapid turnaround global survey. medRxiv. 2020; doi: 10.1101/2020.05.17.20101915.

Received February 2, 2021; Revised March 15, 2021; Accepted March 24, 2021.

[§]These authors contributed equally to this work.
**Address correspondence to:*
Hongzhou Lu and Jianliang Zhang, Shanghai Public Health Clinical Center, Fudan University, No 2901. Caolang Road, Shanghai 201508, China.
E-mail: luhongzhou@fudan.edu.cn (Lu HZ), zhangjianliang@shphc.org.cn (Zhang JL)

Released online in J-STAGE as advance publication March 26, 2021.

Letter

DOI: 10.5582/bst.2021.01046

ChIP-sequencing analysis of E2F transcription factor 2 reveals its role in various biological processes of rheumatoid arthritis synovial fibroblasts

Luwen Li[1,2,3], Yihang Zhang[1,2,3], Lin Wang[1,2,3], Jihong Pan[1,2,3,*]

[1] Biomedical Sciences College & Shandong Medicinal Biotechnology Centre, Shandong First Medical University & Shandong Academy of Medical Sciences, Ji'nan, China;
[2] Key Lab for Biotech-Drugs of National Health Commission, Ji'nan, China;
[3] Key Lab for Rare & Uncommon Diseases of Shandong Province, Ji'nan, China.

SUMMARY The development and progression of rheumatoid arthritis (RA) are complex and the pathogenesis of this disease is not fully understood. E2F transcription factor 2 (E2F2) affects the development and progression of many diseases. To identify the mechanisms underlying the role of E2F2 in RA, chromatin immunoprecipitation was performed followed by sequencing (ChIP-seq) using the E2F2 antibody. Gene Ontology (GO) analysis of differentially expressed genes (DEGs) and Kyoto Encyclopedia of Genes and Genomes (KEGG) pathway enrichment of captured downstream target genes and Metascape analysis of 22 protein molecules partly elucidated the mechanism by which E2F2 affects the progression of RA. Results indicated that E2F2 affects the metabolism of RASFs and the development of ribosome synthesis as well as the stress response. Results indicated that E2F2 can affect multiple biological processes involving RASFs and indicate a unique possibility of targeting E2F2 in the treatment of RA.

Keywords E2F2, ChIP-seq, metabolism, stress response, synthesis of ribosomes

Rheumatoid arthritis (RA) is a chronic autoimmune disease mainly characterized by erosive and symmetrical polyarthritis (*1*). Factors such as heritability, hormones, and the environment are involved in the pathogenesis of RA (*2*); however, its etiology and pathogenesis are complex and have not been fully elucidated. E2F2 is a member of the E2F family of transcription factors and affects the development and progression of many diseases. E2F2 also affects various cellular processes, such as the cell cycle, proliferation, apoptosis, invasion, and migration (*3*). E2F2 promotes the secretion of inflammatory factors in RA synovial fibroblasts (RASFs) and influences the development of RA (*4*). However, additional mechanisms underlying the role of E2F2 in the development and progression of RA need to be elucidated.

The current authors conducted a study to further identify the mechanisms of E2F2 in RASFs in order to study RA in-depth. The synovial tissue of a patient with RA (female, 56 years of age, DAS28: 3.7; RF: 56; CRP: 59 mg/L; anti-CCP: 26 E/mL; and time of onset: 16 months) was collected during knee replacement surgery. The synovial tissue was collected at Shandong Provincial Hospital (Ji'nan, China), and informed consent was obtained from the patient. The research plan was approved by the Ethics Committee of the Shandong Academy of Medical Sciences. The patient met the American College of Rheumatology diagnostic criteria for RA. Fetal calf serum was purchased from Invitrogen, Carlsbad, CA, USA. Anti-E2F2 antibody (SAB2108118) was purchased from Sigma-Aldrich, St. Louis, MO, USA.

As were used in previous studies, type II and III collagenases were used to digest synovial tissue for 6 hours (*5*) and RASFs were cultured. RASF cells (1×10^6) were harvested and crosslinked with formaldehyde. Cells were then lysed and sonicated, and anti-E2F2 antibody was used in immunoprecipitation (IP). This was followed by water bath decrosslinking, DNA purification, construction of a sequencing library, amplification, and high-throughput sequencing. The protocol is as described by Park (*6*).

Gene Ontology (GO) was used to perform enrichment analysis on the functions of peak-related genes, and the Kyoto Encyclopedia of Genes and Genomes (KEGG) was used to perform significant

enrichment analyses on the pathway functions of related genes. Finally, Metascape was used to analyze protein molecules.

GO function annotation and enrichment analysis of KEGG metabolic pathways were performed on high-throughput E2F2 ChIP-seq results. GO annotation indicated that differentially expressed genes were mainly enriched in the nitrogen compound metabolic process, cellular nitrogen compound metabolic process, cellular component organization, or biogenesis (Figure 1A). KEGG pathway annotation indicated that the genes participated in 19 metabolic pathways including ribosomes, Parkinson's disease, and oxidative phosphorylation (Figure 1B).To further explore the mechanism by which E2F2 influences the progression of RA, protein molecules from ChIP-seq were screened and enriched for E2F2. Twenty-two proteins (Figure 1C) were identified, and enrichment analysis was performed with Metascape. Metascape indicated that the main pathways included localization, the response to stimulus, the metabolic process, and biological regulation (Figure 1D). These results are in accordance with the results described earlier and further illustrate that downstream genes regulated by E2F2 are closely related to the metabolic process. The current results also indicate that E2F2 may affect the body's stress response. Interestingly, two of the 22 proteins, thrombospondin-1 (THBS1) and derlin-1, are related to endoplasmic reticulum (ER) stress. Moreover, THBS1 may be a biomarker of early RA (*7*). Abnormal ER stress may promote the

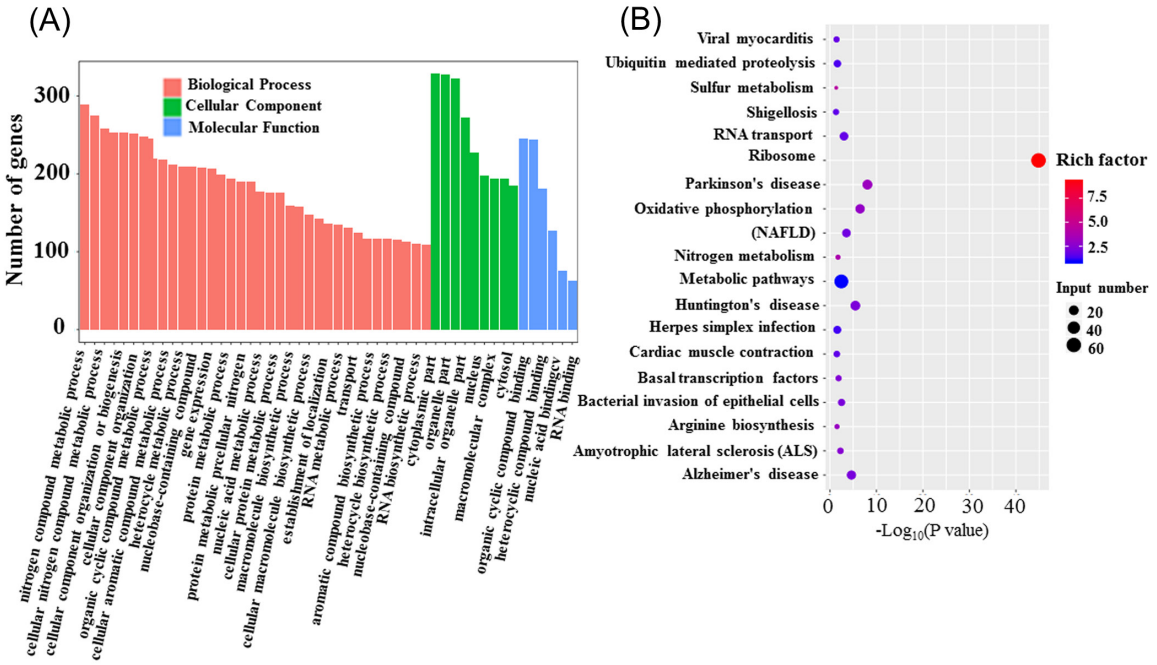

(C)

RAC1	GPR37L1	PLA2G12B	BRD9	THBS1
EYA3	ERVV-2	TBC1D12	EPRS1	ADCK1
CIAO3	MED4	DERL1	ECSIT	VANGL1
MBOAT1	SOCS2	SRSF4	OR6C1	RFESD
CLPTM1	ERAS			

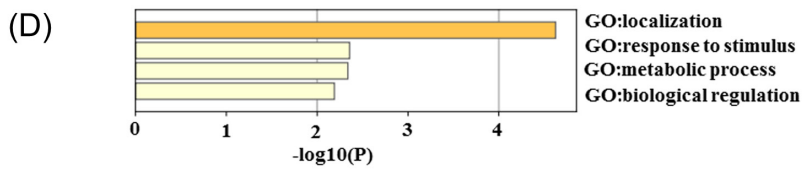

Figure 1. Enrichment of differential genes. (A) Number of genes identified for specific GO annotation terms. **(B)** KEGG pathway enrichment indicating the significance of enrichment. The size of the dot indicates the number of genes in the KEGG pathway, and the shade of the dot indicates the degree of rich factor enrichment. **(C)** The 22 proteins identified by screening and enrichment from E2F2 ChIP-seq. **(D)** Metascape was used to enrich the 22 corresponding genes; enrichment terms are represented in terms of their degree of enrichment. This is expressed as a -log10 [*P*-value], where a higher value indicates more significant enrichment **(B,D)**.

pathogenesis of RA through abnormal cell proliferation and production of pro-inflammatory cytokines (*8,9*). The 22 identified genes also encoded some proteins related to cellular processes (RAC1, CLPTM1, and ERAS), signal conversion-related proteins (GPR37L1.ECSIT), transcription-related proteins (MED4 and BRD9), and ubiquitin ligase in protein degradation. These molecules represent different aspects of the complexity of the pathogenesis of RA.

In summary, the current results indicated that E2F2 influences metabolism, the stress response, and ribosome synthesis of RASFs, thereby affecting the development and progression of RA. Therefore, a promising strategy would be to intervene in metabolism, the stress response, and ribosome synthesis to combat the progression of RA. Accordingly, E2F2 is likely to serve as a potential target in the treatment of RA.

Funding: This research was supported by a grant from the National Sciences Fund Committee (NSFC) of China (Grant No. 81671624).

Conflict of Interest: The authors have no conflicts of interest to disclose.

References

1. Liu Y, Jin J, Xu H, Wang C, Yang Y, Zhao Y, Han H, Hou T, Yang G, Zhang L, Wang Y, Zhang W, Liang Q. Construction of a pH-responsive, ultralow-dose triptolide nanomedicine for safe rheumatoid arthritis therapy. Acta Biomater. 2021; 121:541-553.
2. Smolen JS, Aletaha D, McInnes IB. Rheumatoid arthritis. Lancet. 2016; 388:2023-2038.
3. Evangelou K, Havaki S, Kotsinas A. E2F transcription factors and digestive system malignancies: How much do we know? World J Gastroenterol. 2014; 20:10212-10216.
4. Zhang R, Wang L, Pan JH, Han J. A critical role of E2F transcription factor 2 in proinflammatory cytokines-dependent proliferation and invasiveness of fibroblast-like synoviocytes in rheumatoid Arthritis. Sci Rep. 2018; 8:2623.
5. Wang L, Zheng Y, Xu H, Yan X, Chang X. Investigate pathogenic mechanism of TXNDC5 in rheumatoid arthritis. PLoS One. 2013; 8:e53301.
6. Park PJ. ChIP-seq: Advantages and challenges of a maturing technology. Nat Rev Genet. 2009; 10:669-680.
7. Rahmati M, Moosavi MA, McDermott MF. ER stress: A therapeutic target in rheumatoid arthritis? Trends Pharmacol Sci. 2018; 39:610-623.
8. Yamasaki S, Yagishita N, Tsuchimochi K, Nishioka K, Nakajima T. Rheumatoid arthritis as a hyper-endoplasmic-reticulum-associated degradation disease. Arthritis Res Ther. 2005; 7:181-186.
9. Park YJ, Yoo SA, Kim WU. Role of endoplasmic reticulum stress in rheumatoid arthritis pathogenesis. J Korean Med Sci. 2014; 29:2-11.

Received January 27, 2021; Revised March 26, 2021; Accepted April 22, 2021.

**Address correspondence to:*
Jihong Pan, Biomedical Sciences College & Shandong Medicinal Biotechnology Centre, Shandong First Medical University & Shandong Academy of Medical Sciences, No. 6699 Qingdao Road, Ji'nan 250117, China.
E-mail: panjihong@sdfmu.edu.cn

Released online in J-STAGE as advance publication April 29, 2021.

BST
BioScience Trends

Guide for Authors

1. Scope of Articles

BioScience Trends (Print ISSN 1881-7815, Online ISSN 1881-7823) is an international peer-reviewed journal. *BioScience Trends* devotes to publishing the latest and most exciting advances in scientific research. Articles cover fields of life science such as biochemistry, molecular biology, clinical research, public health, medical care system, and social science in order to encourage cooperation and exchange among scientists and clinical researchers.

2. Submission Types

Original Articles should be well-documented, novel, and significant to the field as a whole. An Original Article should be arranged into the following sections: Title page, Abstract, Introduction, Materials and Methods, Results, Discussion, Acknowledgments, and References. Original articles should not exceed 5,000 words in length (excluding references) and should be limited to a maximum of 50 references. Articles may contain a maximum of 10 figures and/or tables. Supplementary Data are permitted but should be limited to information that is not essential to the general understanding of the research presented in the main text, such as unaltered blots and source data as well as other file types.

Brief Reports definitively documenting either experimental results or informative clinical observations will be considered for publication in this category. Brief Reports are not intended for publication of incomplete or preliminary findings. Brief Reports should not exceed 3,000 words in length (excluding references) and should be limited to a maximum of 4 figures and/or tables and 30 references. A Brief Report contains the same sections as an Original Article, but the Results and Discussion sections should be combined.

Reviews should present a full and up-to-date account of recent developments within an area of research. Normally, reviews should not exceed 8,000 words in length (excluding references) and should be limited to a maximum of 10 figures and/or tables and 100 references. Mini reviews are also accepted, which should not exceed 4,000 words in length (excluding references) and should be limited to a maximum of 5 figures and/or tables and 50 references.

Policy Forum articles discuss research and policy issues in areas related to life science such as public health, the medical care system, and social science and may address governmental issues at district, national, and international levels of discourse. Policy Forum articles should not exceed 3,000 words in length (excluding references) and should be limited to a maximum of 5 figures and/or tables and 30 references.

Communications are short, timely pieces that spotlight new research findings or policy issues of interest to the field of global health and medical practice that are of immediate importance. Depending on their content, Communications will be published as "Comments" or "Correspondence". Communications should not exceed 1,500 words in length (excluding references) and should be limited to a maximum of 2 figures and/or tables and 20 references.

Editorials are short, invited opinion pieces that discuss an issue of immediate importance to the fields of global health, medical practice, and basic science oriented for clinical application. Editorials should not exceed 1,000 words in length (excluding references) and should be limited to a maximum of 10 references. Editorials may contain one figure or table.

News articles should report the latest events in health sciences and medical research from around the world. News should not exceed 500 words in length.

Letters should present considered opinions in response to articles published in *BioScience Trends* in the last 6 months or issues of general interest. Letters should not exceed 800 words in length and may contain a maximum of 10 references. Letters may contain one figure or table.

3. Editorial Policies

For publishing and ethical standards, BioScience Trends follows the Recommendations for the Conduct, Reporting, Editing, and Publication of Scholarly Work in Medical Journals (*http://www.icmje.org/recommendations*) issued by the International Committee of Medical Journal Editors (ICMJE), and the Principles of Transparency and Best Practice in Scholarly Publishing (*https://doaj.org/bestpractice*) jointly issued by the Committee on Publication Ethics (COPE), the Directory of Open Access Journals (DOAJ), the Open Access Scholarly Publishers Association (OASPA), and the World Association of Medical Editors (WAME).

BioScience Trends will perform an especially prompt review to encourage innovative work. All original research will be subjected to a rigorous standard of peer review and will be edited by experienced copy editors to the highest standards.

Ethics: *BioScience Trends* requires that authors of reports of investigations in humans or animals indicate that those studies were formally approved by a relevant ethics committee or review board. For research involving human experiments, a statement that the participants gave informed consent before taking part (or a statement that it was not required and why) should be indicated. Authors should also state that the study conformed to the provisions of the Declaration of Helsinki (as revised in 2013). When reporting experiments on animals, authors should indicate whether the institutional and national guide for the care and use of laboratory animals was followed.

Conflict of Interest: All authors are required to disclose any actual or potential conflict of interest including financial interests or relationships with other people or organizations that might raise questions of bias in the work reported. If no conflict of interest exists for each author, please state "There is no conflict of interest to disclose".

Submission Declaration: When a manuscript is considered for submission to *BioScience Trends*, the authors should confirm that 1) no part of this manuscript is currently under consideration for publication elsewhere; 2) this manuscript does not contain the same information in whole or in part as manuscripts that have been published, accepted, or are under review elsewhere, except in the form of an abstract, a letter to

the editor, or part of a published lecture or academic thesis; 3) authorization for publication has been obtained from the authors' employer or institution; and 4) all contributing authors have agreed to submit this manuscript.

Cover Letter: The manuscript must be accompanied by a cover letter prepared by the corresponding author on behalf of all authors. The letter should indicate the basic findings of the work and their significance. The letter should also include a statement affirming that all authors concur with the submission and that the material submitted for publication has not been published previously or is not under consideration for publication elsewhere. The cover letter should be submitted in PDF format. For example of Cover Letter, please visit: Download Centre (*https://ircabssagroup.com/downcentre*).

Copyright: When a manuscript is accepted for publication in *BioScience Trends*, the transfer of copyright is necessary. A JOURNAL PUBLISHING AGREEMENT (JPA) form will be e-mailed to the authors by the Editorial Office and must be returned by the authors as a scan. Only forms with a hand-written signature are accepted. This copyright will ensure the widest possible dissemination of information. Please note that your manuscript will not proceed to the next step in publication until the JPA Form is received. In addition, if excerpts from other copyrighted works are included, the author(s) must obtain written permission from the copyright owners and credit the source(s) in the article.

Peer Review: *BioScience Trends* uses single-blind peer review, which means that reviewers know the names of the authors, but the authors do not know who reviewed their manuscript. The external peer review is performed for research articles by at least two reviewers, and sometimes the opinions of more reviewers are sought. Peer reviewers are selected based on their expertise and ability to provide high quality, constructive, and fair reviews. For research manuscripts, the editors may, in addition, seek the opinion of a statistical reviewer. Consideration for publication is based on the article's originality, novelty, and scientific soundness, and the appropriateness of its analysis.

Suggested Reviewers: A list of up to 3 reviewers who are qualified to assess the scientific merit of the study is welcomed. Reviewer information including names, affiliations, addresses, and e-mail should be provided at the same time the manuscript is submitted online. Please do not suggest reviewers with known conflicts of interest, including participants or anyone with a stake in the proposed research; anyone from the same institution; former students, advisors, or research collaborators (within the last three years); or close personal contacts. Please note that the Editor-in-Chief may accept one or more of the proposed reviewers or may request a review by other qualified persons.

Language Editing: Manuscripts prepared by authors whose native language is not English should have their work proofread by a native English speaker before submission. If not, this might delay the publication of your manuscript in *BioScience Trends*.

The Editing Support Organization can provide English proofreading, Japanese-English translation, and Chinese-English translation services to authors who want to publish in *BioScience Trends* and need assistance before submitting a manuscript. Authors can visit this organization directly at *http://www.iacmhr.com/iac-eso/support.php?lang=en*. IAC-ESO was established to facilitate manuscript preparation by researchers whose native language is not English and to help edit works intended for international academic journals.

4. Manuscript Preparation

Manuscripts are suggested to be prepared in accordance with the "Recommendations for the Conduct, Reporting, Editing, and Publication of Scholarly Work in Medical Journals", as presented at *http://www.ICMJE.org*.

Manuscripts should be written in clear, grammatically correct English and submitted as a Microsoft Word file in a single-column format. Manuscripts must be paginated and typed in 12-point Times New Roman font with 24-point line spacing. Please do not embed figures in the text. Abbreviations should be used as little as possible and should be explained at first mention unless the term is a well-known abbreviation (*e.g.* DNA). Single words should not be abbreviated.

Title page: The title page must include 1) the title of the paper (Please note the title should be short, informative, and contain the major key words); 2) full name(s) and affiliation(s) of the author(s), 3) abbreviated names of the author(s), 4) full name, mailing address, telephone/fax numbers, and e-mail address of the corresponding author; and 5) conflicts of interest (if you have an actual or potential conflict of interest to disclose, it must be included as a footnote on the title page of the manuscript; if no conflict of interest exists for each author, please state "There is no conflict of interest to disclose"). Please visit Download Centre and refer to the title page of the manuscript sample.

Abstract: The abstract should briefly state the purpose of the study, methods, main findings, and conclusions. For articles that are Original Articles, Brief Reports, Reviews, or Policy Forum articles, a one-paragraph abstract consisting of no more than 250 words must be included in the manuscript. For Communications, Editorials, News, or Letters, a brief summary of main content in 150 words or fewer should be included in the manuscript. Abbreviations must be kept to a minimum and non-standard abbreviations explained in brackets at first mention. References should be avoided in the abstract. Three to six key words or phrases that do not occur in the title should be included in the Abstract page.

Introduction: The introduction should be a concise statement of the basis for the study and its scientific context.

Materials and Methods: The description should be brief but with sufficient detail to enable others to reproduce the experiments. Procedures that have been published previously should not be described in detail but appropriate references should simply be cited. Only new and significant modifications of previously published procedures require complete description. Names of products and manufacturers with their locations (city and state/country) should be given and sources of animals and cell lines should always be indicated. All clinical investigations must have been conducted in accordance with Declaration of Helsinki principles. All human and animal studies must have been approved by the appropriate institutional review board(s) and a specific declaration of approval must be made within this section.

Results: The description of the experimental results should be succinct but in sufficient detail to allow the experiments to be analyzed and interpreted by an independent reader. If necessary, subheadings may be used for an orderly presentation. All figures and tables must be referred to in the text.

Discussion: The data should be interpreted concisely without repeating material already presented in the Results section. Speculation is permissible, but it must be well-founded, and discussion of the wider implications of the findings is encouraged. Conclusions derived from the study should be included in this section.

Acknowledgments: All funding sources should be credited in the Acknowledgments section. In addition, people who contributed to the work but who do not meet the criteria for authors should be listed along with their contributions.

References: References should be numbered in the order in which they appear in the text. Citing of unpublished results, personal communications, conference abstracts, and theses in the reference list is not recommended but these sources may be mentioned in the text. In the reference list, cite the names of all authors when there are fifteen or fewer authors; if there are sixteen or more authors, list the first three followed by *et al*. Names of journals should be abbreviated in the style used in PubMed. Authors are responsible for the accuracy of the references. The EndNote Style of *BioScience Trends* could be downloaded at **EndNote** (*https://ircabssagroup.com/examples/BioScience_Trends.ens*).

Examples are given below:

Example 1 (Sample journal reference):

Inagaki Y, Tang W, Zhang L, Du GH, Xu WF, Kokudo N. Novel aminopeptidase N (APN/CD13) inhibitor 24F can suppress invasion of hepatocellular carcinoma cells as well as angiogenesis. Biosci Trends. 2010; 4:56-60.

Example 2 (Sample journal reference with more than 15 authors):

Darby S, Hill D, Auvinen A, *et al*. Radon in homes and risk of lung cancer: Collaborative analysis of individual data from 13 European case-control studies. BMJ. 2005; 330:223.

Example 3 (Sample book reference):

Shalev AY. Post-traumatic stress disorder: Diagnosis, history and life course. In: Post-traumatic Stress Disorder, Diagnosis, Management and Treatment (Nutt DJ, Davidson JR, Zohar J, eds.). Martin Dunitz, London, UK, 2000; pp. 1-15.

Example 4 (Sample web page reference):

World Health Organization. The World Health Report 2008 – primary health care: Now more than ever. *http://www.who.int/whr/2008/whr08_en.pdf* (accessed September 23, 2010).

Tables: All tables should be prepared in Microsoft Word or Excel and should be arranged at the end of the manuscript after the References section. Please note that tables should not in image format. All tables should have a concise title and should be numbered consecutively with Arabic numerals. If necessary, additional information should be given below the table.

Figure Legend: The figure legend should be typed on a separate page of the main manuscript and should include a short title and explanation. The legend should be concise but comprehensive and should be understood without referring to the text. Symbols used in figures must be explained. Any individually labeled figure parts or panels (A, B, *etc*.) should be specifically described by part name within the legend.

Figure Preparation: All figures should be clear and cited in numerical order in the text. Figures must fit a one- or two-column format on the journal page: 8.3 cm (3.3 in.) wide for a single column, 17.3 cm (6.8 in.) wide for a double column; maximum height: 24.0 cm (9.5 in.). Please make sure that the symbols and numbers appeared in the figures should be clear. Please make sure that artwork files are in an acceptable format (TIFF or JPEG) at minimum resolution (600 dpi for illustrations, graphs, and annotated artwork, and 300 dpi for micrographs and photographs). Please provide all figures as separate files. Please note that low-resolution images are one of the leading causes of article resubmission and schedule delays.

Units and Symbols: Units and symbols conforming to the International System of Units (SI) should be used for physicochemical quantities. Solidus notation (*e.g*. mg/kg, mg/mL, mol/mm^2/min) should be used. Please refer to the SI Guide *www.bipm.org/en/si/* for standard units.

Supplemental data: Supplemental data might be useful for supporting and enhancing your scientific research and *BioScience Trends* accepts the submission of these materials which will be only published online alongside the electronic version of your article. Supplemental files (figures, tables, and other text materials) should be prepared according to the above guidelines, numbered in Arabic numerals (*e.g.*, Figure S1, Figure S2, and Table S1, Table S2) and referred to in the text. All figures and tables should have titles and legends. All figure legends, tables and supplemental text materials should be placed at the end of the paper. Please note all of these supplemental data should be provided at the time of initial submission and note that the editors reserve the right to limit the size and length of Supplemental Data.

5. Submission Checklist

The Submission Checklist will be useful during the final checking of a manuscript prior to sending it to *BioScience Trends* for review. Please visit Download Centre and download the Submission Checklist file.

6. Online Submission

Manuscripts should be submitted to *BioScience Trends* online at *http://www.biosciencetrends.com*. The manuscript file should be smaller than 5 MB in size. If for any reason you are unable to submit a file online, please contact the Editorial Office by e-mail at *office@biosciencetrends.com*

7. Accepted Manuscripts

Proofs: Galley proofs in PDF format will be sent to the corresponding author *via* e-mail. Corrections must be returned

to the editor (*proof-editing@biosciencetrends.com*) within 3 working days.

Offprints: Authors will be provided with electronic offprints of their article. Paper offprints can be ordered at prices quoted on the order form that accompanies the proofs.

Page Charge: Page charges will be levied on all manuscripts accepted for publication in *BioScience Trends* ($140 per page for black white pages; $340 per page for color pages). Under exceptional circumstances, the author(s) may apply to the editorial office for a waiver of the publication charges at the time of submission.

Misconduct: *BioScience Trends* takes seriously all allegations of potential misconduct and adhere to the ICMJE Guideline (*http://www.icmje.org/recommendations*) and COPE Guideline (*http://publicationethics.org/files/Code_of_conduct_for_journal_editors.pdf*). In cases of suspected research or publication misconduct, it may be necessary for the Editor or Publisher to contact and share submission details with third parties including authors' institutions and ethics committees. The corrections, retractions, or editorial expressions of concern will be performed in line with above guidelines.

(As of June 2020)

BioScience Trends
Editorial and Head Office
Pearl City Koishikawa 603,
2-4-5 Kasuga, Bunkyo-ku,
Tokyo 112-0003, Japan.
E-mail: office@biosciencetrends.com